PARTS OF THE ORIGINAL DOCUMENT

ARE OF POOR REPRODUCTIVE QUALITY

CERTAINES PARTIES DU DOCUMENT ORIGINAL

SONT DE PIÈTRE QUALITÉ DE REPRODUCTION

State-of-the-Art Track Technology and its Application to Improve Track Component Performance and Track Maintenance Management

A. Mohrenstein
S.L. Lawson
J.D. Michaud
C.J. Boon

CIGGT Report No. 86-15
Transport Canada Report No. [illegible]

CA2 ON
UQU 325
86
R35
c.2

CA2ON
QQ4325
86
R35
c.2

CIGGT Project No. PRO-313

CIGGT Report No. 86-35
Transport Canada Report No. TP 8524E

STATE-OF-THE-ART TRACK TECHNOLOGY AND ITS APPLICATION TO IMPROVE TRACK COMPONENT PERFORMANCE AND TRACK MAINTENANCE MANAGEMENT

Library and Information Centre /
Centre de Documentation (CSLA)
RECEIVED / REÇU LE
MAR 10 1988
Transport Canada / Transports Canada

A. Moucessian
S.T. Lamson
J.C. Michaud
C.J. Boon

prepared for

Transportation Development Centre, Transport Canada

Canadian Institute of Guided Ground Transport
Queen's University
Kingston, Ontario
K7L 3N6

April 1987

369460

ACKNOWLEDGEMENTS

The authors wish to acknowledge the assistance and cooperation of Mr. Wayne Rowan of the Transport Canada's Transportation Development Centre during the course of this project. Thanks are also extended to CN Rail, CP Rail, the Association of American Railroads, and the Transportation Development Centre for providing the necessary data and funding for this project.

ISBN 0 88911 049 2

Un sommaire en français de ce rapport est inclus avant la Table des matières.

This report resulted from research conducted through the Canadian Institute of Guided Ground Transport. The report represents the views of the authors and does not necessarily have the endorsement of the University or the other participating organizations.

REPORT DOCUMENTATION FORM

1. Transport Canada Report No.
TP 8524E

2. TDC Project No.
6059, 6749

3. Recipient's Catalogue No.

4. Title and Subtitle
STATE-OF-THE-ART TRACK TECHNOLOGY AND ITS APPLICATION TO IMPROVE TRACK COMPONENT PERFORMANCE AND TRACK MAINTENANCE MANAGEMENT

5. Report Date
April 1987

6. Performing Organization Report No.
86-35

7. Author(s)
A. Moucessian, S.T. Lamson, J.C. Michaud, C.J. Boon

8. Transport Canada File No.
D1465-401-2

9. Performing Organization Name and Address
Canadian Institute of Guided Ground Transport (CIGGT)
Queen's University
Kingston, Ontario
K7L 3N6

10. DSS File No.
11SD.T8200-3-3524

11. DSS or Transport Canada Contract No.
OSD83-00120

12. Sponsoring Agency Name and Address
Transportation Development Centre (TDC), Guy Favreau Complex, Ste 601, West Tower, 200 Dorchester Blvd. W., Montreal, P.Q. H2Z 3E4
CN Rail (CN), P.O. Box 8100, Montreal, P.Q. H3C 3N4
CP Rail (CP), P.O. Box 6042, Station A, Montreal, P.Q. H3C 3E4
Assoc. of American Railroads (AAR), 50 F Street, Washington, D.C. 20001

13. Type of Report and Period Covered
final

14. Sponsoring Agency Code
TDC 6749

15. Supplementary Notes
See also "Subballast and Geotextiles for Railway Track Support Separation Applications," CIGGT 85-12, TP 7383E

16. TDC Project Officer
Wayne Rowan

17 Abstract

State-of-the-art track technology and its application to improve track component performance and track maintenance management are presented. Research findings on the degradation nature of each of the track components, namely rail, tie, ballast, sub-ballast and subgrade, are reviewed, together with the use of geotextiles in track rehabilitation. The review is extended to methods of performance evaluation and improvement of each track component. Some of the track component degradation processes are then mathematically modelled in a number of computer programs which together make up a track system model that may be used for better and more efficient management of track maintenance.

18. Key Words
Track, rail, tie, ballast, sub-ballast, subgrade, geotextile, mathematical modelling

19 Distribution Statement
Available on request from CIGGT or TDC

20. Security Classification (of this report)
unclassified

21. Security Classification (of this page)
unclassified

22. No. of Pages
98 + append.

23. Price

TDC CDT 79-005

FORMULE DE DOCUMENTATION POUR RAPPORT

1. Nº du rapport Transports Canada
TP 8524E

2. Nº de l'étude — CDT
6059, 6749

3. Nº de catalogue du destinataire

4. Titre et sous-titre
STATE-OF-THE-ART TRACK TECHNOLOGY AND ITS APPLICATION TO IMPROVE TRACK COMPONENT PERFORMANCE AND TRACK MAINTENANCE MANAGEMENT

5. Date du rapport
Avril 1987

6. Nº du rapport de l'organisme exécutant
86-35

7. Auteur(s)
A. Moucessian, S.T. Lamson, J.C. Michaud, C.J. Boon

8. Nº de dossier Transports Canada
D1465-401-2

9. Nom et adresse de l'organisme exécutant
Canadian Institute of Guided Ground Transport (CIGGT)
Queen's University
Kingston, Ontario
K7L 3N6

10. Nº de dossier — ASC
11SD.T8200-3-3524

11. Nº de contrat — ASC ou Transports Canada
OSD83-00120

12. Nom et adresse de l'organisme parrain
Centre de développement des transports (CDT), Com. Guy Favreau, Ste 601, Tour Ouest, 200 o., boul. Dorchester, Montréal, P.Q. H2Z 1X4
CN Rail (CN), C.P. 8100, Montréal, P.Q. H3C 3N4
CP Rail (CP), C.P. 6042, succursale A, Montréal, P.Q. H3C 3E4
Assoc. of American Railroads (AAR), 50, rue F, Washington, D.C. 20001

13. Genre de rapport et période visée
final

14. Code de l'organisme parrain
TDC 6749

15. Remarques additionnelles
Voir aussi "Subballast and Geotextiles for Railway Track Support Separation Applications," CIGGT 85-12, TP 7383E

16. Agent de projet — CDT
Wayne Rowan

17. Résumé

Ce rapport fait le point sur l'état actuel de la technologie des voies ferrées et sur les applications destinées au relèvement de leurs caractéristiques et de la gestion de maintenance. La recherche a concerné le processus de dégradation des éléments d'une voie ferrée : rails, traverses, ballast, sous-couches et sol support, ainsi que les géotextiles entrant dans la réfection des voies. La recherche a porté également sur les procédés d'expertise de chacun de ces éléments en vue d'en relever les performances. Certains des processus sont écrits sous forme de programmes informatiques dont l'ensemble forme un modèle qui permettra de déboucher sur des méthodes de gestion de la maintenance améliorées et perfectionnées.

18. Mots-clés
Voie, rail, traverse, ballast, sous-couche, sol support, géotextiles, modélisation mathématique

19. Diffusion
Disponible sur demande auprès du CIGGT ou du CDT

20. Classification de sécurité (de ce rapport)
non classifié

21. Classification de sécurité (de cette page)
non classifiée

22. Nombre de pages
98 + append.

23. Prix

CDT TDC 79-005

EXECUTIVE SUMMARY

This report is arranged in two main parts. The first part (Section 2) consists of a state-of-the-art review of track technology and highlights the latest theories on and understanding of the deterioration mechanism and performance improvement techniques of rail, tie, ballast and sub-ballast, as well as the use of geotextiles in track rehabilitation. The second part (Section 3) describes the development of a Track System Model which incorporates some of the theories on track component deterioration.

Although not fully illustrated in this report, the Track System Model may be used effectively to improve track component life and optimize track management decisions. The development of an effective and reliable track system model requires good data bases on track component deterioration and maintenance operations to calibrate the model. Most of the existing data bases fall short of providing all the data required. These shortfalls have been highlighted in the report.

A summary of the material covered in this report is given below.

STATE-Of-THE-ART TRACK TECHNOLOGY REVIEW

Rail

Fatigue- and wear-associated defects are the main cause of rail deterioration. Plastic flow is another defect which can lead to serious damage and deterioration of the track. Also contributing to rail deterioration is the existence of shatter cracks in the rail steel, a fault associated with high hydrogen content in the rail steel. This problem can be controlled effectively by applying appropriate techniques during the rail manufacturing process.

Fatigue-type defects can be successfully controlled by reducing the stresses developed during wheel/rail interaction, by changing the wheel and rail profiles, and by increasing the capacity of rail head steels to withstand such stresses.

The most effective way to reduce wear is by the proper use of rail lubrication. Decreasing the angle of attack between the flange of the wheel and the gauge face of the rail, increasing the hardness of the rail steel, and a more refined structure for the rail steel are other means of reducing rail wear.

Increasing the yield strength and controlling the wheel/rail contact position (e.g. through rail grinding) are effective measures for reducing the plastic flow problem.

Ties

North American railroads are the greatest users of wood ties. The use of concrete ties, however, is becoming quite common with some railroads in certain terrain. The realization of some of the advantages of concrete ties together with the constant threat of a shrinking natural resource are the main factors contributing to this trend. There is a great effort on the part of steel producers to encourage the use of steel ties. However, the use of steel ties in North America has so far been on a very small scale and on an experimental basis.

Each type of tie offers certain advantages, but the choice of a given tie on a system-wide basis is dependent on many factors. An assessment of the comparative features of the various types of ties is one component of the decision-making process. Such a comparison includes consideration of the ability of each type of tie to hold proper track gauge and alignment, consideration of the influence of the resulting impact forces transferred to the ballast and their effect on track settlement, the electrical insulation and corrosion properties of each type of tie, and so on.

Ballast, Sub-ballast and Subgrade

Ballast, sub-ballast and subgrade make up the track support system. For the ballasted track to perform satisfactorily, the track support system must keep the development and growth of track geometry errors to within acceptable limits. These errors arise through two degradation mechanisms, namely the settlement of the support system and the breakdown and subsequent fouling of the ballast layer. Both mechanisms are driven largely by the repeated loadings imposed on the support system through the rails and ties by the movement of traffic over the track. However, the latter mechanism is also affected by physical and chemical weathering processes unrelated to the traffic history of the track.

The above-mentioned deterioration processes can be effectively controlled by considering a number of key factors in the design and construction of new track. These considerations are as follows:

- preservation or creation of stable subgrade conditions
- separation of the ballast and subgrade layers to prevent the upward migration of subgrade fines into the ballast
- specification of free-draining ballast materials resistent to wear and weathering breakdown
- establishment and preservation of good drainage.

Geotextiles

Geotextiles are used primarily to limit ballast contamination. To achieve this broad objective they must be able to:

- drain water away from the track roadbed, on a long-term basis, both laterally along the plane of the geotextile and by gravity, without buildup of excessive hydrostatic pressure
- withstand the abrasive puncture forces of moving aggregate caused by the tamping/compaction process during cyclic maintenance, tamping during initial compaction and by the passage of trains
- retard the migration of fine particles while allowing the passage of water, so as to separate the ballast and subgrade materials under the influence of repeated loading and of water migration.

TRACK SYSTEM MODELLING

The Track System Model (TSM) which was developed by incorporating some of the key parameters identified in Section 2, consists of four modules as follows:

- Dynamic Wheel Force Model
- Rail Life Model
- Tie Life Model
- Surface Life Model.

Dynamic Wheel Force Model

The difference between one traffic category and another, in terms of track degradation, begins with the various characteristics of their dynamic wheel load. Therefore, an estimate of the dynamic wheel load for each traffic category is necessary in order to work out the contribution to total track maintenance costs of different traffic types in a traffic mix. This model gives the required wheel loads.

For each traffic type, there are two principal load components, namely vertical and lateral, each with two principal terms: steady-state and dynamic variation. The steady-state term represents the reaction of the vehicle to the average track parameters such as nominal alignment. The dynamic term represents the reaction of the vehicle to the instantaneous changes in track parameters, such as alignment errors.

The loads obtained from this model are then transferred to the following models, where they are used in determining their effect on the life of the particular track component.

Rail Life Model

Rail damage and associated costs are basically caused by an accumulation of various wheel-loading cycles, each with a different force, depending on vehicle characteristics, operating conditions, and track quality. The wheel loads, as obtained from the Wheel Force Model, are separated into high and low rail forces, and also into flange and tread forces, each causing a particular type of damage. The forces can be normalized so that each equivalent load cycle causes equal amounts of damage, thus establishing the unit of rail cost per cycle.

The key to this approach is to accurately estimate the dynamic force exerted on the rail by each traffic category, and the relative extent of damage the rail sustains when subjected to a cycle of such force.

Tie Life Model

The strategy in this program is that a distinct series of track conditions can be identified and grouped into a finite number of classes. Each track class is considered to represent a unique set of track characteristics, as related to tie damage. The total traffic is also broken into a distinct, finite set of traffic classes, each one representing a unique set of traffic characteristics as related to tie damage.

The analysis is then carried out by considering the net effect on each track class when subjected to loading by each traffic class. A final summation of tie damage allows the total effect per route to be determined.

Surface Life Model

The analysis is carried out on a per-track-class, per-traffic-class basis, until a number of normalized wheel load cycles are generated. The normalization standardizes all traffic-loading cycles according to their relative significance to track surface degradation. After the total number of normalized wheel load cycles is calculated for a track class, the surfacing cycle and required lift are estimated.

The three models predicting rail life, tie life, and required lift and surfacing cycle have to be calibrated using existing data before they can be used in predicting future maintenance requirements. Typical calibration procedures are illustrated in the report.

SOMMAIRE

Le présent rapport se présente en deux parties principales. La première (section 2) passe en revue les procédés de maintenance d'une voie ferrée et les met en rapport avec les théories et les connaissances les plus récentes concernant le processus de dégradation des voies ferrées et le relèvement des armements : rails, traverses, ballast et sous-couches; elle traite aussi des géotextiles utilisés pour la remise en état des voies. La seconde (section 3) décrit la mise au point d'un modèle informatique intégrant quelques-unes des théories sur le processus de dégradation.

Bien qu'il soit incomplètement illustré, on peut affirmer que ce modèle peut servir utilement à prolonger la vie utile des armements et aide efficacement à la prise de décisions concernant la gestion des voies ferrées. La mise au point d'un tel modèle nécessite des bases de données fiables sur le processus de détérioration, ainsi que sur le processus de maintenance, afin de pouvoir caler adéquatement le modèle. Or, d'importantes lacunes existent dans les bases existantes; ce rapport les met en évidence.

Un sommaire des sujets traités dans celui-ci est donné ci-après.

REVUE DES PROCÉDÉS DE MAINTENANCE

Rails

La dégradation des rails provient tout d'abord des défauts causés par la fatigue et l'usure, auxquels s'ajoutent les phénomènes d'écoulement plastique ainsi que les microfissures, défaut lié à une haute teneur en hydrogène des aciers pour rails, teneur pouvant cependant être maîtrisée par des précautions prises en cours de fabrication.

Les défauts de fatigue peuvent être enrayés par divers moyens : atténuation des contraintes sour la charge des roues, modification du profil des rails et augmentation de la résistance des champignons aux types de contraintes considérés.

Le meilleur moyen de baisser le taux d'usure est de lubrifier convenablement les rails. Mais il en est d'autres également : réduire l'angle d'attaque entre le boudin et la face intérieure du rail, augmenter la dureté de l'acier et affiner sa microstructure.

Quant à l'écoulement plastique, les moyens efficaces de lutter contre ce phénomène consistent à relever la limite d'élasticité de l'acier et à maintenir le point de contact roue-rail dans des limites étroites (par un profilage adéquat des rails).

Traverses

Les sociétés nord-américaines de chemins de fer sont les plus grandes consommatrices de traverses en bois, bien que l'usage des traverses béton commence à se répandre dans certaines sociétés pour certains besoins. Les avantages évidents des traverses béton et l'épuisement mondial des ressources forestières contribuent à cet essor. Les sidérurgistes, eux, verraient d'un bon oeil une utilisation plus étendue des traverses en acier; en Amérique du Nord, elles ne sont cependant que très peu utilisées et seulement dans des applications de nature purement expérimentale.

Si chaque type de traverse possède des avantages intrinsèques, il reste que le choix d'un type particulier pour l'ensemble d'un réseau doit tenir compte d'un très grand nombre de facteurs. L'analyse comparative des caractéristiques des divers types de traverses est un des éléments de la prise de décision. Elle doit tenir compte de l'aptitude de la traverse à maintenir l'écartement et l'alignement des rails dans les limites prévues et à transférer convenablement les efforts au ballast, de l'effet de ceux-ci sur le tassement, des caractéristiques isolantes de la traverse, de sa tenue à la corrosion, etc.

Le ballast et les sous-couches

Le ballast et les sous-couches constituent la structure de soutien de la voie ferrée. Pour que celle-ci joue bien son rôle, la structure de soutien doit maintenir l'amplitude des défauts géométriques de la voie dans des limites acceptables. Ces défauts naissent de deux processus de dégradation : le tassement de la structure de soutien et l'effritement du ballast, suivi de sa contamination. Ces deux processus sont largement reliés aux charges cycliques exercées sur la structure de soutien par l'intermédiaire des rails et des traverses. Mais le deuxième processus dépend aussi de phénomènes physico-chimiques qui ne sont par liés intrinsèquement au trafic écoulé.

On peut se prémunir contre des processus de dégradation en prenant en compte, lors de l'étude et la construction d'une voie ferrée, les facteurs clés suivants:

- création ou conservation des conditions de stabilité du sol support;
- séparation du ballast et des sous-couches afin de prévenir la contamination du premier par les seconds;
- utilisation d'un ballast drainant librement, résistant à l'usure et à l'effritement;
- mise en place d'un bon système de drainage bien protégé.

Les géotextiles

Les géotextiles sont surtout utiles pour empêcher la contamination du ballast et ce :

- en permettant à l'eau d'évacuer la plate-forme aussi bien dans le plan du géotextile que par gravité, sans qu'il en résulte une pression hydrostatique excessive;
- en résistant aux forces de perforation abrasive exercées par les granulats en mouvement sous l'action des opérations de bourrage/compactage en maintenance cyclique, du bourrage durant la mise en place initiale et, enfin, du passage des trains;
- en empêchant les remontées de fines particules sans gêner l'évacuation de l'eau, agissant ainsi comme écran entre le ballast et les sous-couches malgré les efforts cycliques et le ruissellement.

LE MODELE INFORMATIQUE

Ce modèle qui tient compte de certains paramètres clés identifiés à la section 2, comporte les quatre modules suivants :

- module dynamique,
- module rails,
- module traverses,
- module nivellement.

Module dynamique

Pour bien caractériser les différents types de trafics en fonction des dégradations qu'ils provoquent, il faut commencer par bien déterminer les charges dynamiques qui les caractérisent. Il faut donc connaître approximativement les charges dynamiques correspondant à chaque type de trafic avant de pouvoir établir la quote-part de ceux-ci dans le coût total de maintenance. Ce module fournit les données nécessaire à cet égard.

Tout trafic se décompose en deux composantes principales de charge : charges verticales et charges transversales, celles-ci à leur tour se définissant par le régime qui peut être soit permanent, soit transitoire. Par régime permanent, on entend la composante correspondant aux valeurs moyennes des paramètres clés, le nivellement nominal, par exemple. Par régime transitoire, on entend la composante correspondant aux valeurs instantanées de ces paramètres, les défauts d'alignement, par exemple.

Les valeurs de charge tirées de ce module sont alors transférées aux modules suivants qui s'en servent pour calculer leur effet sur l'élément de voie les intéressant.

Module rails

Les avaries de rails et les coûts y afférents sont induits par la conjonction de trafics, donc de cycles de charge très variables en nature, vitesse et intensité. Les valeurs de charge tirées du module dynamique sont décomposées en forces exercées sur les rails extérieurs et intérieurs, mais aussi en forces latérales et forces verticales, chacune de ces forces induisant des avaries de type particulier. Ces forces peuvent être normalisées de façon que les cycles de charge équivalents induisent des effets égaux, dont il sera possible par la suite de tirer des coûts unitaires par cycle.

L'essentiel de cette approche est d'estimer avec précision les charges dynamiques par type de trafic ainsi que la sévérité correspondante des avaries.

Module traverses

La stratégie qui sous-entend ce module consiste à identifier des séries de conditions géométriques de voie et à les grouper à l'intérieur d'un nombre fini de classes distinctes, chacune représentant un ensemble particulier de caractéristiques géométriques rapportées aux défauts induits dans les traverses. Quant au trafic total, il est, lui aussi, subdivisé en un nombre fini de types de trafics distincts, chacun représentant un ensemble particulier de caractéristiques de trafic rapportées aux défauts induits dans les traverses.

L'analyse consiste alors à identifier l'effet net de chacun des types de trafics sur chacune des classes de voies pour en tirer par sommation l'effet total induit dans les traverses par l'ensemble du trafic sur la ligne considérée.

Module nivellement

L'analyse consiste, ici aussi, à identifier l'effet des différents trafics sur les différentes classes de voies, aboutissant à un certain nombre de cycles de charge normalisés qui definissent la relation entre trafic et charge, d'une part, et dégradation de nivellement, d'autre part. A un nombre de cycles de charge normalisés donné, calculé à l'égard d'une voie donnée, correspondra un cycle pour les opérations de nivellement et une amplitude pour les opérations de soufflage, à décider.

Cependant, avant de pouvoir obtenir des prévisions de maintenance utilisables, il faudra procéder au calage des trois modules rails, traverses et nivellement, à partir des valeurs mesurées, calage qui se fait selon la procédure type expliquée dans le rapport.

TABLE OF CONTENTS

1. INTRODUCTION 1
   1.1 Objective 1
   1.2 Scope and Strategy of Research Program 2

2. STATE-OF-THE-ART TRACK TECHNOLOGY REVIEW 4
   2.1 Rail -- Nature of Rail Degradation/Method for Performance Evaluation and Improvement 4
      2.1.1 Fatigue-associated Defects 4
      2.1.2 Wear-associated Defects 5
      2.1.3 Defects Associated with Plastic Flow 6
      2.1.4 Shatter Cracks 8
      2.1.5 Summary 8
   2.2 Tie -- Nature of Tie Degradation/Method for Performance Evaluation and Improvement 8
      2.2.1 Wood Ties 9
         2.2.1.1 Tie loading environment 9
         2.2.1.2 Wood properties 11
         2.2.1.3 Failure modes 11
         2.2.1.4 Data base 12
      2.2.2 Concrete Ties 13
         2.2.2.1 Types of concrete ties 13
         2.2.2.2 Loading conditions 14
         2.2.2.3 Design Criteria 14
         2.2.2.4 Other Demands 17
         2.2.2.5 Rail Fastening Systems 17
         2.2.2.6 Rail Pads 19
      2.2.3 Steel Ties 19
         2.2.3.1 Design of the tie section 20
         2.2.3.2 Rail fastening systems and pads 22
      2.2.4 Comparative Performance of Wood, Concrete and Steel Ties 22
         2.2.4.1 Track gauge 22
         2.2.4.2 Track alignment 23
         2.2.4.3 Impact forces 23
         2.2.4.4 Track settlement 24
         2.2.4.5 Electrical insulation 25
         2.2.4.6 Corrosion 25
      2.2.5 Tie Usage in North America 26
      2.2.6 Summary 26
   2.3 The Track Support System 27
      2.3.1 Track Support Degradation Mechanisms 28
         2.3.1.1 Track support settlement 29
         2.3.1.2 Ballast breakdown and the effects of ballast quality 40
      2.3.2 Sub-ballast 45
   2.4 Geotextiles 48
      2.4.1 Purpose of Geotextiles 48

3. TRACK SYSTEM MODELLING 51
3.1 Overview 51
3.2 Computer Model 52
3.2.1 Model Structure 53
3.2.2 Vehicle Dynamics Model 55
3.2.2.1 Introductory remarks 55
3.2.2.2 Model outline 56
3.2.2.3 Vertical forces 59
3.2.2.4 Lateral forces 60
3.2.2.5 Track quality indices 61
3.2.3 Rail Life Model 62
3.2.3.1 Model Outline 62
3.2.3.2 Working equations 63
3.2.3.3 Procedure to establish rail cost data . . . 65
3.2.4 Tie Life Model (Wood) 67
2.3.4.1 Model outline 67
3.2.4.2 Working equations 68
3.2.4.3 Simplification of stress equations 76
3.2.4.4 Model Calibration 78
3.2.5 Surface Life Model 79
3.2.5.1 Introductory Remarks 79
3.2.5.2 Model outline 81
3.2.5.3 Working equations 81
3.2.5.4 Surface Life Model calibration 91
3.3 Application of Track System Model to Component Improvement and Maintenance Management 92
3.4 Recommmendations for Further Work on the Track System Model 93

REFERENCES 94

Appendix A: DEVELOPMENT OF AN EMPIRICAL RELATIONSHIP FOR VERTICAL DYNAMIC WHEEL FORCE VARIATION OF A 100-TON CAR AS A FUNCTION OF TRACK ROUGHNESS AND VEHICLE SPEED

Appendix B: DEVELOPMENT OF AN EMPIRICAL RELATIONSHIP FOR THE STEADY-STATE LATERAL FORCE OF A 100-TON CAR IN CURVING

Appendix C: MODEL CALIBRATION REQUIREMENTS AND PROCEDURES

Appendix D: "DYNFOR", "TIELIF" AND "SURLIF" PROGRAM INTERRELATIONSHIP AND INPUT DATA FORMAT

Appendix E: "DYNFOR" PROGRAM LISTING, INPUT AND OUTPUT

Appendix F: "TIELIF" PROGRAM LISTING, INPUT AND OUTPUT

Appendix G: "SURLIF" PROGRAM LISTING, INPUT AND OUTPUT

LIST OF TABLES

2.1 Impact Forces from a 100-Ton Hopper Car at 60 24
2.2 Basic Ballast Characteristic Test Limits 42
2.3 Sub-Ballast Grinding Limits 46

LIST OF FIGURES

2.1 Wear of rails in curves under heavy traffic conditions 6
2.2 Various forms of rail corrugation 7
2.3 Tie loading environment 10
2.4 Basic types of concrete tie 14
2.5 BHP heavy axle load tie 20
2.6 Rail insulation on steel and timber tie track: before, during and after a rain storm 25
2.7 Typical cross-section, conventional railway ballasted track structure 27
2.8 Effect of track modulus variation on maximum vertical stress in track support resulting from a single static axle load 33
2.9 Effect of track modulus variation on maximum vertical stress in track support resulting from two coupled G-75 trucks 33
2.10 Subgrade settlement with traffic 38
2.11 General test arrangement 40
2.12 Plastic axial strain observed in triaxial tests on railroad ballasts 43
2.13 Mainline maintenance cycle related to aggregate index 43
2.14 Typical track cross-section for new double-track construction 44
2.15 Grading curves of suggested sub-ballast and its alternative options 47
2.16 Canal effect created by undercutting operation prior to removal of shoulder ballast 49

3.1 Track system 51
3.2 Track System Maintenance Model 54
3.3 Sample vertical wheel force variation of a 100-ton car at 65 mph running over jointed rail track 57
3.4 Sample lateral wheel force variation of a 100-ton car running through a 1.43 degree curve 57
3.5 Sample wheel load distribution for passenger and freight traffic 58
3.6 Dynamic Wheel Force Model flowchart 58

3.7 Dynamic lateral load factor versus vehicle speed 61
3.8 Concept of rail life/cost model 62
3.9 Tie Life Model flowchart 67
3.10 Effect of stress and tie age on tie deterioration rate 75
3.11 Annual tie replacement 78
3.12 Idealized representation of track geometry errors 79
3.13 "Percent poor track" as a criterion for mechanized tamping cycle 80
3.14 Surface Life Model flowchart 81
3.15 The vertical profiles of a section of track towards the end of four maintenance cycles 83
3.16 Track differential settlement and error growth 83
3.17 Total track settlement measured at rail level 85
3.18 Subgrade settlement measured at top of subgrade, 20" below base of tie 85
3.19 Upper ballast deterioration rate versus abrasion number for different gradations 90

1. INTRODUCTION

Canadian railways have experienced a rapid increase in traffic volume during the last two decades. To accommodate this growth, axle loads, train speeds and train lengths were increased and significant capital invested to expand effective track capacity on some of the most heavily used lines. Track maintenance expenditures also rose significantly during this period, to offset the accelerated track deterioration rates resulting from operation of heavier and faster trains.

Continued traffic growth and competitive pressures will create demands for further increases in axle loads, train lengths and traffic density without additional large-scale investment to expand track capacity. This prospect has led some railways to experiment with different train consists. The Hamersley and Mount Newman iron ore railways recently evaluated a train of 230 cars with 35-tonne axle loads and a speed of 85 km/h. In North America, serious consideration has been given to using 125-ton cars (approximately 35-tonne axle load) for freight service, and a speed of 200 km/h (125 mph) or more for passenger traffic. If these changes are implemented, rail and tie degradation and track geometry deterioration are likely to increase, creating a greater requirement for track maintenance, precisely when less track occupancy time can be made available for maintenance. As well, financial constraints and increasingly competitive markets for North American railways have led to the need for more effective management tools to aid in the decision-making process.

For a relatively long time, the railroads have maintained extensive computerized data bases on track performance. Partial information is now available on the degradation history and current status of track components and geometry. Information is also available on the related traffic characteristics. A computer model linking traffic history to track degradation would allow the railroads to make better use of the available information. With the recent development of microcomputers, such tools can be used not only by head office management but also by local track maintenance managers to improve overall productivity.

1.1 Objective

The work reported herein had as its primary objectives the development and identification of:

- practical and cost-effective techniques to reduce track geometry and component deterioration
- a systematic approach to track maintenance planning to improve cost and time efficiency.

The secondary objective was to ensure that basic track support and structures research would focus on key problem areas so as to support track maintenance innovations.

This three-year work program was sponsored by the Transport Canada Transportation Development Agency (TDC), CN Rail, CP Rail, and the Association of American Railroads.

1.2 Scope and Strategy of Research Program

This report describes the achievements of the program and outlines further work logically stemming from the results of this project. These achievements fall into two main areas:

- research into track component improvements
- track system modelling.

The requirements for improvements in track components were identified from investigation of the "state-of-the-art" in three main areas:

- **Rail**, including the nature of rail degradation due to fatigue, wear and plastic flow, together with manufacturing defects. Methods for improving rail performance and increasing service life, such as rail profile grinding, are discussed.

- **Ties**, including the comparative features and in-track performance of wood, concrete and steel ties. The unique features and requirements of each type of tie, such as failure modes, fastening systems, design criteria, etc., are discussed.

- **Ballast**, including the nature of ballast degradation and its influence on track settlement and other related problems. Specifications and guidelines for effective application of geotextiles and sub-ballast in construction and rehabilitation of track structures are outlined.

Track systems research at CIGGT has led to the development of several computerized tools intended to aid railway personnel in track maintenance planning. The most important of these tools is the Track System Model (TSM). This model consists of four linked components:

- Vehicle Dynamics Models
- Rail Life Model
- Tie Life Model
- Surface Life Model.

Modelling of the track system has highlighted the shortcomings of existing data on the behaviour of track components. In addition, review of the latest knowledge and understanding of track components has revealed important areas which need more attention in future research activities.

From fundamental inputs, the vehicle models generate the key components of wheel loading in the vertical and lateral dynamic modes and in the steady-state curving mode. Outputs from these models feed into the Rail, Tie and Surface Life Models to permit calculation of track component and geometry degradation and, ultimately, of maintenance costs.

2. STATE-OF-THE-ART TRACK TECHNOLOGY REVIEW

The track structure, consisting of rails, ties, tie plates, fasteners, ballast, sub-ballast and subgrade, is a complex system of interrelated components which are in constant interaction with each other. Proper track structure performance is dependent on the correct behaviour of each component under the loads and conditions imposed by nature and by the wheels of passing trains. In the following sections, the nature of the degradation process of each component is discussed, together with methods of performance evaluation and improvement.

2.1 Rail -- Nature of Rail Degradation/Method for Performance Evaluation and Improvement

The various types of rail deterioration are identified and described in this section, together with factors which enhance or retard the deterioration process.

2.1.1 Fatigue-associated Defects

Shelling, transverse or detail fractures, surface checking or flaking, and horizontal split heads are all fatigue defects of rail. These defects can occur independently or together, and so contribute to varying degrees to the overall maintenance cost of the track.

A review of the literature in this area [1] showed that the occurrence of shelling and other fatigue-type defects can be successfully reduced by:

(a) reducing the stresses developed during rail/wheel interaction (e.g. by changes in rail and wheel profiles, and/or

(b) increasing the capacity of rail head steels to withstand such stresses (by increasing the yield strength, tensile strength and fatigue limit of steel).

Independent studies conducted at U.S. Steel Research Laboratories [2] and BHP Melbourne Research Laboratories [3] have shown that fatigue-type defects in the rail head are invariably nucleated at large, complex, exogenous calcium aluminate or calcium aluminum silicate inclusions. Clearly, the service lives of the rails would have been longer if the inclusions responsible for crack initiation had not been present. Rail deterioration by fatigue occurs in three stages: (a) nucleation, (b) growth, and (c) catastrophic failure once the crack reaches critical size. Stress, of course, has a major effect on each of these stages. However, material characteristics also influence the degradation process. For example:

- nucleation is influenced by steel cleanliness and the fatigue limit of the steel, which in turn is proportional to the ultimate tensile strength

- growth is influenced by microstructure and, in particular, by presence of grain boundary ferrite [4]

- final fracture is influenced by the fracture toughness of the material.

2.1.2 Wear-associated Defects

The various forms of wear have been categorized by Ghonem et al. [5] as follows:

(a) **Adhesive wear (or mild wear)**: This occurs on the top surface and gauge corner of the rail as a result of wheel/rail sliding. In this mechanism, as in the case of sliding bodies, wheel and rail surface asperities come into contact and adhere strongly to form asperity junctions. Subsequent separation of wheel and rail surfaces break these junctions, generating particles which are termed adhesive wear particles. This mode of wear occurs most frequently on tangent track and in curved regions with starved lubrication conditions. The presence of lubricant or contaminants on the rail retards the adhesion process and, while it may be eliminated, it is not the dominant factor in the overall wear process of lubricated curved rails.

(b) **Abrasive wear**: When hard materials, such as adhesive wear particles or uncrushed sand grains, are held between the wheel and rail sliding surfaces, these hard particles slide on the rail surface and are able to deform the rail outer surface by plowing. The accumulation of plastic strain in surface layers during plowing produces singular changes in the microstructure and chemistry of the surface, giving rise to subsurface deformation. This surface layer damage is what permits, on subsequent passage of hard particles, a micro-cutting to take place, generating wear product in the form of chips.

Several studies on rail wear (e.g. references 1, 6, 7, 8 and 9) have indicated that a decrease in wear, especially on the gauge face of high rails, can be achieved by:

- the proper use of rail lubrication

- a decrease in the angle of attack (and thus the curving force) between the flange of the wheel and the gauge face of the rail

- an increase in the hardness of the rail steel

- an increase in the work-hardenability. Materials with higher rates and maximum levels of work-hardening should also exhibit lower rates of wear.

- a more refined microstructure. For fully pearlitic steels, the wear rate can be reduced considerably by refining the microstructure, i.e. by decreasing the interlamellar spacings. Also, at equivalent hardnesses, both bainitic and quenched and tempered martensitic microstructures exhibit higher wear rates than a fully pearlitic microstructure.

- a lower level of sulphide and oxide inclusions.

The first measure is potentially the most cost-effective. Laboratory work by Kalousek and field tests at FAST have shown that its effect on wear reduction can override the influence of other measures.

A detailed account of the last measure which relates to rail steel cleanliness was given recently by Moucessian et al. [10] in a report prepared for Algoma Steel Corporation.

2.1.3 Defects Associated with Plastic Flow

For curved track under heavy traffic conditions, the gauge side of the high rail and the field side of the low rail tend to suffer considerable plastic flow, as shown in Figure 2.1. Beside the problem of rail head geometry distortion, plastic flow also leads to rail fatigue and, under certain conditions, rail corrugation (Figure 2.2).

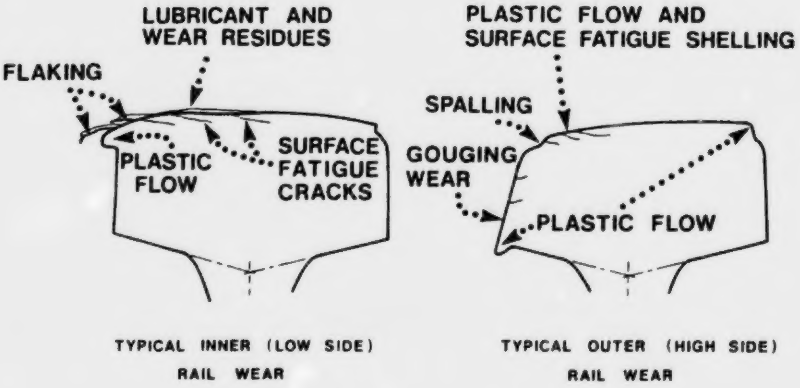
LUBRICANT AND WEAR RESIDUES
FLAKING
PLASTIC FLOW
SURFACE FATIGUE CRACKS
PLASTIC FLOW AND SURFACE FATIGUE SHELLING
SPALLING
GOUGING WEAR
PLASTIC FLOW
TYPICAL INNER (LOW SIDE) RAIL WEAR
TYPICAL OUTER (HIGH SIDE) RAIL WEAR

Source: J. Kalousek and A.E. Bethune [11]

Figure 2.1 Wear of rails in curves under heavy traffic conditions

The first problem often exhibits itself in the form of surface cracks on the rail surface. These cracks normally do not penetrate deep into the rail head, and hence are not critical to rail performance. However, with increased accumulation of traffic, several cracks join to form large shells which often necessitate premature rail replacement.[1]

The problem of rail corrugation is more serious. It presents itself in several forms, as shown in Figure 2.2, and has been a major cause of premature rail replacement in a number of railroads. The surface waviness causes a considerable increase in dynamic loads and vehicle/track vibration. The dynamic wheel/rail interaction may also lead to derailment due to wheel lift or rail break.

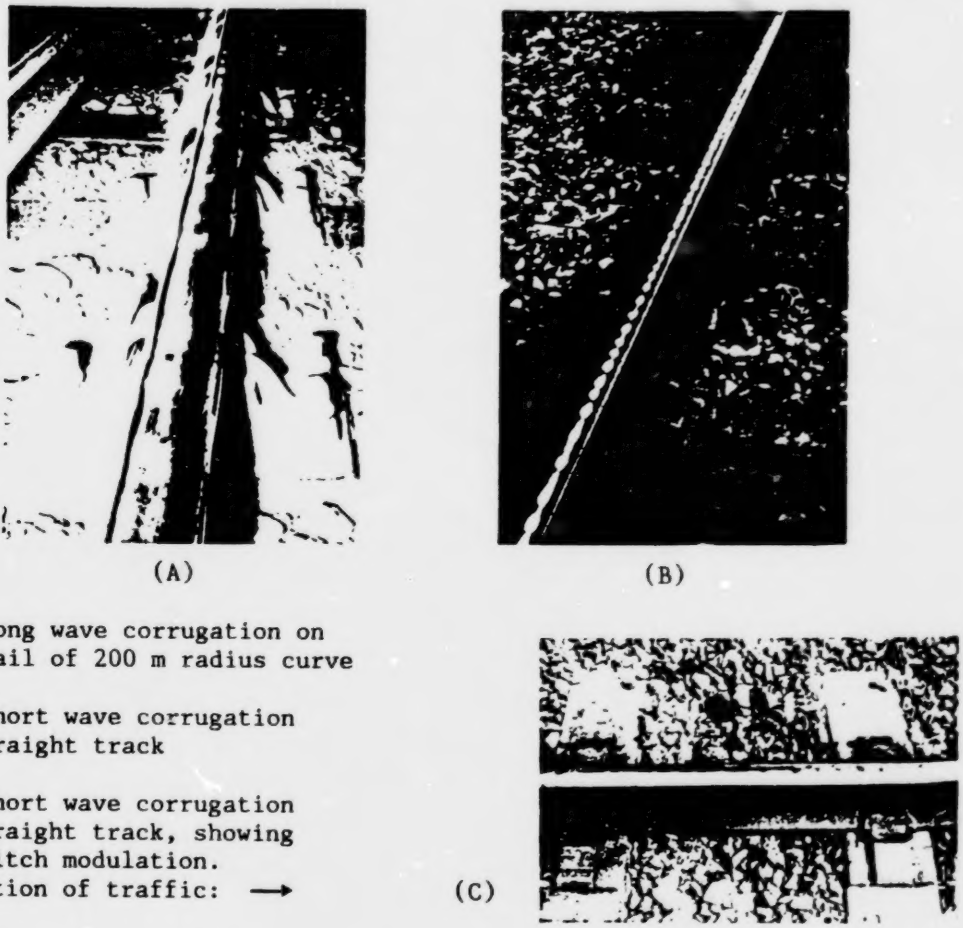

(A)

(B)

(a) Long wave corrugation on low rail of 200 m radius curve

(b) Short wave corrugation on straight track

(c) Short wave corrugation on straight track, showing tie pitch modulation. Direction of traffic: →

(C)

Source: R. Clark [12]

Figure 2.2 Various forms of rail corrugation

---

[1] i.e. rail replaced when head wear has not reached the allowable rail head loss limit

Research work supported by field tests and selected field applications has shown that increasing the yield strength and controlling the wheel/rail contact position are effective measures for reducing the plastic flow problem [13,14]. The latter is in fact one of the key strategies in the state-of-the-art rail profile grinding technique which has been successfully used to improve rail life on a number of heavy-haul railways [15,16].

2.1.4 Shatter Cracks

Shatter cracking is associated with high hydrogen content (greater than three parts per million) in the rail steel [17]. The amount of hydrogen present in rail steels is mainly a function of the manufacturing process. The alloying and other accompanying elements also influence shatter cracking. This problem is controllable by use of appropriate techniques during the manufacturing process of rail steels (Moucessian et al. [10]).

2.1.5 Summary

The various defects of rails in track have been discussed. It has been noted that defects can be associated with fatigue or wear, as well as related to plastic flow of the steel and to manufacturing process flaws such as undesirable inclusions in the steel. Techniques such as rail lubrication and rail grinding were found to have improved the service performance of rails.

2.2 Tie -- Nature of Tie Degradation/Method for Performance Evaluation and Improvement

The purpose of a tie is to distribute the wheel load to the ballast and to maintain track geometry. To meet these objectives, it must provide good control of track gauge and alignment, absorb and dissipate part of the wheel impact load, and transmit remaining forces to the track support at contact pressures below its allowable bearing strength. In most railroads, ties also provide the electrical insulation between rails for train control circuitry. Therefore, electrical insulation is also a requirement. The number of ties per unit length required to perform these tasks is affected by a number of factors, including subgrade strength, ballast quality, maximum axle load, rail weight, and track alignment.

Until the early 1940s, wooden ties were standard for North American railroad track construction, because wood was widely available and relatively inexpensive. However, growing axle loads on tracks of high curvature and gradient reduced wood tie life cycles to unacceptable levels. The expected life of a wood tie in curved track is typically less than twenty years, much less than the historical thirty to forty years. This decreasing tie life has resulted in an incremental cost of one billion dollars annually (labour, equipment and material costs) to replace ties on U.S. railroads. The decision to replace a specific tie is usually left up to an individual tie inspector who may spend, at best, a few seconds making the replacement decision.

Recent studies to improve system performance and cost control have concentrated on developing better decision-making procedures for tie replacement, and on incorporating such procedures in predictive models (Section 3.2.4). Another consideration for better system performance has been the development of concrete and steel ties, due in part to wood shortages and corresponding high prices, especially in Europe. More recently, plywood, wood composite and even plastic ties have been used for special trials or applications.

In the following sections, the findings of recent studies on the nature of wood, concrete and steel tie degradation will be described, together with the development of methods for performance evaluation and service improvement.

2.2.1 Wood Ties

In North America there are currently more than a billion wood ties in track [18], with an annual replacement rate of more than thirty million [19]. After rail costs, ties are the second most important cost item in track maintenance. Any attempt to reduce this cost must start with a better understanding of the loading environment, wood properties and failure modes of the wooden tie.

2.2.1.1 Tie loading environment

Figure 2.3 outlines the loading environment which normally applies to wood ties in service. Train traffic interacts with track conditions to create a spectrum of wheel loads. These are distributed onto the ties through the rail seats, causing tie stress. Together with climatic conditions (e.g. rain, snow, etc.), these stresses cause ties to fail, usually in the form of end splitting, plate cutting or spike kill. The weather and biological action can also cause ties to fail from decay, but this more commonly occurs concurrently with the other tie failure modes. Wheel loads are usually applied in three forms:

- **vertical load,** which has a mean component proportional to the vehicle weight and a dynamic component which varies as a function of vehicle speed and track roughness

- **lateral load,** which has a mean component related to the vehicle steady-state curving performance and a dynamic component which varies as a function of vehicle speed and random track alignment errors

- **longitudinal load,** which is normally associated with lateral load during vehicle curving. The mean component is dependent on the curving capability of the truck. A dynamic component may also exist but would be relatively small, since there is no random track roughness input to wheels in the longitudinal direction.

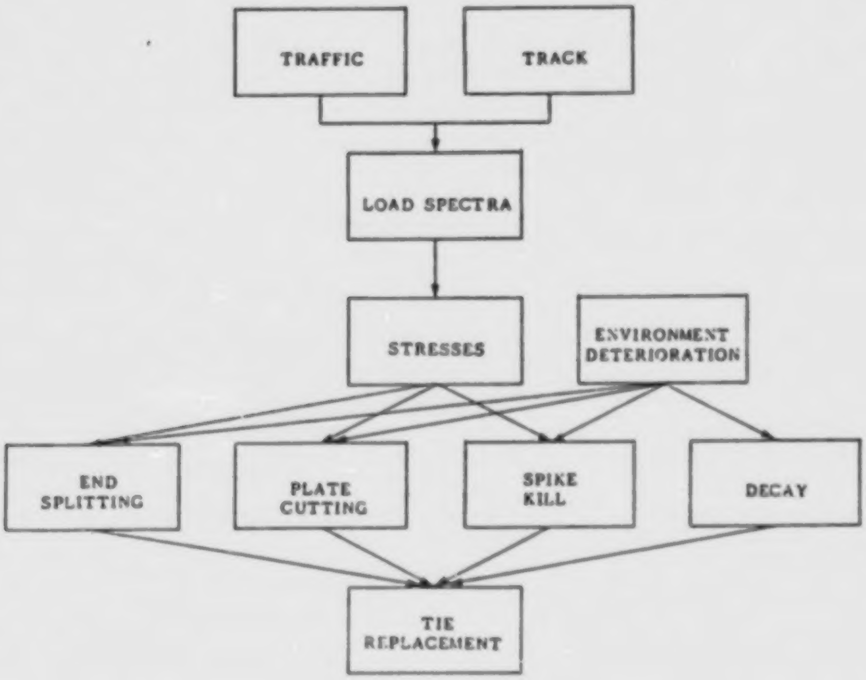
TRAFFIC
TRACK
LOAD SPECTRA
STRESSES
ENVIRONMENT DETERIORATION
END SPLITTING
PLATE CUTTING
SPIKE KILL
DECAY
TIE REPLACEMENT

Source: S.T. Lamson and B. Dowdall [18]

Figure 2.3 Tie loading environment

Each of these wheel load components must be accurately estimated to correctly differentiate the contribution of different traffic categories in a traffic mix to total tie replacement. Currently, there is no practical way to estimate these components on a large scale. Vehicle dynamic models have been constructed, but can only be applied to a very limited track length. Existing simple formulae such as the AREA formula for the dynamic input factor:

$$\varphi = 1 + 5.21\ V/D$$

where: V is vehicle speed

D is wheel diameter

may not only be inaccurate, but also useless to tie life modelling, since these formulae generally do not adequately differentiate one type of vehicle from another. The AREA formula, for example, treats 100-ton cars the same as passenger coaches if they both have the same size wheels. Other factors which are very significant to dynamic load (unsprung mass, suspension characteristics, etc.) are not included.

2.2.1.2 Wood properties

The properties of wood vary considerably, both from species to species and within each species. This variation is further compounded by various wood/tie preservation techniques (creosote, nailing plates, dowels, vapour drying, etc.). The strength of wood is dependent on its grain orientation as well as its moisture content. Being a generally tough material, it has good fatigue resistance. The endurance limit for hardwood is approximately 27 MPa (3,900 psi), which is well above typical tie plate loads. This, plus the fact that in service ties do not go through a full stress reversal cycle, indicates that fatigue fracture of wood ties is unlikely.

A number of standard testing methods are available to determine wood properties. Of these, hardness and cleavage appear to be most relevant to performance. Details of these tests, typical results, and the effect of climatic conditions are described in Appendix A of reference [18].

2.2.1.3 Failure modes

There are many different causes of tie failure. These causes can be classified, but not without some overlap. The most common modes of failure are:

- plate cutting
- splitting
- spike kill
- decay
- crushing
- derailment
- metal sickness

The reaction between the iron spike and wood (so-called "metal sickness") is not significant enough to be considered. Derailments are a unique occurrence involving more than tie deterioration. Crushing is sometimes quoted as a separate failure but is more likely linked to plate cutting. Spike kill results from the removal of rail, requiring re-spiking. There are many products on the market that can be used to fill in the old spike holes, but their success is still being assessed. Re-spiking reduces tie life as the fibres are separated and dirt and moisture can enter the non-preserved heart of the tie. The rate of rail replacement determines the amount of re-spiking. Decay is a factor that affects all ties and is time- and environment-dependent. The main causes of tie failures are, however, plate cutting and splitting.

Plate cutting is caused by the mechanical action between the tie plate and the tie, resulting in abrasion of the tie. Tie plates can move vertically, horizontally and longitudinally, depending on the dynamic load condition of a wheel cycle. In curves where the lateral force is high, an overturning moment is placed on the rail, causing increased stresses on the field end of the tie plate, thus accelerating plate cutting.

Splitting is more common on curves due to the higher lateral force. The length of time before a split appears is influenced by the spike insertion method. If a spike is driven in, the fibres are crushed and damaged, leading to an earlier split. If the hole is pre-drilled, the fibres are left in much better condition, and are able to resist splitting longer.

Splitting occurs from the spike to the end of the tie. Nailing plates and "S" irons driven into the tie ends have been used in an effort to reduce splitting. As most ties now have nailing plates, it is assumed that the split begins at the spikes under the pressure of the lateral forces which push the spike into the wood fibres like a splitting wedge.

Once the split has been initiated, other factors can influence its propagation. Water and dirt can enter the split, weakening the wood and braking down the fibre bond. This effect may also be accelerated with the introduction of fungi into the split. However, it is often not clear on the surface if splitting or decay is prevalent in the failed tie.

2.2.1.4 Data base

Any tie life calculation based on today's level of understanding of various aspects of tie behaviour must make reference to actual past experience. Data bases on ties vary from railway to railway. Usually, annual tonnage and replacement are recorded. This information, however, is not sufficient for a reliable and useful tie life prediction. The following additional information is needed:

- traffic category breakdown: tonnage, axle load, vehicle type, speed
- track category breakdown: length, geometry, environment, tie type
- tie failure breakdown: cutting, splitting, decay, etc.

Historical data on tie replacement, if available, are often affected by outside factors such as delayed replacement due to shortage of funds or accelerated replacement due to track upgrading. These factors further reduce the usefulness of the data base in model development. However, despite these data-related shortcomings, tie life models are being developed and improved as more data becomes available. One such model is described in Section 3.2.4.

2.2.2 Concrete Ties

There are currently an estimated three billion ties in service in the world, more than four hundred million of which are concrete [20]. Of the total number of ties, some 2 to 5 percent have to be removed every year. Today, concrete ties cover more than 50 percent of the annual tie demand in many parts of the world, such as in most of Europe, in the Soviet Union, in Japan, and in some African countries. In other areas, such as the United States, Canada and Australia, a much smaller proportion of concrete ties are used.

CN Rail has been a leader in the use of alternative ties in North America [21]. The premium price for concrete ties was deemed acceptable if the increasing maintenance and material expenses associated with wood ties could be eliminated. With this philosophy, CN Rail installed about 2.5 million concrete ties in British Columbia and northern Ontario between the early 1920s and the early 1980s [22], on track where curves exceed 2° and tonnage exceeds 20 million gross tons (MGT) per year [21].

The following are excerpts from a state-of-the-art report on concrete ties prepared by the FIP Commission on Prefabrication.

2.2.2.1 Types of concrete ties

Over the years, several types of concrete ties have been developed and used in track systems. Due to the nature of the dynamic loading, there are variations in the pressure distribution between the ballast and the tie. Therefore, the tie may be subjected to a wide range of bending moments, both positive and negative. This situation has led to two different design systems. In one there is one rigid concrete block under each rail and a flexible central piece made of steel between them -- the "two-block tie." In the two-block tie the rail loads will be transmitted to the track support in a well-defined way. Bending moments in the tie will be small, even if the bedding support is not quite uniform, but the relative twist and inclination of the rail seats may vary. The other system, the "monoblock tie," consists of one single rigid beam which must resist those larger moments which arise in different sections of the tie. The two main types of tie are shown in Figure 2.4.

Monoblock ties are almost exclusively prestressed (to resist the assumed dynamic bending moment distribution). They are normally pretensioned, although some post-tensioned types are also produced.

Some non-standard types of ties are also used for switches, crossings, bridges, and other special structures.

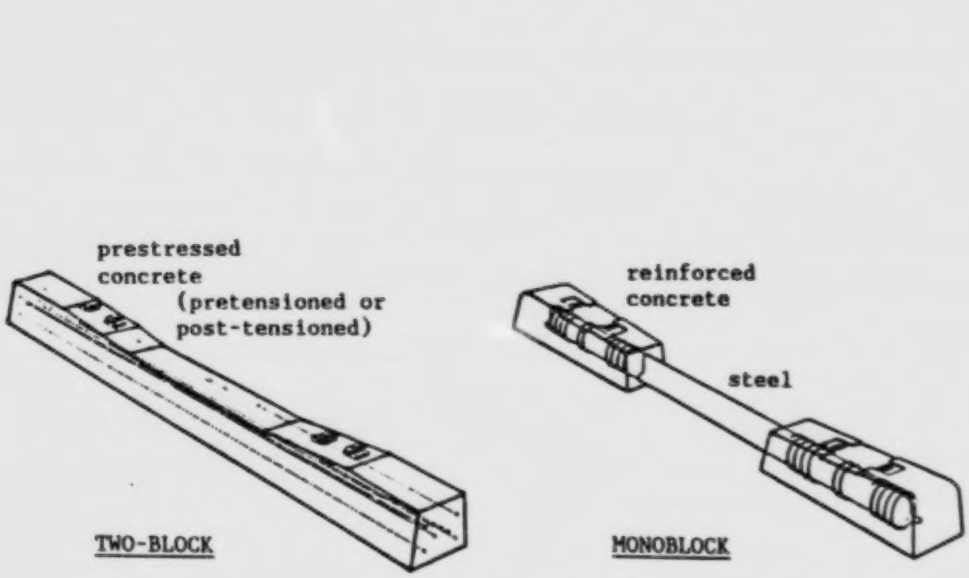

Source: J. Buekett [31]

Figure 2.4 Basic types of concrete tie

2.2.2.2 Loading conditions

Tie loading conditions on a concrete tie are essentially the same as those noted in Section 2.2.1.1. The nature of load resistance and distribution, however, is somewhat different and needs special consideration.

The loads on the tie not only depend on the axle loads and spacing, but also on the properties of the rail (primarily its vertical stiffness) and the rail fastening system (primarily its vertical elasticity).

Load peaks depend to a large degree on the condition of the rolling stock (roundness of wheels), as well as the condition of the rail joints (horizontal and vertical gaps) and rail surface conditions (spalling, shelling and corrugation).

The majority of railway authorities assume a uniform distribution of the pressure beneath the tie (at least as one loading case), allowing pressures of between 0.4 and 0.5 MPa.

However, pressure is sometimes assumed to be concentrated more towards the ends of the tie and less in the centre, because normally the centre of the tie does not (and should not) rest on the ballast.

Other pressure distributions relating to non-symmetrical axle loads, as in sharply curved track, are trapezoidal or triangular in shape.

2.2.2.3 Design Criteria

Since mass production started in the late 1940s, pretensioned concrete monoblock ties have generally had the shape of a doubly symmetrical beam with a basically trapezoidal section, often variable over the length. The underside, resting on the ballast, is usually plain, whereas the contours of the side faces and of the upper face are sometime intricate. The inclination of the rail seats normally varies from 1:40 to 1:20

towards the centre. Most tie lengths are between 2,500 and 2,600 mm (extremes 2,300/2743 mm) for standard gauge and between 2,000 and 2,200 mm for narrow gauge, respectively.

The governing requirements for concrete monoblock tie dimensions are essentially as follows:

(a) The area of the underside must be such that the average contact pressure under full load does not exceed a certain value, normally 0.4 to 0.5 MPa.

(b) The end faces should preferably be of a size and shape to provide maximum resistance to lateral movement.

(c) Since the prestressing tendons are parallel to the bottom surface, the cross-section can be varied so that the geometry of a particular section may be used to provide prestress eccentricity to best match the bending moments, positive or negative, experienced at that point. Usually positive rail seat bending moments are the maximum, although negative centre bending moments may be even higher for broad-gauge ties. Consequently, the typical shape of the tie body is tapered from both ends to the centre in height and sometimes width, with gentle changes of the sectional profile used to prevent stress concentrations.

In concrete tie design, consideration should be given to tie service and behaviour and fatigue resistance, and in certain cases to ultimate failure.

The service stage. The loading of the tie does not depend on the wheel or axle loads of the rolling stock alone, but on a variety of factors representing the complex elastic rail/fastening/tie/ballast system as well as the dynamics of the loading. However, it is difficult to accurately quantify the various influences, and, as a consequence, the design parameters are usually based on assumed safety factors resulting from long-term experience.

The loading case which determines the tie design is defined as the maximum wheel load acting directly above the tie with some modifying factors, namely:

- an impact factor to account for the dynamic loading (due to anomalies of rolling stock and/or rails), including fastening and ballast attenuation effects

- a distribution factor to account for the vertical stiffness of the rail.

Under this loading, a prestressed concrete monoblock tie should not crack, even under an almost unlimited number of cycles between zero and full load.

However, many railways have found cracks due to severe overloads occurring, if infrequently, during the life of the tie. These cracks need not result in reduced service life as long as full prestress is maintained at the rail seat by a reliable tendon bond-transfer or anchorage system.

As a rule, the most critical bending moment along the tie-body occurs at the rail seat under maximum wheel load, causing tensile stresses at the underside. Those positive and negative bending moments which occur in other sections of the tie are usually of less importance. Therefore, the design and degree of prestressing is primarily dictated by the conditions at the rail seat.

The most important parameters that have an effect on the rail-seat bending moment are as follows:

- maximum static axle loads (symmetrical) and wheel loads (non-symmetrical due to curves), respectively
- impact effects due to condition of rolling stock and rails
- maximum train speed
- maximum track radius
- tie length
- bearing conditions of tie on ballast, especially in the centre part
- relative stiffness of rail/tie/ballast
- elastic properties of rail fastening system
- tie spacing
- axle spacing.

Fatigue. As railway ties are by definition subjected to cyclic loading during their entire lifetime, special care must be taken with regard to the fatigue resistance of all materials involved, including that of the prestressing steel. This is why a crack-free tie body under dynamic axle loading is desirable, because cracks in the concrete due to bending moments lead to a large increase of the stress range of the prestressing steel, which in turn could cause a fatigue failure.

As long as all sections of the tie body remain homogeneous (i.e. crack-free) there normally is no risk of a fatigue failure of the prestressing steel. If cracking were to occur, however, the fatigue resistance could be critical. It is noteworthy that a high-quality prestressing wire or strand is apt to withstand a stress variation of only 5 to 10 percent of its ultimate tensile strength [24].

For these reasons, most railway authorities are conservative in allowing concrete tensile stresses as the basis for the moment capacities and a few authorities even exclude any tensile stresses.

Ultimate failure. Ultimate failure moments are occasionally specified, and then most often for the rail seat only. In the few cases where reliable figures could be obtained, the failure moment is between 1.4 and 2.6 times the corresponding bending moment capacity. If possible, the failure mode should not be brittle, i.e. the compressive strength of the concrete should allow the prestressing steel to elongate well into the plastic range before the ultimate capacity is reached.

2.2.2.4 Other Demands

Some of the other demands on the concrete tie are electrical isolation and durability.

Most concrete ties are used in electrically controlled signal territory. It is necessary to provide insulation between the rails and the ties. This is usually accomplished by means of plastic insulators inserted between the spring clips and the rail (Pandrol), insulating plastic screw inserts (MH), or insulated pins (FIST). In all cases, the pad placed under the rail must also provide electrical isolation. A typical value for signal insulation is the requirement of a minimum impedance of 20,000 ohms per tie when ac energy of 10 volts, 60 Hertz is applied to the rail fastening assembly.

The concrete used for the manufacture of prestressed concrete ties is, of necessity, high quality and therefore can generally be expected to be durable. In cold climates where concrete ties would be exposed to freeze/thaw conditions, the use of air entrainment (3 to 4 percent) can greatly improve durability.

2.2.2.5 Rail Fastening Systems

The purpose of a rail fastening system is to accurately maintain the position of the rail on the tie and to transmit the forces exerted on the rail by the passage of a vehicle onto the tie. These forces are primarily those from the action of the vehicle on the rail, although environmental conditions (e.g. temperature) also have an influence. As well as its primary load-carrying role, the system has important requirements from the point of view of installation and maintenance and other operating requirements of the railway.

The following demands are placed on a fastening system:

(a) The system must hold the rails to the correct gauge and inclination.

(b) The system must safely transmit the rail forces to the tie. These include vertical axle loads, side forces and longitudinal creep.

(c) The system must attenuate the shock loads to prevent the tie from suffering vibration impact or abrasion damage. The system must not suffer from wear due to attrition.

(d) The fastening must have sufficient elasticity and fatigue resistance to give a good service life.

(e) Installation and maintenance costs should be minimized; the system must be easily installed using either manual or mechanized techniques.

(f) Electrical insulation must be good so that track circuits may be used if desired.

(g) The components must be inexpensive and should be easily and inexpensively replaceable. If not, then they should have a durability equal to the life of the tie (e.g. cast-in components).

(h) The components must be designed so that they do not put expensive constraints on the tie design and production methods.

(i) The system should be vandal-proof.

Fastenings are of two main types: rigid and elastic. Rigid systems are expensive and do not have the required resilience when used with concrete ties. They have been superseded by the newer, elastic fastening systems which fall broadly into three main groups:
6f

- sprung spikes
- screw systems
- clip systems.

A description of the various systems is beyond the scope of this report, but was dealt with in some detail by Dixon et al. [65].

2.2.2.6 Rail Pads

The rail pad has an important role to play in attenuating impact loads from bad joints, track irregularities and faults in rolling stock. The pads should stay in place and not work out in use and should not degrade in normal use.

Pads are made typically of rubber, rubber-bonded cork, high-density polyethylene (HDPE), polyurethane and ethyl vinyl acetate (EVA). Pad thicknesses vary between 5 and 10 mm normally. Pad stiffnesses are typically in the range 100 to 600 x 10^3 N/mm^2.

On heavy-haul railroads the elastic behaviour of the pad is of less significance than for track where the speed exceeds 100 km/h. Therefore, durability is the overriding requirement and plastic materials such as EVA are used. Because HDPE becomes brittle at low temperatures, it is not suitable for use where freezing conditions occur.

On higher-speed tracks, profiled Neoprene or SBR rubber pads are most widely used. Recent research has shown that a pad thicker than the normal 5 mm will provide better attenuation of the impact loads included by rail head and wheel defects. In France, 9 mm pads are in use for high-speed lines.

However, many soft pads are less durable than harder alternatives. In most cases, the softer and sometimes thicker pad permits greater deflection of the elastic rail clips. This places the clips in a more severe fatigue environment and may reduce long-term toe load, which in turn reduces the longitudinal resistance of the fastener system.

This conflict between requirements for low stiffness versus durability and longitudinal restraint is one of the principal challenges facing the fastener supplier.

A detailed evaluation of a number of pads and insulators for use on concrete ties is given in reference 25.

2.2.3 Steel Ties

Railway ties made of steel have been used for more than a century [26] but generally not on railways operating with high axle loads. Three specific problems have hindered acceptance of steel ties. These problems are as follows:

- wear of the rail fastener and rail seat
- difficulties in tamping
- incompatibility with use of track circuits.

More recent developments in tamping equipment and fastener systems, together with shortages of good timber in certain parts of the world, have prompted the consideration of steel ties. However, the future use of steel ties, especially in heavy-haul track, is rather uncertain.

North American railways have been reluctant to use steel ties. Where alternatives to wood ties have been necessary or desirable, concrete ties have been the obvious choice. The Australian heavy-haul railways are currently experimenting with steel ties. Their decisions on future use of steel ties could be an important factor in the future of the steel tie.

In the following sections some of the requirements and considerations in the design of steel ties are described.

2.2.3.1 Design of the tie section

Several types of steel tie have been developed (e.g. the "I" beam and pot types) but most modern steel ties have a cross-section of inverted trough shape, as shown in Figure 2.5 [26], which permits efficient use of material and provides for mating between the tie and ballast structure. There are two fundamentally different types of trough tie: namely, those of uniform wall thickness and those with cross-sectional shape comprising a thick "top," thin "legs" and bulbous "toes" (Figure 2.5). The former is manufactured by pressing flat skelp and the latter either by pressing a profile section or by hot-rolling the final shape. The latter method permits more nearly optimum use of material and is particularly suited to heavy ties, where the cost saving in material outweighs the saving due to simplicity of the other method of manufacture.

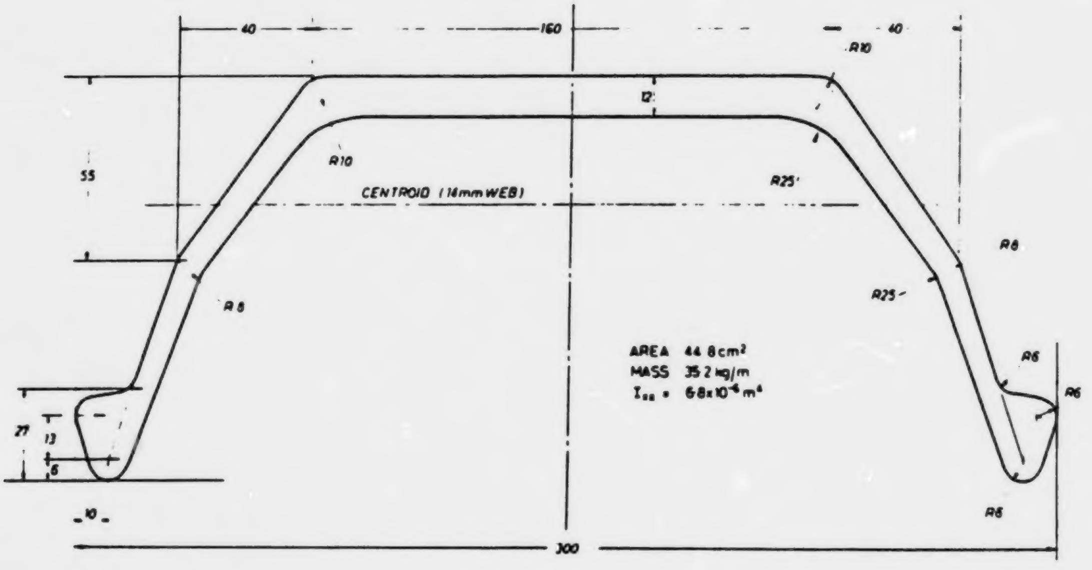

Source: Brown and Skinner [26]

Figure 2.5 BHP heavy axle load tie

The life of a steel tie is dependent principally on its fatigue performance and this may be characterized by the performance of that part of the tie which is most susceptible to fatigue damage -- namely the rail fastener.

Rail fasteners suitable for steel ties comprise two categories: those with a rail base plate and those without. The former type is usually attached to the tie by welding and the latter either by welding or by notches and tunnels pressed in the tie (see Section 2.2.3.2). The use of high-performance bolts is not favoured due to the relatively higher cost of the bolt compared to an equivalent weld.

The procedure for designing a steel tie was outlined by Brown and Skinner as follows:

(1) establish maximum permissible working stress by considering the tie versus a welded beam

(2) compute the permissible maximum stress using loading history

(3) use beam-on-elastic-foundation analysis to establish moment of inertia

(4) establish cross-sectional shape

(5) compare results with other ties of known performance

(6) finalize rail fastener, mode of cant and insulation.

The initial aim is to establish the necessary section properties of the tie with due consideration to the following points.

For steel ties in heavy haul railways, the failure criterion is usually fatigue rather than static overload. The number of fatigue cycles which the tie must withstand (i.e. number of passing axles) is determined using the known traffic conditions on the track. In assessing the cumulative fatigue damage to the tie [27], the loading history on the tie must be considered, because the load range exerted by passing axles will differ, depending on the spacings of the axles, trucks and ties. It should be noted that it is the range of load which causes fatigue damage, not the absolute value, when considering welded connections which have high tensile residual stress. After establishing the load range, the required section properties (area and moment of inertia) of the tie may be calculated using a method such as beam-on-elastic-foundation theory.

Having established a moment of inertia value, the shape of the tie can then be selected. In determining the shape, the following factors must be considered:

- mass (cost) should be minimized but must be consistent with strength requirements

- the contact area should be maximized to reduce ballast pressure and consequent degradation and track deformation [28]

- the depth should not exceed that above which it is difficult to ballast the tie.

The above factors are interrelated such that:

- reduction of mass by reducing tie width causes least reduction in the amount of inertia, but increases the number of ties required per kilometre

- thinning the web (say concavely) reduces the moment of inertia significantly

- thinning the toe and/or reducing the overall height lowers the moment of inertia very significantly.

This interrelationship makes the optimization of the steel tie section rather difficult.

Other factors affecting the design of steel ties are loss of mass due to corrosion (estimated to be 15 percent over 50 years in a dry, open environment) and the effect of centre-binding (less likely in trough-shaped ties than flat-bottomed ones). Provision of lateral stability of trough-shaped ties is provided by fixtures at each end. Some of the fixtures are in the form of a welded plate, a lanced flap, a pressed spade, and so on. Laboratory and cost evaluations have shown that ties with the pressed spade end perform best [29].

2.2.3.2 Rail fastening systems and pads

The general requirements and types of fastening systems and selection of a suitable pad (geometry, material and insulating characteristics) are similar to those for the concrete tie and are not elaborated here (see Sections 2.2.2.5 and 2.2.2.6).

2.2.4 Comparative Performance of Wood, Concrete and Steel Ties

In an assessment of steel railway ties, Driscoll and Lamson [30] discussed the ability of wood, concrete and steel ties to meet the various requirements imposed on them for good track performance. Their findings are summarized below.

2.2.4.1 Track gauge

Track gauge widening under train traffic is one of the major maintenance problems in curves [31,32]. It is well known that superior gauge control is one of the major advantages used to justify concrete ties. In this respect, steel ties offer the same performance as concrete ties.

Total dynamic gauge widening in wood tie track is due to lateral rail bending, worn spike holes, worn rail and worn wheels. The first two factors are related to tie performance.

Concrete and steel ties provide far better gauge control. This improvement is due to the precise manufacturing tolerances and the positive fasteners which are typically employed. If wood ties were converted to use elastic fasteners (e.g. Pandrol, Trakloc models), the performance disparity would be much reduced.

It should be further noted that the abrasive wear of the insulated shoulder pads on concrete and steel ties (about one-quarter inch thick) has been found to cause about one-quarter inch gauge widening.

2.2.4.2 Track alignment

The ability of track to maintain proper alignment under load depends on the resistance of the (rail + tie) structure to vertical, lateral and longitudinal movement. Weight, surface area and shape of tie, as well as the torsional resistance of the fastener, all influence this problem.

Wood ties have low weight, low drag (simple square shape), and a small area of contact with the ballast. The conventional cut spike arrangement provides little torsional resistance. Consequently, wood ties have the lowest lateral resistance and can sustain the least temperature increase before buckling. Concrete ties are about three times heavier and have more ballast contact area, and hence have more alignment holding capability. Steel ties weigh approximately the same as wood ties (about 200 lb) but have a larger ballast contact area and a better drag shape. As a result, they have at least as good, if not slightly better, alignment control capabilities as concrete ties. Steel ties installed in a 12 degree curve on a trial basis by BC Rail have resulted in very satisfactory alignment retention.

2.2.4.3 Impact forces

It is well known that concrete-tie track gives rise to higher peak impact loads than wood-tie track. The high impact force in concrete-tie track is attributable to its high mass and stiffness. Wood and steel ties do not have this problem, their responses to impact loading being of the same order of magnitude.

Table 2.1 shows typical impact forces from a 100-ton hopper car travelling at 60 mph, as calculated by Driscoll and Lamson [30] using British Rail's P_1 and P_2 impact force equations. P_1 is a high-frequency impact force affecting track support (i.e. ballast and subgrade) and P_2 is a low-frequency impact force. The equations allow for common wheel/rail surface irregularities such as dipped rail joints and flat wheels.

TABLE 2.1

IMPACT FORCES FROM A 100-TON HOPPER CAR AT 60 MPH

	WT (lb)	U (lb/in/in)	M1 (lb-sec^2 /in.)	M2 (lb-sec^2 /in.)	P_1 (lb)	P_2 (lb)
hardwood	210	2,500	0.67	3.37	61,370	36,100
steel	220	3,500*	0.62§	2.97	60,300	37,170
concrete	615	15,000	1.42	3.45	71,600	40,080

* estimated
§ lower track mass due to wider tie spacing

The other parameters in the table represent the following:

WT = tie weight (lb)

U = track module (lb/in./in.)

M_1 = effective mass of rail and tie (lb-sec^2/in.)

M_2 = effective track mass (lb-sec^2/in.)

In a recent CN field test, Scott [33] found that the impact by flat wheels on concrete-tie track could be as high as 125 kips at 60 mph.

2.2.4.4 Track settlement

Concrete ties, due to their high weight and stiffness, give rise to significantly higher impact forces than steel and wood ties. This would partially offset the benefit of larger tie width (compared to wood ties). Steel ties, however, do not have the high weight and stiffness problem, and hence should provide an improvement in track settlement.

Track settlement leads to track geometry errors which require maintenance. There has been concern that steel ties would be difficult to tamp due to their trough shape. This could be a temporary problem as it takes time to adjust equipment and procedures to maintain steel ties. It is worth noting that the heavy-haul railroads which have recently used steel ties (Mount Newman Mining, the Quebec North Shore and Labrador Railway (QNS&L), British Columbia (BC) Rail) have not reported any major problems with tamping. It is important during installation to rework the ballast to remove the selective consolidation of the ballast resulting from previous tie spacing.

2.2.4.5 Electrical insulation

Rails are used as a conductor for train control circuitry. Left and right rails must be insulated from each other. Wood has a natural insulating property, and hence has been very satisfactory in this respect.

Concrete ties, when wet, create some conductivity. This is, however, very effectively controlled with a simple insulation pad arrangement (a polymer pad under the rail seat and two polymer pads on the rail base/clip shoulder portion).

Steel ties have a potential problem because the insulation pad must provide all the insulation. BHP has designed and tested a pad which has proven to be satisfactory in Australia's semi-arid climate. Figure 2.6 shows test results [34] which indicate that the insulation property of steel ties (with insulating pads) is comparable to that of wood ties during and after a rainfall.

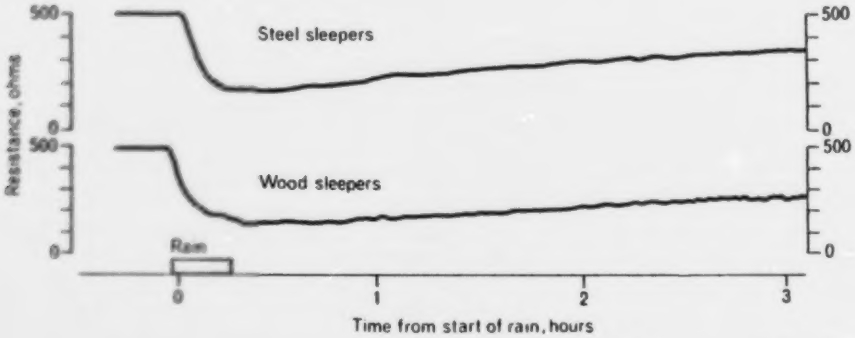

Source: J.H. Brown [34]

Figure 2.6 Rail insulation on steel and timber tie track: before, during and after a rain storm

The Mount Newman Mining Railway in Australia has been operating steel-tie track since 1980 without any significant problems. In the Canadian climate, however, which is more humid and includes a long period of wet snow and ice, there is a potential problem with steel ties. However, the QNS&L Railway has not reported any problems. Their insulation is on one side only, alternating sides at every tie.

2.2.4.6 Corrosion

A major concern with regard to steel ties is corrosion. Corrosion can lead to wear and fatigue of ties, especially at the fastener connections. While it is quite simple to provide extra section thickness to compensate for the accumulation of corrosion in the expected long tie life span (about fifty years), it is much more difficult to prevent corrosion-led fatigue. The problem is more significant in areas with highly acidic rainfalls. For North American application, this is the second factor which has deterred the railroads' interest in steel ties. Careful design of fastener attachments, to avoid stress concentration as a consequence of corrosion, is necessary.

2.2.5 Tie Usage in North America

Past tie purchases for U.S. and Canadian railroads illustrate the dominant position of wood ties. "Other" ties have been principally concrete (CN Rail in Canada and Amtrak routes in the U.S.). CN's concrete tie installations have been in higher curvature and tonnage track. Amtrak's objectives in using concrete ties are to achieve higher running speeds and a more comfortable ride for its passenger operations. In 1982, premium tie usage for Canada and the U.S. was a mere two percent of total tie requirements.

If it is assumed that the U.S. railroads and CP Rail will follow CN's lead in the same proportion, then there is a potential premium tie market of over four million ties per year (premium tie market share approximately 18 percent of total tie replacements) [30].

The QNS&L Railway has had the longest experience with steel ties in heavy-haul service in Canada. They have 590 special heavy section, nine foot long Kawasaki ties in a 7.5 degree curve. The railway installed Pandrol E and True Temper fasteners using welded shoulders. Both the shoulders and the fasteners had problems related to failure under extreme cold and loading, which have been corrected. The steel ties, once set in alignment with three tamping passes, have maintained good surface and alignment.

CP Rail is skeptical about the ability of steel ties to maintain surface and alignment sufficiently to justify their use. In CP's opinion, comparative data on track moduli for steel versus wood and steel versus concrete is needed to objectively weigh the long-term effects of steel tie usage.

BC Rail is also active in the use of premium ties on a trial basis. They have had satisfactory results with the installation of 500 Omark (BHP design) steel ties in a 12 degree curve on the Squamish line.

2.2.6 Summary

A review of wood, concrete and steel ties has indicated the dominant use of wood ties by North American railways. Although concrete and steel ties have been and are being used both as a supplement to wood ties and in special cases (mainly on an experimental basis in the case of steel ties), it will be a long time before wood ties are replaced by concrete or steel ties in any significant numbers. Therefore, development of efficient data bases and computer models is essential for proper management of tie replacement policies. Such an approach has been used to develop the Tie Life Model which is described in Section 3.2.4.

2.3 The Track Support System (Ballast, Sub-ballast and Subgrade)

This section of the report deals with the behaviour under load of the granular materials which form the engineered track support (the ballast and sub-ballast) and of the underlying surficial materials (the subgrade).

Figure 2.7 shows a schematic cross-section of a typical ballasted railway track, consisting of (from top to bottom) a ballast layer enveloping the ties, a layer of sub-ballast, and, finally, the subgrade. The upper layer, and ideally the sub-ballast, are of selected granular materials. The subgrade may be the naturally occurring surficial material, fill material from a point closely adjacent to the track, or, in the case of recently constructed lines, selected superior material brought in from some distance.

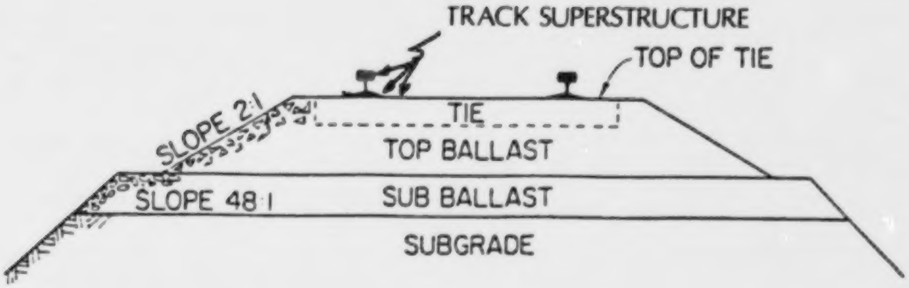

Figure 2.7 Typical cross-section, conventional railway ballasted track structure

The ballast layer, which is typically made up of coarsely-graded selected crushed rock or base-metal slag, serves two principal purposes:

- it provides resilient, free-draining vertical, lateral and longitudinal support for the track superstructure so as to retain the desired alignment and facilitate subsequent maintenance
- it attenuates and distributes the forces imposed by the movement of traffic so as to keep unit area loadings at the ballast/sub-ballast and especially at the sub-ballast/subgrade interfaces within the bearing strength limits of these materials under "worst case" conditions.

The current use of selected crushed-rock ballast contrasts with the practices prevalent during the peak periods of railway construction in the latter 19th and early 20th centuries. Cinders, steel-making slag, and various pit-run sand and gravel mixes were used, depending on what was readily available and cheapest. In most cases, these original inferior materials were never removed, but simply covered over with better ballast during later maintenance and upgrading activities.

The sub-ballast layer, which in modern construction consists of more finely graded, free-draining granular materials such as coarse sand, acts as a filter to control the upward migration of subgrade particles into the ballast. A proper sub-ballast also provides some additional attenuation and distribution of imposed loads. However, as noted above, most track was originally constructed to lower standards and does not incorporate a distinct sub-ballast layer. The granular material adjacent to the subgrade surface is usually the original ballast in a badly fouled condition, with attendant poor drainage characteristics.

The subgrade is the effective "foundation" on which the track is built. With occasional local exceptions, the subgrade for track built prior to the 1940s consists of the original surficial material, or of pit-run fill taken from sites immediately adjacent to or within the right-of-way. Consequently, the engineering properties of subgrade materials may vary widely at different points along a given route, and can change quite dramatically in a matter of a few metres. Recent construction practices stress removal or stabilization of structurally weak subgrade materials, sometimes to a considerable depth. However, the length of track so constructed remains a small proportion of the total track operated.

2.3.1 Track Support Degradation Mechanisms

For ballasted track to perform satisfactorily, the track support system must keep the development and growth of track geometry errors to within acceptable limits.[2] These errors arise through two degradation mechanisms which affect the track support system:

- the settlement of the support system
- the breakdown and subsequent fouling of (primarily) the ballast layer.

Both mechanisms are driven largely by the repeated loadings imposed on the support system through the rails and ties by the movement of traffic over the track. However, the latter mechanism is also affected by physical and chemical weathering processes unrelated to the traffic history of the track.

---

[2] The development, measurement and maintenance to control these errors is discussed in greater depth in Section 3.2.5.3 of this report.

2.3.1.1 Track support settlement

The nature, rate and magnitude of track support settlement is affected by a number of factors, including subgrade strength and stability, the design and construction standards of the original track, the traffic and maintenance histories of the track, the depth and quality of granular materials above the subgrade surface, and the quality of support system drainage.

Track support settlement can take two forms. The first, uniform settlement, results from compaction of the granular materials and/or the plastic deformation of the subgrade in a consistent fashion over extended distances. This will not in itself give rise to track geometry defects, provided that the support section remains free-draining. However, deformations of even a few millimeters are sufficient to cause ponding, and can result in the saturation and softening of poorly draining subgrade materials. These small-scale deformations will occur even with well-designed and constructed track on good-quality subgrades, regardless of the degree of subgrade compaction prior to construction. The necessity of maintaining good drainage throughout the support section, including the subgrade, cannot be overemphasized, and must form the cornerstone of both track design and track maintenance and rehabilitation efforts [35].

Because both the track support system and the imposed loading history usually vary substantially over relatively short distances, the more typical form of track settlement is differential settlement. This type of settlement, which results in the development and growth of track geometry errors, can arise from a number of sources, both current and historical, and has major implications both for track design and construction and track maintenance practices.

For the design and construction of new track, the key considerations with respect to the track support system are:

- preservation or creation of stable subgrade conditions

- separation of the ballast and subgrade layers to prevent the upward migration of subgrade fines into the ballast

- specification of free-draining ballast materials resistent to wear and weathering breakdown

- establishment and preservation of good drainage.

The first consideration entails calculation of the maximum subgrade stresses associated with the design load of the track, and subsequent selection of a sufficient depth of granular cover to keep these stresses below the safe bearing stress of the subgrade. A number of different approaches to estimation of ballast and subgrade stresses have been developed and used over the years, with varying degrees of acceptance and success. These techniques range from simple empirical models to (most recently) detailed, computationally demanding finite element models [36-38]. The manual of the AREA lists two empirical and two theoretical design equations. The empirical equations are those of Talbot (1919) and the JNR. The latter equation was developed for narrow-gauge track; JNR clearly states that it should not be used in the design of standard-gauge track. The theoretical equations are the point load equation of Boussinesq, with the rail seat load taken as the point load, and Love's integration of the Boussinesq equation for a circular loaded area. The loaded area is taken to be equal to an empirically estimated effective tie bearing area under one rail seat.

However, Talbot defined the intensity of pressure between ballast and tie as the average pressure over the entire tie-bearing area. The AREA equation has been modified to use a significantly reduced bearing area. This has the effect of increasing the nominal intensity of pressure per unit area, resulting in a conservative design standard.

Talbot's original work (1919) demonstrated that the theory of a continuous beam-on-elastic-foundation (BOEF) (or, more correctly, a linear spring [Winkler] foundation) gave calculated bending moments for the rails close to those measured in freshly tamped track. The validity of this theory has since been confirmed by many investigators, including the Association of American Railways (AAR). The American Railway Engineering Association (AREA), in their Manual for Railway Engineering, also endorse this approach as producing results "within the acceptable limits of accuracy" [39].

This design method results in the representative differential equation for the elastic beam (rail) subject to a vertical (wheel) load, P, of:

$$EI \frac{d^4z}{dx^4} + Uz = 0$$

where: E is the elastic modulus of the beam

I is the second moment of area of the beam

z is the deflection at a point x from the applied load

x is the distance along the beam from the point of application of the load

U is the modulus of the elastic support commonly known as the track modulus. (Note that the track modulus as used in common practice and in the AREA Manual relates to a single rail.)

For a single wheel load, P, on an infinitely long beam, the solutions to this equation are well known and are:

$$z_x = \frac{\beta P}{2U} (\cos \beta x + \sin \beta x) \exp(-\beta x)$$

$$M_x = \frac{P}{4\beta} (\cos \beta x - \sin \beta x) \exp(-\beta x) \qquad (3)$$

where $\beta = [U/(4EI)]^{0.25}$

The maximum values of z and M are directly below the load at x = 0.

$$z_o = \beta P/(2U)$$

$$M_o = P/(4\beta)$$

Alternatively, but less commonly, a deformation wave length of $2\pi/\beta$ is used. From the above equations, the rail seat loads are commonly calculated as:

$$Q_x = z_x US = \frac{1}{2} \beta SP (\cos\beta x + \sin\beta x) \exp(-\beta x)$$

where S is the crosstie spacing. For a crosstie placed directly below the load (x = 0):

$$Q_o = \beta SP/2$$

Since the BOEF theory is based on elastic response, the theorem of superposition applies, and the effect of multiple wheels or axles can be simply calculated:

$$z_j = \Sigma z_x$$

$$M_j = \Sigma M_x$$

$$Q_j = \Sigma Q_x$$

where the different values of x are the distances of each wheel load from the position point j.

The rail seat load produced by multiple axles (Q_j), as calculated above, can then be used to calculate the tie bearing pressure and subgrade stress. Therefore, it is reasonable to assume that below each seat there is a rectangular area of crosstie which transmits the rail seat load to the ballast. This permits the use of the solutions developed by Love (1928), who extended Boussinesq's solution to a loaded rectangular area. The AREA Manual specifies that the area of the crosstie bearing surface for each rail seat, A_b, may be calculated according to:

$$A_b = b(\ell - \ell_r) \{ 1 - \frac{C(\ell - \ell_r)}{t^{0.75}} \}$$

where: b = width of crosstie

ℓ = length of crosstie

ℓ_r = distance centre to centre between rails

t = thickness of crosstie

C = constant = 0.04 (0.018) if dimensions are in millimeters (inches). (Note constant is dependent on units.)

An alternative approach is to assume that the area is proportional to the distance either side of the rail which is affected by mechanized tamping. The AREA method results in rail seat bearing areas the width of the crosstie and a length determined by the formulate for A_b.

This "length" value is 879 mm (34.6 inches) for a 178 mm (7 inch) deep by 2.55 m (8 foot 6 inch) long crosstie, and 975 mm (38.4 inches) for a 178 mm (7 inch) deep by 2.70 m (9 foot 0 inch) long crosstie. For the latter approach, the bearing length of each rail seat has been taken to be 914 mm (36 inches). This is considered the approximate distance influenced by the tamper tines.

Figure 2.8 shows the underlying maximum vertical support stress resulting from a single axle load on 68 kg/m (136 lb/yd) rail and 279 mm (11 inch) crossties spaced at 610 mm (24 inch) centres for different values of track modulus. The contact pressure or vertical stress at zero depth for a single axle load increases as the fourth root of the track modulus (i.e. an increase of track modulus by a factor of sixteen doubles the contact stress). The difference in vertical stress decreases rather slowly with depth, so that even 0.8 metres (32 inches) below the rail seat, the effect of track modulus variation on subgrade stress from the single axle is considerable.

Figure 2.9 shows the results of similar calculations, using the same cross tie size and spacing, for two coupled G75 trucks with uniform 294 kN (33 ton) axle loads. At lower values of track modulus, the interaction between axle loads is sufficient to cause a considerable increase in the contact pressure or vertical stress at zero depth. This has the effect of making maximum contact pressure and maximum subgrade stress less sensitive to variations in track modulus. For the two highest values of track modulus, the interaction effects actually reduce the maximum value of contact pressure/subgrade stress from those calculated for a single axle.

With respect to dynamic increments, Kenney (1954) has shown that for a beam-on-elastic-foundation perfect track transversed by perfect wheels, the dynamic component of track force rises very slowly with speed, reaching resonance with standard track construction around 1,600 km per hour.

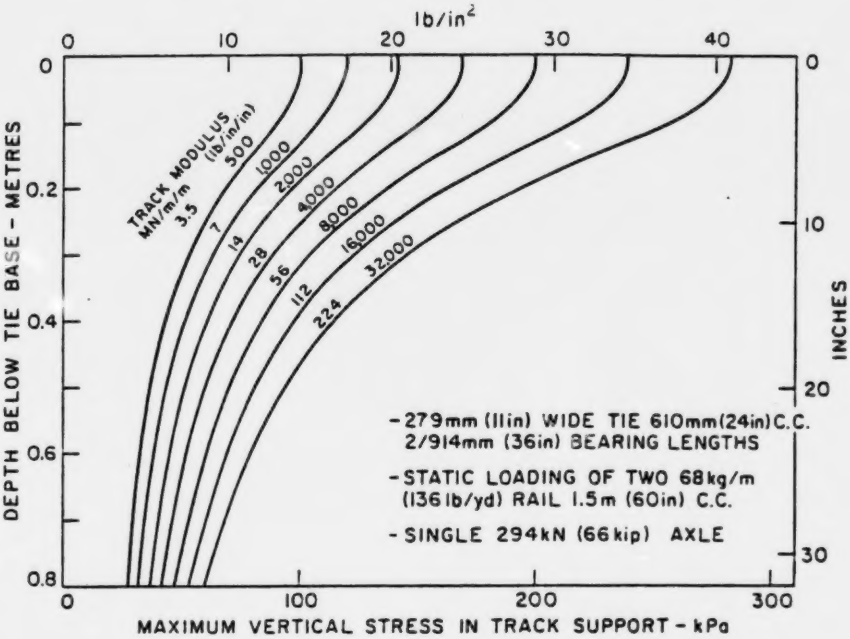

Figure 2.8 Effect of track modulus variation on maximum vertical stress in track support resulting from a single static axle load

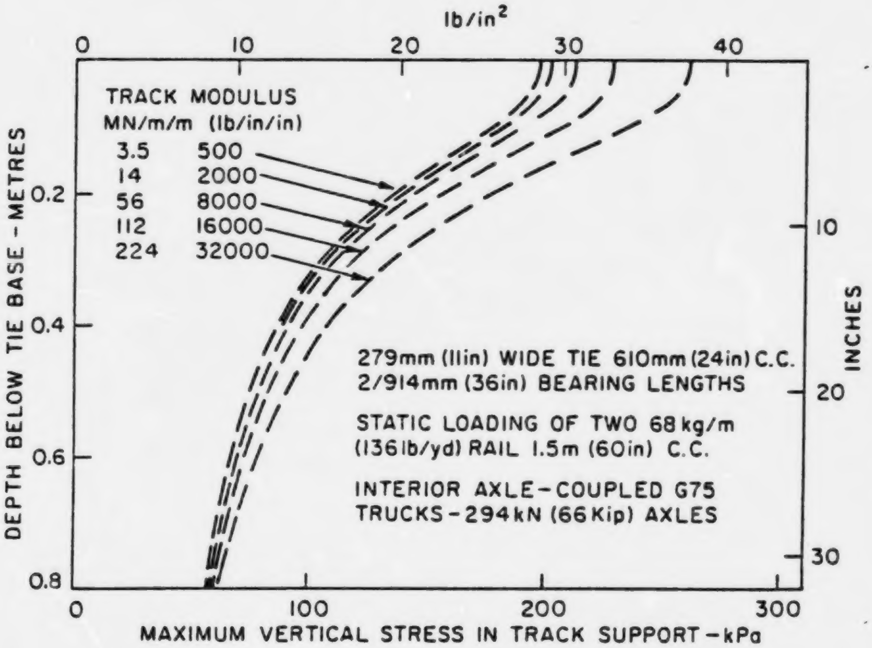

Figure 2.9 Effect of track modulus variation on maximum vertical stress in track support resulting from two coupled G-75 trucks

However, since track is a relatively loose assemblage of rail, fasteners, ties, ballast, sub-ballast and subgrade, resonance could occur within any one of these components. Such resonance has not been recorded on well-designed and maintained track up to speeds of 300 km/h. Within the limitations of Kenney's solution, track and/or wheel irregularities are the principal causes of significant dynamic track forces under current operating practices.

Theories dealing with such irregularities are complex. However, by separating the various interacting forces into a steady-state component and a dynamic component, useful equations have been developed. These equations are described in Section 3, where they are incorporated into computer models for analysis of the track structure.

Once the rail seat loads have been obtained, the stress below each rail seat may be simply calculated by assuming a uniform contact pressure over an area equal to the crosstie width times the rail seat bearing length.

The stress at any depth below a given surface point can then be calculated, using solutions developed by Love (1928) for the stresses below a loaded rectangular area, as the sum of all the contributions from each and every rail seat load. For standard gauge track, the nominal centreline separation of the rails is taken to be 1500 mm.

It is critical that the imposed subgrade stresses or loads not exceed the bearing capacity of the subgrade material under "worst case" conditions (maximum static plus dynamic load imposed on a saturated subgrade). Work carried out by Heath et al. [40] for British Rail clearly established that for cohesive soils (which are typical of natural subgrades), there is a threshold level of stress, above which repeated applications of load cause large permanent deformations, and below which permanent deformations are small and self-limiting.

British Rail developed a method of track foundation design based on this work, in which the depth of granular material required to prevent excessive subgrade loading could be predicted from laboratory repeated-load testing and the forecast traffic loading for the line. This approach was subsequently validated by field measurements at a number of BR sites, and by the work of Sheeran et al. at McGill University [41]. However, this method tends to overstate the required depth of material for well-drained, less cohesive subgrade materials such as gravel, sand, and low-compressibility silts [42].

Subsequent investigations by Shenton [43] and others have established that if threshold stresses are exceeded at any point in the operating history of a particular section of track, so that differential and excessive subgrade settlement occurs, the track will tend to resume this deformed profile despite subsequent maintenance and re-establishment of the correct profile. These points of permanent deformation correspond to areas of inherently weak subgrade (such as saturated clays or organic soils), or to points of high dynamic stress increment, such as rail joints (during the portion of the track's loading history when jointed rails were used) or welds in continuous welded rail.

To avoid subgrade failures under new track, it is now normal practice to remove the topsoil for future use and proof-roll the surface of the subgrade excavation to locate unacceptably weak zones, especially in cuts and low fills. Such zones of weakness are usually excavated to remove the unacceptable material, compacted, and filled to the selected subgrade surface with a selected fill material. Acceptable areas are often scarified to a depth of about 0.15 metres, and recompacted to 90 percent of maximum density as defined by ASTM D-1557, or 95 percent maximum density as defined by ASTM D-698. However, even when these precautions are taken, the strength of the compacted subgrade, when saturated, may be sufficiently weak that a depth of granular cover greater than the AREA minimum recommended depth of 105 mm (12 inches) of ballast plus 150 mm (6 inches) of sub-ballast may be required. Where granular materials are scarce, it may be acceptable to treat a layer of subgrade material with lime, flyash, cement or other suitable additives (e.g. BIO CAT 300-1) to increase the strength of the uppermost subgrade surface. However, the use of flyash as a soil stabilizing material has to be considered with care. Graham and Dawley [67] have shown that flyash combined with cement can significantly improve the properties of subgrade materials, whereas the use of flyash (Battle River, Class F Ash in their tests) as the sole treatment agent can improve soil properties only to a limited extent, if at all.

The treated subgrade is regarded as equivalent to unbound granular material. This is due to the fact that the modified soil layer is generally quite brittle. Although quite hard, it will fracture under dynamic loading produced by traffic. It is questionable whether integrity of the layer can be maintained even under static axle loading. Unless the supporting subgrade layer has a large modulus, the tensile stress in the treated layer will be quite large, resulting in tension cracks. These cracks allow water to penetrate to the underlying untreated soil during wet weather, and also allow drying of the untreated material during dry weather. This results in erosion below the treated soil layer, with resulting fouling of the ballast. To control this process, the treated layer should be covered with a non-cementing, non-plastic granular material graded to act as a filter to the subgrade.

Numerous methods of subgrade treatment are available. Of most interest in this context are techniques which emphasize mechanical stabilization and/or compaction of the layer immediately below the sub-ballast.

Early earthwork practice permitted the construction of embankments and subgrades without compaction. Unfortunately, consolidation of most soils by nature alone is inadequate, resulting in many failures due to the lack of adequate compaction. Indeed, failures often occur on clay embankments even with compaction. These failures are more frequent and of greater magnitude under heavier axle loads.

Adequate compaction assists in achieving three desirable conditions:

- a decrease in the susceptibility of the soil to permanent settlement
- a decrease in subgrade permeability
- an increase in subgrade bearing capacity (e.g. California Bearing Ratio or CBR).

Settlement is caused primarily by compression of subgrade voids. For a given level of compaction, maximum density results in minimum void volume, and a corresponding minimum settlement.

Since water must permeate through the voids, achieving maximum density generally also means achieving minimum permeability. Capillary water movements are also minimized.

When the subgrade is not saturated, its bearing capacity can be large, even at less than maximum density. However, when the soil is saturated, its bearing capacity for a given density drops significantly. For a saturated soil, maximum bearing capacity occurs at maximum density. This is of particular concern in North America, and especially in Canada, since virtually all Canadian subgrade soils are classified as "moist" (i.e. not drained and subject to saturation) [44]. The engineering of adequate drainage at the time of construction or rehabilitation, and its subsequent maintenance, must form an integral part of any systematic track improvement program.

The moisture content required to permit the applied compaction effort to produce maximum dry density is known as the optimum moisture content. Compaction of untreated soils is generally performed at one or two percentage moisture content above this optimum moisture value. This results in a more workable and compactable soil. Soil compacted at moisture values below the optimum also tends to have an unstable orientation of particles. On wetting, this unstable particle matrix collapses (or swells), causing greater movements than would be the case had the soil been compacted at a higher moisture content. On large jobs, optimum moisture content is obtained from field trials using the actual construction equipment. Otherwise standard laboratory techniques, such as ASTM D-698 or D-1557, are used.

Where direct compaction will not yield acceptable subgrade strength, other techniques involving treatment of the subgrade material may be applied. One such technique is the use of a liquid additive called BIO CAT 300-1. This product catalyzes the potential of natural soil and aggregate materials (during the process of wetting, mixing, placement and compaction) to attain high density, increased internal cohesion, and a reduced percentage content of void and soil pore spaces.

The technique of cement stabilization involves pulverizing the soil, to a specific depth, adding and mixing the cement with the soil, then watering and compacting the mixture in the usual manner. Because it is generally about 30 percent cheaper to combine the cement and soil in place than to batch mix, this is the most common method of treatment. When the cement hydrates, the soil is stabilized and will be stronger and more resistant to penetration by water. Care must be taken to avoid soils having more than 1 to 2 percent organic matter, and those with sulphate contents over 5000 ppm SO_4. Even 2000 ppm SO_4 or less may cause problems. Where soils with high sulphate contents are used, seal coats of waterproofing should be applied. Seal coats should also be used on expanding-lattice clays. Sulphate action causes disintegration and softening of the stabilized soil layer when the moisture content exceeds that necessary for compaction. This may occur any time, even after several years of satisfactory performance.

The addition of small quantities (1 to 2 percent) of cement will modify the properties of soil, while larger amounts (4 per cent or more) cause major property alterations. The effects of the two processes -- cement "modification" and "stabilization" -- differ principally by degree. Recent applications to subgrade work has tended away from the practice of producing concrete-like layers.

Stabilization of soils with hydrated lime is similar to cement stabilization. It is generally applied to high-liquid-limit clays, and is rarely used with granular soils unless plastic fines are present. Lime or lime slurry may be added as a soil conditioner.

Lime stabilization is achieved with calcium hydroxide (hydrated lime) or calcium oxide (quicklime). Because of environmental and safety considerations, the former chemical is more commonly used. Both contain a high percentage (about 90 percent) of calcium and magnesium oxide. The stabilizing effect results from chemical reactions causing the formation of cementitious components (calcium silicates). Calcium carbonate (agricultural lime) does not form silicates, and so is unacceptable as a stabilizing material.

Unlike cement-stabilized soils, which need compaction as soon as possible after mixing, lime-stabilized soils require a 72-hour rot period after mixing and before compaction. Lime stabilized soils generally increase in strength with the addition of lime up to a given limit, beyond which point additional lime has little value.

On chronically unstable clay subgrades under existing track, it is essential to undertake some form of subgrade/embankment strengthening before increasing the axle load limit on the tie. Lime Slurry Pressure Injection (LSPI) roadbed stabilization is an accepted procedure used throughout the United States by most of the major railroads to treat the chronic track problems associated with high-plasticity soils. Cement and cement grout injection is also used in deep ballast pockets. The slurry is injected into the ground under pressure, expelling water from voids in the subgrade. The slurry flows through available voids, fissures, desiccation cracks, failure planes, and coarse geological formations. Certain physio-chemical changes occur at the interface of the grout seams, where direct contact is made with the soil, as well as in the soil between the seams due to supernatant impregnation. The stabilized grout-impregnated seams form impervious barriers that impede the movement of moisture and add considerable strength and reinforcement to the subgrade.

The field behaviour of soil is difficult to predict, even after extensive laboratory investigations. A typical set of equilibrium resilient moduli values determined after repetitive loading tests on fine-grained Leda Clay soil were found to be dependent on the magnitude of the axial stress difference, despite the fact that the confining pressure was held constant. For this clay, the threshold value was about 50 percent of the unconfined compressive strength. This is in agreement with the range of values obtained by Heath at al. in their studies for British Rail. A similar but less dramatic drop in moduli with variations in stress difference was obtained in tests on a fine sand. Triaxial tests at constant confining pressure on gravel-sized particles, however, showed less variation in moduli with variations in axial stress difference.

For finer grained soils, reduction of the applied stress level by increasing the depth of granular cover can have quite a dramatic effect on the deformation of the underlying subgrade.

Recent experimental work carried out by CN [45] for track constructed on Lake Edmonton (varved) clays and on coarse silt showed that subgrade settlement rates decreased markedly with increasing depth of granular material below the ties, up to a depth of about 17 inches (45 cm), but were much less sensitive to depth increases beyond that point, as shown in Figure 2.10. This work suggests that for the subgrade and traffic loading conditions prevailing at these sites, granular depths of 17 to 30 inches would be adequate to prevent excessive subgrade deformation, depending on the traffic density.

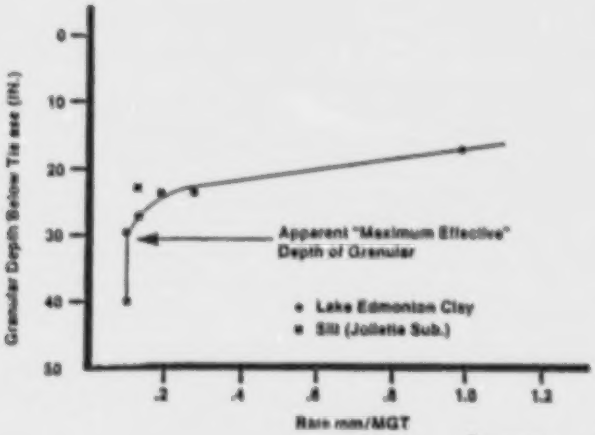

Source: J.F. Scott [45]

Figure 2.10 Subgrade settlement with traffic

These results were obtained by attaching deformation gauges to wood crossties on the field side (not between the rails) beyond the end of the tie plate. These gauges measured the compression of the granular material below the tie, and the total deformation of both the granular layers and the Edmonton clay subgrade to a depth of about 3 m. These results are consistent with the earlier results for the Leda clay discussed above. Had the equilibrium resilient modulus remained constant, then the proportion of measured deflection within the subgrade would have remained relatively high, even with 1 m of granular cover. These findings are very significant, since they indicate that a small increase in the depth of granular cover can have a dramatic effect on the measured track modulus, and on the magnitude of track settlement.

When track has been designed, constructed and maintained to standards compatible with its subgrade bearing capacity and subsequent loading history (i.e. where loading in excess of its threshold limit has not occurred), most of the track settlement will occur within the ballast and sub-ballast layers. Various laboratory investigations of ballast settlement, from small-scale triaxial tests to large-sale ballast box studies, have indicated a general trend to increasing permanent track settlement with increasing applied stress on the ballast. However, the relationship is not well defined due to the complexity of the vehicle/track superstructure/ballast/subgrade system.

Extensive experimental investigations by Raymond, Roney, Bathurst and various other collaborators between 1975 and 1987 [42,46,47], Adegoke [48], Yoo [49], Shuga [50], and Selig [51], and others have shown that track settlement after a given number of loading cycles is proportional to ballast stress raised to a power of between 1 and 3. Exponent values close to one are associated with adequate depths of strong ballast subjected to relatively light traffic loads. Higher exponent values correspond to lower-quality ballast subjected to relatively heavy traffic loads.

A recent study of track settlement [47] using a large-scale ballast box, as illustrated in Figure 2.11, found that track settlement for a given tonnage was directly proportional to the applied load for load levels below the threshold value, but that for load levels in excess of the threshold, the settlement was proportional to the applied load raised to powers up to 3. The threshold load was defined as the load level beyond which large track settlement occurred (as in Heath et al. [40]). This relationship indicates that for a given number of wheel-loading cycles, the track settlement rate is more than proportional to ballast stress.

The effects of long-term load cycle accumulation on the settlement of the track support system have been the subject of numerous experimental investigations, including those of Shenton [52], Selig [53], Raymond [46] and Sheeran et al. [41]. The results of most triaxial (repeated-loading) laboratory tests of ballast settlement show permanent settlement as a function of the number of load cycles (N) (i.e. settlement α log N). However, a four-year investigation of actual track settlements on instrumented CN track [54] generated data that show a clear linear increase in long-term permanent track settlement as a function of the number of load cycles (i.e. settlement α N). Interestingly, repeated-load triaxial tests on samples from these instrumented lines showed the log-linear relationship [41].

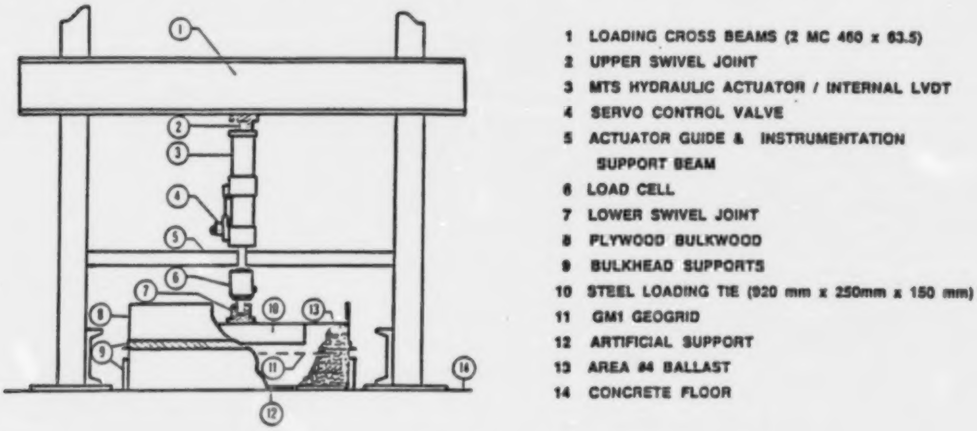
1 LOADING CROSS BEAMS (2 MC 460 x 63.5)
2 UPPER SWIVEL JOINT
3 MTS HYDRAULIC ACTUATOR / INTERNAL LVDT
4 SERVO CONTROL VALVE
5 ACTUATOR GUIDE & INSTRUMENTATION SUPPORT BEAM
6 LOAD CELL
7 LOWER SWIVEL JOINT
8 PLYWOOD BULKWOOD
9 BULKHEAD SUPPORTS
10 STEEL LOADING TIE (920 mm x 250mm x 150 mm)
11 GM1 GEOGRID
12 ARTIFICIAL SUPPORT
13 AREA #4 BALLAST
14 CONCRETE FLOOR

Figure 2.11 General test arrangement

The difference between laboratory test results and field test results may be attributed to the fact that the laboratory tests reflect the results for short-term settlement of clean ballast. In practice, large surface lifts (e.g. during ballast undercutting and cleaning) rarely occur, while small surface lifts (e.g. during mechanized tamping) occur only infrequently (e.g. every few years). The log N relationship, therefore, is expected to be relevant only for the short period following a surface lift, when the ballast is relatively clean. For most of the remaining time of a surfacing cycle (from two to ten years), a linear relationship would prevail. This is consistent with the rapid return to a linear pattern following frost heaving noted by Dalton and Scott (see Figures 3.17 and 3.18). For practical purposes, the linear relationship can be used and the rapid settlement following a surface lift treated as part of the overall efficiency of the tamping process (i.e. an effective lift equals actual lift minus immediate settlement).

2.3.1.2 Ballast breakdown and the effects of ballast quality

Ballast breakdown is one of the major contributors to track settlement and the degradation of track geometry. This effect encompasses the mechanical wear processes caused by traffic loading (abrasion and fracturing), the physical and chemical weathering processes which are largely independent of traffic (freeze/thaw effects, solutional weathering), and the secondary deterioration which arises from contamination of the ballast by evolved particulate fines (fouling), with subsequent reduction of free-draining capability and the development of cemented or pumping track. Particulate fines derived from above (blown dust, ladings, etc) or below (subgrade) the ballast may also contribute to the fouling process.

To perform well in track, a ballast material must be hard enough to resist breakdown through abrasion, tough enough to resist breakdown through fracturing under impact, and dense enough to resist lateral forces and anchor the ties in place. The material also must be resistant to freeze/thaw action and to chemical weathering, and should remain free-draining and elastic. Both the original crushed aggregate and the finer material evolved through wear processes should form shapes which are stable when subjected to low and/or high frequency vibrations. These stable particles, which are approximately cuboid, have superior interlocking properties and resistance to both lateral and vertical deformation.

The in-track performance of a ballast material is dependent on the physical properties of the aggregate, and on the specified grading and percent compaction employed in a given application.

The physical properties of the ballast are determined by geological attributes -- the minerals present and their stability, the size, shape and orientation of individual grains, the presence or absence of structural elements such as joints or fractures -- which affect the hardness and toughness of the material, its specific gravity, the permeability of fine materials evolved through physical breakdown, and its resistance to the adverse effects of vibration.

Raymond et al. [54] presented a comprehensive ballast selection and evaluation protocol based on the results of a four-year investigation of ballast properties. One of the key recommendations of this research program was the use of an Aggregate Index, I_a, to characterize the resistance to fracturing and abrasion exhibited by each material.

I_a is defined as:

$$I_a = LAA + 5MA$$

where: LAA is the Los Angeles Abrasion test value for the material under evaluation

MA is the Mill Abrasion test value for the material under evaluation.

The Los Angeles Abrasion test provides a measure of the toughness (resistance to fracture of the ballast, while the Mill Abrasion test provides a measure of the hardness (resistance to abrasion) of the ballast. The lower the I_a value, the better the ballast. This approach allows a quantifiable tradeoff between these key ballast properties, and in combination with other test values, facilitates quality ranking for different materials. Table 2.2 summarizes the acceptable limits for different track classes recommended by Raymond et al. Using these criteria, rankings were developed for 10 CN and 11 CP ballasts. By far the best material was the "Sudbury Slag," a silicate slag obtained from Inco. At the other extreme were four "dirty" limestones, a badly weathered volcanic rock, and two gravels.

TABLE 2.2

BASIC BALLAST CHARACTERISTIC TEST LIMITS

Track/Ballast Class	A	B	C	D	Remarks
Mill Abrasion and Los Angeles Abrasion (weight percent)	LAA ≤ 30 MA ≤ 4 but LAA + 5MA ≤40	LAA ≤ 35 MA ≤ 5 but LAA + 5MA ≤50	LAA ≤ 40 MA ≤ 6 but LAA + 5MA ≤60	LAA ≤ 50 MA ≤ 8 but LAA + 5MA ≤80	
Cement Value (MPa)	CV < 1.0 + 0.2 MA				
Magnesium Soundness* (percent)	≥ 3	3	5	5	5 cycles
Bulk Specific Gravity	≤ 2.65	2.65	2.50	2.50	
Shape Factor	≤ 2.00	2.25	2.50	2.75	

* May be replaced by the freeze/thaw test.

Laboratory test data from this research program (Raymond [42,46,54]) showed a strong correlation between ballast quality and plastic strain (i.e. settlement). Figure 2.12 shows typical results for plastic strain for different grades of ballast materials. The Sudbury Slag showed the smallest cumulative strain after 10^5 load cycles, while the greatest deformation occurred with a soft, weak coarsely crystalline marble, a non-ballast; one of the "dirty" crushings was the poorest performer among the ballast materials.

Data on the actual track maintenance cycles shown in Figure 2.13 indicate that low-quality limestone and granite ballasts ($I_a \geq 60$) last less than 75 MGT between maintenance cycles, while high-quality basalts and sulphide slag ($I_a \leq 30$) last up to 185 MGT between maintenance cycles.

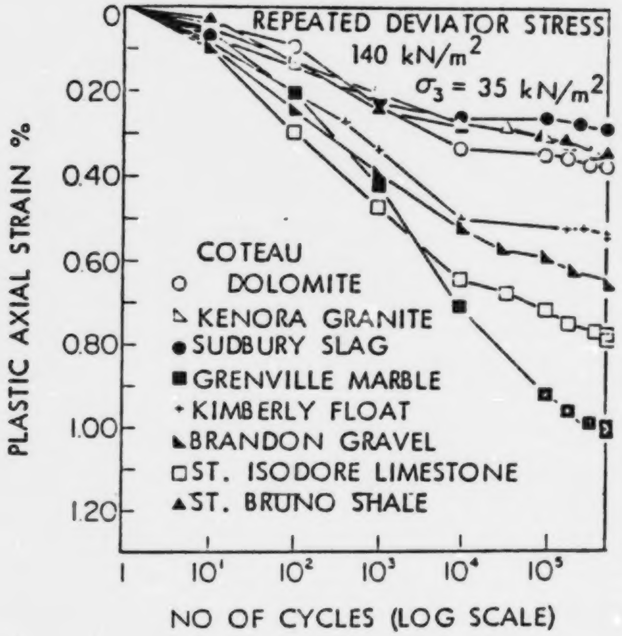

Source: G.P. Raymond [54]

Figure 2.12 Plastic axial strain observed in triaxial tests on railroad ballasts

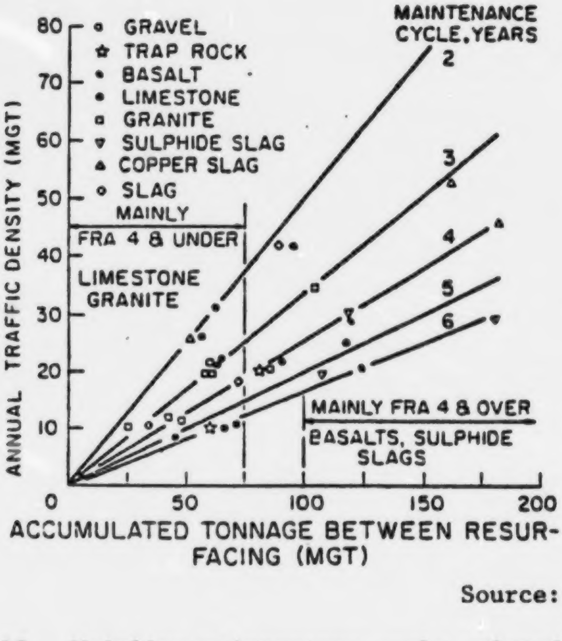

Source: G.P. Raymond [54]

Figure 2.13 Mainline maintenance cycle related to aggregate index

As the ballast material abrades during traffic loading, it generates fine particles. These fines, plus other exogenous material such as wind-blown dust and/or lading spills, tend to migrate downward in the ballast and accumulate in the voids or pore spaces. These fines will absorb and retain moisture, and can act as a lubricant to facilitate further compaction and abrasion of the ballast. For most ballast materials, these fines are plastic and will tend to cement in dry weather and pump in wet weather. At this stage, with most voids filled with evolved or exogenous materials, the ballast is said to be fouled, and cleaning and/or replacement with uncontaminated materials is required. However, not all fines behave in this fashion. Some materials, such as the silicate slag noted above, produce fines that remain free-draining, and tend to promote good interlocking of the larger ballast fractions.

The key to maintenance of superior track conditions is good drainage. If the ballast material is selected so as to avoid rock types that generate plastic, cementing fines, and if the material is graded to minimize the fine fraction placed in track, the ballast section can be maintained in a free-draining condition. Adequate depth of track-side ditching and the sloping of subgrade and sub-ballast surfaces to encourage lateral drainage, as shown in Figure 2.14, must be provided and maintained.

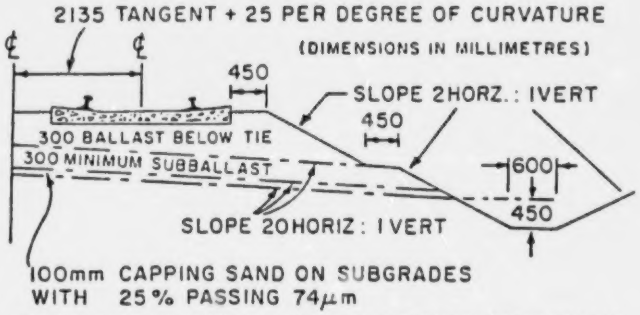
2135 TANGENT + 25 PER DEGREE OF CURVATURE
¢
¢
(DIMENSIONS IN MILLIMETRES)
450
SLOPE 2HORZ.: 1VERT
450
300 BALLAST BELOW TIE
300 MINIMUM SUBBALLAST
600
450
SLOPE 20HORIZ: 1VERT
100mm CAPPING SAND ON SUBGRADES
WITH 25% PASSING 74μm

- CAPPING SAND TO MEET ASTM D1241 AND BE CONTINUOUSLY GRADED WITHIN GRADING LIMITS D, E OR F OF D1241.
- SUBBALLAST IF USED WITHOUT CAPPING SAND SHALL MEET A.R.E.A. Ch. 1, ART. 2.10. - WHERE CAPPING SAND COVERED BY A GEOTEXTILE IS USED, SUBBALLAST GRADING SHOULD BE VOID OF SIZES LESS THAN 3mm.
- IN HIGH FREEZING INDEX LOCATIONS REQUIRED GRANULAR COVER MAY BE REDUCED 15 THICKNESSES FOR EACH THICKNESS OF STYROFOAM HI-60 OR SIMILAR. STYROFOAM TO EXTEND 1300mm BEYOND TIE ENDS AND TO BE PLACED ON GEOTEXTILE THAT IS ON 100mm SUB-LAYER. STYROFOAM MAY NOT BE USED TO REDUCE GRANULAR COVER REQUIRED DUE TO WEAK SUBGRADE.
- MINIMUM FROST PROTECTION GRANULAR COVER TO BE 50% OF FROST DEPTH GIVEN BY AVERAGE YEARLY FREEZING INDEX.
- BALLAST - HARD MINERAL - TOUGH - LOW AGGREGATE INDEX. GRADING A.R.E.A. No. 4 OR 24.

Figure 2.14 Typical track cross-section for new double-track construction

2.3.2 Sub-ballast

As noted above, the primary function of sub-ballast is to act as a filter to prevent the upward migration of subgrade fines into the ballast section, and secondarily, to reduce the traffic loading at the subgrade surface. Both functions are facilitated by good drainage.

Regardless of the amount of compaction a subgrade receives during construction, some degree of permanent deformation will occur due to traffic loading. This deformation is greatest beneath the rail. On good subgrades, this depression may only be millimeters deep, but this can be sufficient to cause water ponding and considerable softening of fine-grained subgrade materials (clays and fine silts). To prevent silt-sized or smaller fines from penetrating upwards from such subgrades, sub-ballast that incorporates non-plastic sand-sized materials grading down to the 74 micron (No. 200) sieve should cover the subgrade soils or a non-plastic, sand-sized granular capping material should be provided. To be effective, this material must act as a filter to prevent subgrade fines from being vibrated and/or pumped upwards. Similarly, sub-ballast or capping sand should be either graded to prevent its finer particle sizes from vibrating upwards into the ballast or a non-woven geotextile should be placed on the sub-ballast or capping sand to prevent such movement (see Section 2.4 for a discussion of geotextile applications).

Raymond [55], on the basis of over ten years' investigation of track behaviour, states that:

> Sub-ballast should be either in conformity with the (AREA) Manual for Railway Engineering, or be an aggregate screening of 19 mm maximum size, 3 mm minimum size, placed on a sub-layer of sand in conformity to ASTM D1241 and one of its gradings D, E or F. Alternatively, the above aggregate screening may be used upon a 100 mm thick capping sand covered by a 280 g/m^2 geotextile.

Table 2.3 presents a range of possible sub-ballast grading limits for different methods of application.

TABLE 2.3

SUB-BALLAST GRINDING LIMITS

Sieve Size	Capping* Sand	Filter** Sand	Open§ Graded Sub-ballast	Broadly Graded Sub-ballast
1"		100	100	100
1/2"			51-100	51-100
3/8"		80-100	30-80	48-80
No. 4	100	65-100	0-15	40-65
No. 8		55-85	0-3	
No. 16	70-100	45-70		25-45
No. 50	25-70	25-45		10-25
No. 100	14-40	14-30		5-14
No. 200	5-15	5-15		3-5

* Capping sand shall be covered by 280 g/m^2 geotextile.

** Filter sand should, preferably, be covered by open-graded sub-ballast or 280 g/m^2 geotextile on heavy-tonnage lines

§ Open-graded sub-ballast to be used only on filter sand or on geotextile.

Note: Ballast must not be placed directly on capping sand.

The use of a broadly graded granular ballast follows the AREA Manual, and is one solution. Another alternative is to use a capping sand to filter the subgrade fines. This capping sand would then be covered by a geotextile or by an open-graded fine gravel. The ballast would be placed directly on the open fine gravel or the geotextile. The geotextile could also be covered with an open-graded granular covering of fine-gravel-sized particles as a protective layer against ballast penetration and the effects of tamping. A third alternative would be to use a broadly graded sand that would include both some fine gravel sizes and some fines (i.e. minus 74 microns). These gradings are shown as typical grading curves in Figure 2.15. Figure 2.15 also shows CN's (1985) ballast grading and CP's (1985) maximum ballast grading. In all cases, the top surface of the sub-ballast should be sloped to encourage lateral drainage.

The required minimum depth of sub-ballast is a matter of some debate. Raymond recommends 30 cm, with at least 30 cm of ballast under the tie. The work of Scott and Dalton indicates a requirement for at least 43 cm of total granular section (ballast plus sub-ballast) and a maximum of 75 cm. With 30 cm of ballast, this would allow 13 to 45 cm of sub-ballast; 30 cm could be a useful rule of thumb for mainline applications on "typical" subgrades.

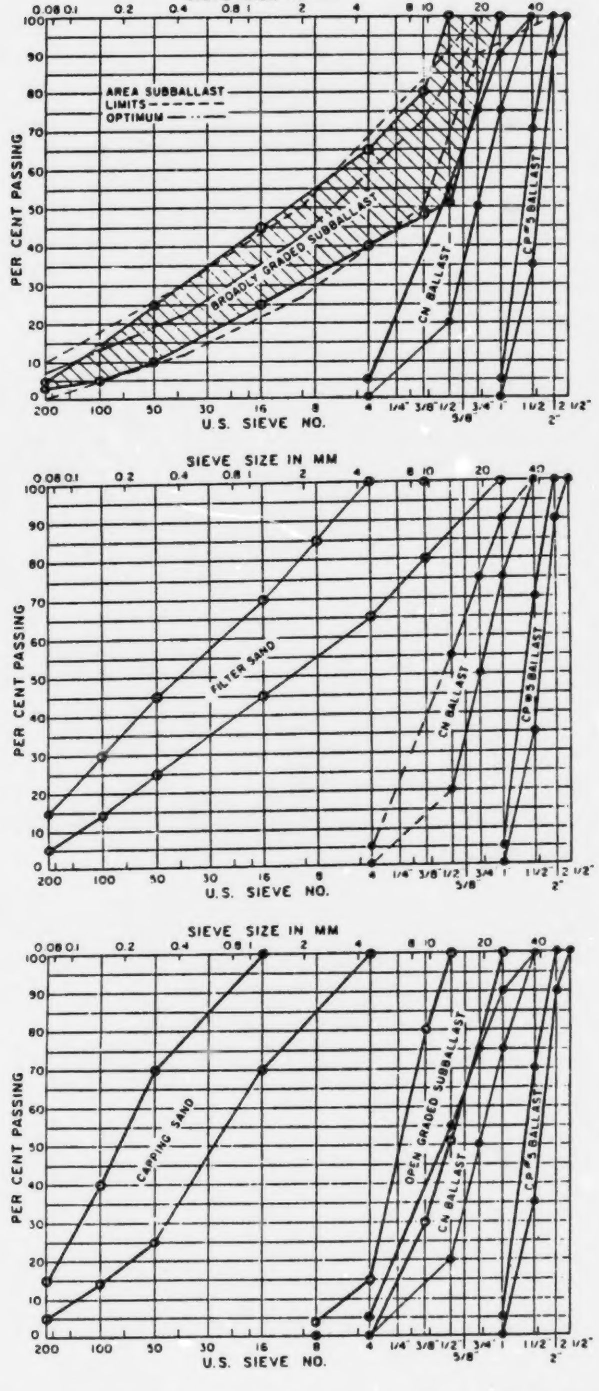

Figure 2.15 Grading curves of suggested sub-ballast and its alternative options

2.4 Geotextiles

2.4.1 Purpose of Geotextiles

The accumulated fines in dirty ballast may arise from a number of sources, including subgrade migration, impermeable fines in the original sub-ballast, aggregate breakdown of either sub-ballast or ballast, transported fines in flood water, freight car droppings, wind-blown sources, locomotive sand, and the like. Geotextiles will not prevent fines from exogenous sources such as lading spills or wind-blown dust from contaminating clean ballast, but are of value where the track support is already contaminated, and action has been taken to prevent or minimize further contamination.

In the presence of excess water, fine materials below a track subject to repetitive wheel loads will migrate upwards through the track structure. The more free water there is, the faster, in general, the upward migration of fines. Thus, drainage improvement (whether the improvement of side ditch drainage dealing with surface water, or the lowering of the ground water to increase the subgrade strength, or drainage of the track area to prevent water seeping up into the subgrade bearing area) should always be the first and most essential item in any subgrade stabilization work. This is true whether or not geotextiles are used.

Special attention should be given to the undercutting of long lengths of track where, as shown in Figure 2.16, a canal effect is produced by undercutters. If, after or before undercutting, the shoulder ballast is not removed and cleaned, drainage from the load-bearing area of the side ditches cannot occur. Where possible, the shoulder undercutting should be deeper than the track undercut. Geotextiles should never be used as a substitute for good drainage. Indeed, if the geotextiles are installed without an ability to drain and discharge by gravity to side ditches or French drains, they will facilitate retention of water within the load-bearing area of the track. Water that is trapped within the load-bearing area of the track will provoke or exacerbate both pumping and frost heaves.

In tangent track, geotextiles have found their greatest use in poorly drained terrain, such as marshes and clay plains. These fabrics are also being used at locations where it is difficult to maintain good drainage, or where localized high-impact loadings occur, such as at grade crossings, diamonds, turnouts and similar track structures.

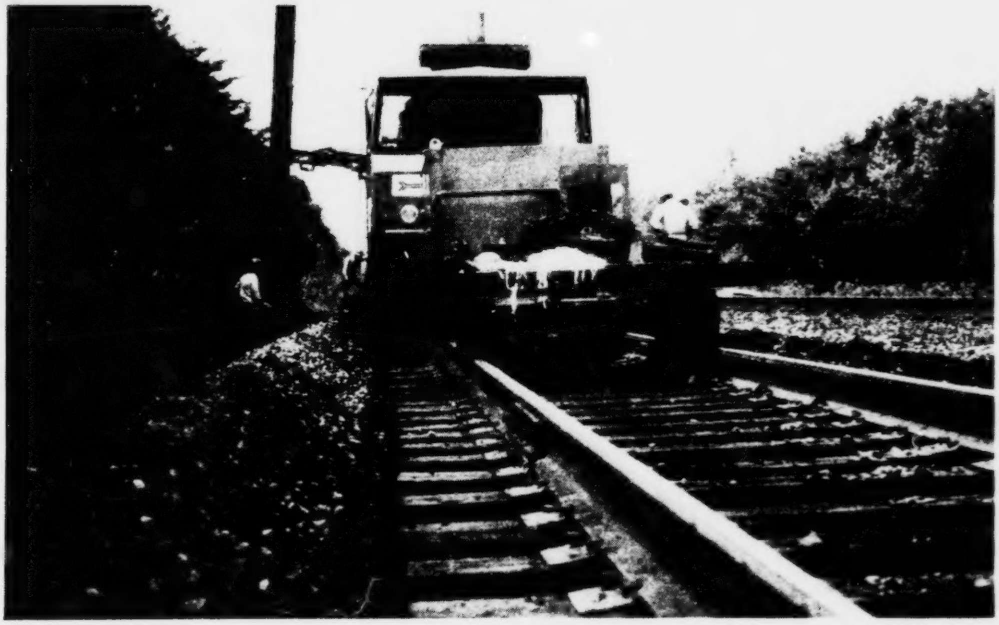

Figure 2.16 Canal effect created by undercutting operation prior to removal of shoulder ballast

Track requiring rehabilitation has generally been in use for a sufficiently long period of time for excessive subgrade settlements to have ceased. Under these circumstances, the geotextile must be very resistant to abrasion and puncture, so as to withstand the harsh environment of ballast or subgrade aggregate particle movement. On undercut, ploughed or sledded track in which the rail remains in place during rehabilitation, the surface prepared to receive the geotextile will contain ballast particles lying on the surface or protruding from the surface. If punctured or worn through, the geotextile will lose some of its ability to filter and separate.

The geotextile must also be able to transmit water within the plane of the geotextile. When an axle or group of axles passes a location, water will escape, or try to escape, along the path of least resistance. Geotextiles with in-plane permeability offer such a path.

The basic functional requirements of geotextiles for use in railroad bed rehabilitation are to:

- drain water away from the track roadbed, on a long-term basis, both laterally along the plane of the geotextile and by gravity without buildup of excessive hydrostatic pressures
- withstand the abrasive puncture forces of moving aggregate caused by the tamping/compaction process

during cyclic maintenance, tamping during initial compaction, and by the passage of trains

- retard the migration of fine particles while allowing the passage of water, so as to separate the ballast and subgrade materials under the influence of repeated loading and of water migration.

References [56] and [57] provide a comprehensive material specification and acceptance testing method for geotextiles intended for use in railroad track applications.

3. TRACK SYSTEM MODELLING

3.1 Overview

Figure 3.1 is a schematic diagram of the track system. It describes the main interactive processes which link the vehicle dynamic force inputs experienced by the track to the deterioration of track components and geometry. As shown, a vehicle of a given design, running over a track section of a given standard, at a given speed, will create a spectrum of track forces.

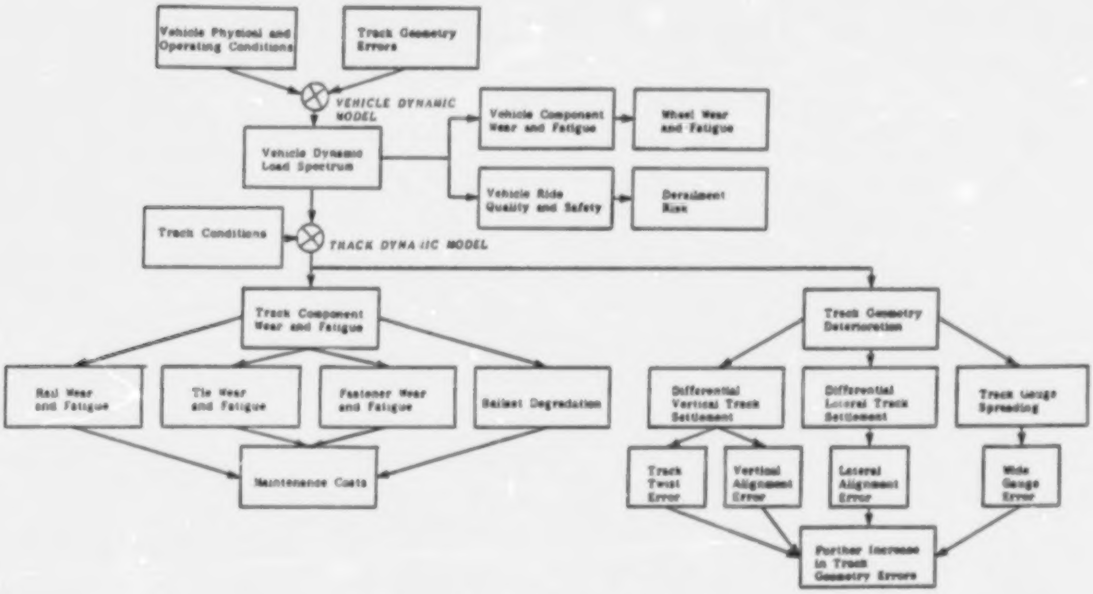
Vehicle Physical and Operating Conditions
Track Geometry Errors
VEHICLE DYNAMIC MODEL
Vehicle Dynamic Load Spectrum
Vehicle Component Wear and Fatigue
Wheel Wear and Fatigue
Vehicle Ride Quality and Safety
Derailment Risk
Track Conditions
TRACK DYNAMIC MODEL
Track Component Wear and Fatigue
Rail Wear and Fatigue
Tie Wear and Fatigue
Fastener Wear and Fatigue
Ballast Degradation
Maintenance Costs
Track Geometry Deterioration
Differential Vertical Track Settlement
Differential Lateral Track Settlement
Track Gauge Spreading
Track Twist Error
Vertical Alignment Error
Lateral Alignment Error
Wide Gauge Error
Further Increase in Track Geometry Errors

Figure 3.1 Track system

These forces are transmitted into the track, causing wear and fatigue of track components and deterioration of track geometry. The distribution of these forces depends on track design and the condition of the track components. Repair and replacement costs are incurred as a result of component wear and fatigue. Deterioration of track geometry causes an increase in track errors and leads to larger dynamic wheel loads as subsequent trains pass. This self-reinforcing cycle continues until track components and geometry are reconditioned. Vehicle performance and track response are clearly inter-related, and the track deterioration process is generally self-accelerating.

To understand and quantify the behaviour and interaction of such systems, the following work must be carried out:

(a) **Determination of track loading.** Each type of vehicle in a traffic mix, operating at a given speed, generates a unique dynamic wheel load spectrum. The variation of load within a spectrum is due to the random variation of physical properties within a vehicle type (e.g. wheel geometry defects) and the random variation of track geometry within a track section (e.g. surface roughness). Conventional North American practice, which represents each type of vehicle by the static axle load or by the static axle load modified by an impact factor based on speed and wheel diameter does not adequately incorporate this variability. For each vehicle type in a traffic mix, the necessary track loading information is its dynamic wheel load spectrum. The minimum information is the steady-state level and dynamic variation of the wheel force in the vertical and lateral directions (see Appendices A and B).

(b) **Determination of track response.** For any given set of dynamic wheel forces from given traffic, there is a corresponding set of forces on ties and ballast. This load distribution varies with track configuration and track component conditions. One common technique for estimating load distribution is based on the theory of beam (rail) on elastic foundation (ties and ballast). Once the load distribution is known, the deflections and stresses in ballast, sub-ballast and subgrade can be estimated.

(c) **Estimation of track component deterioration rate.** Steps (a) and (b) produce data describing the loading (i.e. forces/stresses) on each track component. Based on these data, estimates of wear and fatigue rates for track components such as rails and ties can be made. These will indicate the level of track maintenance effort which a given track design would require in the long term under a specified traffic level.

(d) **Estimation of track geometry deterioration rate.** Since conventional track design is not rigid, the continued application of wheel loads leads to track settlement. Further, because wheel forces and rail support corrections generally vary along the track, the settlement is not uniform. This leads to further increases in track geometry errors and, in turn, to further increases in wheel forces. Research work in the area of track should consider a preliminary model of track differential settlement for use in analyzing track geometry deterioration problems.

3.2 Computer Model

The complexity of the track environment makes the prediction of items (a) through (d) (Section 3.1) difficult. Many theories have been developed in the past to determine the required parameters in what is a fairly unpredictable environment. Actual field data have also been collected at times, but the quality of some of these data is questionable. To make the best use of the current level of knowledge, track behaviour has been modelled mathematically, with the ultimate aim of providing a better tool for track maintenance management. These models incorporate the theories used to obtain track component response and interactions, but use field data to calibrate the model (see Appendix C) for a particular railway operation.

A track system model consisting of four modules has been developed. The modules are:

- the Dynamic Wheel Force Model
- the Rail Life Model
- the Tie Life Model
- the Surface Life Model.

To make these models useful tools for track maintenance management, they should be upgraded regularly as more and better data become available.

3.2.1 Model Structure

Figure 3.2 illustrates the structure of the model. The Dynamic Wheel Force module produces the key components of the dynamic wheel load for each set of traffic/track conditions. Outputs from this module are fed to the Rail, Tie and Surface modules, which calculate track component and geometry degradation rates, from which maintenance costs may be derived.

A key feature of the model structure is the normalization of the wheel loading cycle. This involves converting the actual number of wheel loading cycles of a given traffic category in a traffic mix into the equivalent number of wheel loading cycles of a reference traffic category.

The reference traffic category is normally defined as the traffic category which contributes the most to the overall track maintenance cost and whose characteristics are best understood. For North American main lines, this is generally the 100-ton car.

The normalization is based on the relative contribution to track degradation by a given traffic category compared to that by the reference traffic. For example, if the wheel loading cycle of a six-axle locomotive causes twice as much differential track settlement as that of a 100-ton car (reference traffic), it is equivalent to two cycles.

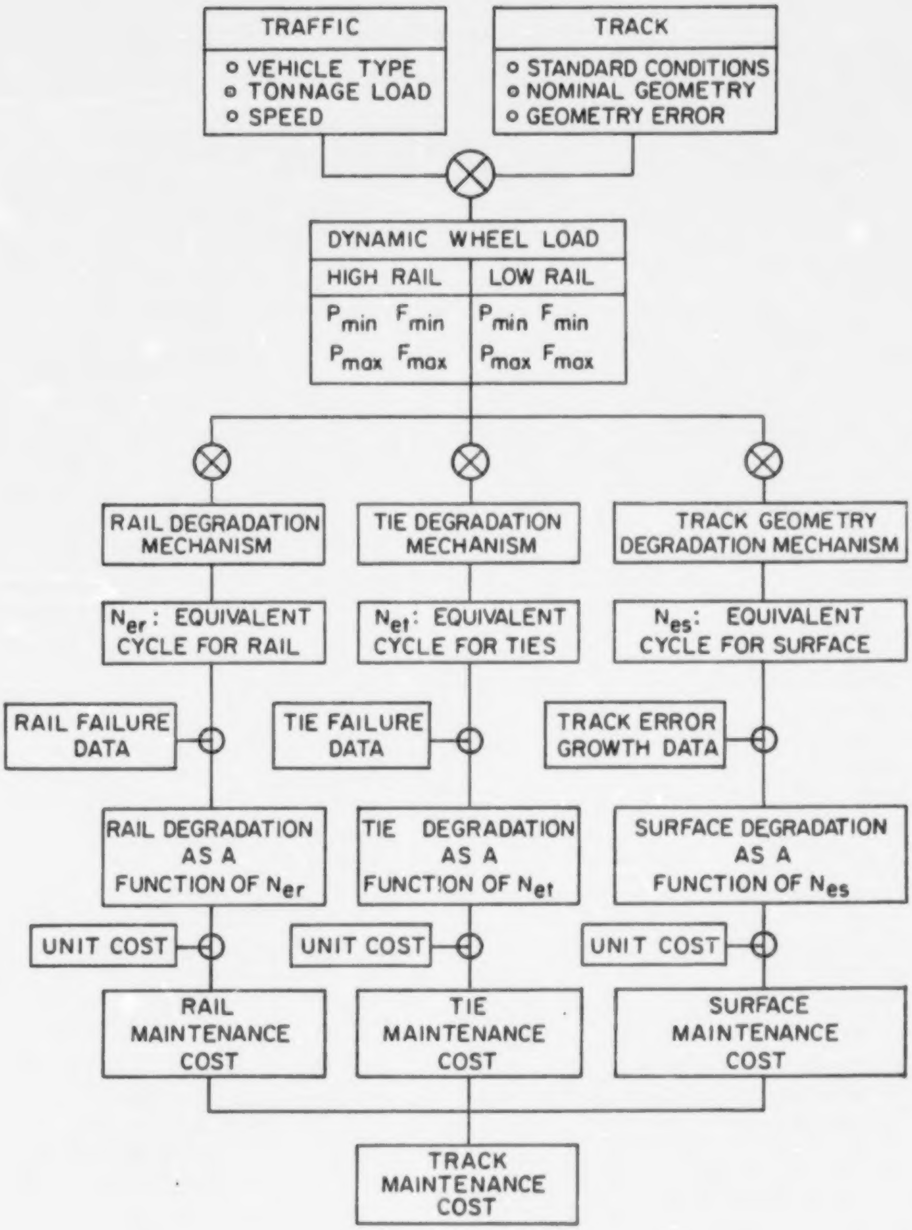
TRAFFIC
o VEHICLE TYPE
o TONNAGE LOAD
o SPEED
TRACK
o STANDARD CONDITIONS
o NOMINAL GEOMETRY
o GEOMETRY ERROR
DYNAMIC WHEEL LOAD
HIGH RAIL
LOW RAIL
P_{min} F_{min}
P_{max} F_{max}
P_{min} F_{min}
P_{max} F_{max}
RAIL DEGRADATION MECHANISM
TIE DEGRADATION MECHANISM
TRACK GEOMETRY DEGRADATION MECHANISM
N_{er}: EQUIVALENT CYCLE FOR RAIL
N_{et}: EQUIVALENT CYCLE FOR TIES
N_{es}: EQUIVALENT CYCLE FOR SURFACE
RAIL FAILURE DATA
TIE FAILURE DATA
TRACK ERROR GROWTH DATA
RAIL DEGRADATION AS A FUNCTION OF N_{er}
TIE DEGRADATION AS A FUNCTION OF N_{et}
SURFACE DEGRADATION AS A FUNCTION OF N_{es}
UNIT COST
UNIT COST
UNIT COST
RAIL MAINTENANCE COST
TIE MAINTENANCE COST
SURFACE MAINTENANCE COST
TRACK MAINTENANCE COST

Figure 3.2 Track System Maintenance Model

This normalization process converts a mixed traffic situation into an equivalent uniform traffic situation. The total equivalent cycles are then compared against the actual failure data to establish an empirical relationship between traffic and track degradation. This empirical relationship can later be applied to future track and/or traffic conditions to predict the future rate of track degradation and maintenance cost. Note that as rail, tie and surface degradation mechanisms are different, the total equivalent cycles for rail, tie and surface will be different, even though the total number of actual cycles is the same.

This model structure is very flexible. It is designed to make the best use of the existing incomplete understanding of track system performance and degradation processes, as well as incomplete track and traffic data. Essentially, the model will give the best possible answer for a given level of knowledge and information. More knowledge and/or more information can be readily incorporated to give better, less uncertain, results. Since complete understanding of track behaviour and complete availability of traffic and track data will never be achieved in absolute terms, this is in fact a reasonable strategy.

For ease of trial application, the first version of the models was set up in a Lotus 1-2-3 work-sheet format. The constraints of a work-sheet format necessitated some simplifications, and hence reduced accuracy. With the exception of the Rail Life Model, all models (Dynamic Wheel Force "DYNFOR", Tie Life "TIELIF" and Surface Life "SURLIF") have now been converted to FORTRAN IV coding.

A description of the working structure of the updated subprograms is given in Appendix D, together with input data requirements.

The subprograms have been applied to the analysis of some aspects of track maintenance on a number of operating railroads. Typical results are given in Appendices E through G, where listings of each subprogram are also given. The output from each subprogram includes an echo of the input data, thus making it easy to check for possible input errors. The subprograms are being upgraded continually as further research findings become available.

A description of the component models (subprograms) in the Track System Maintenance Model is given in the following sections.

3.2.2 Vehicle Dynamics Model

3.2.2.1 Introductory remarks

The difference between one traffic category and another, in terms of track degradation, begins with the different characteristics of their dynamic wheel load. Therefore, an estimate of the dynamic wheel load for each traffic category is necessary in order to work out the contribution to total track maintenance costs of different traffic types in a traffic mix. For each traffic type, there are two principal load components: vertical and lateral, each with two principal terms: steady-state and dynamic variation. The steady-state term represents the reaction of the vehicle to the average track parameters (e.g. nominal alignment). The dynamic term represents the reaction of the vehicle to the instantaneous changes in track parameters (e.g. alignment errors).

Figure 3.3 is an example of the vertical wheel force variation of a 100-ton car running over jointed rail track. The steady-state force is 28 kips (approximate static wheel load), and the dynamic variation (due to surface errors at rail joints) is about ±4 kips (±14 percent of static wheel load).

Figure 3.4 is an example of the lateral wheel force variation of a 100-ton car running through a 1.4 degree curve. The steady-state lateral wheel force on the high rail is 6 kips, and the dynamic variation is about ±1 kip (±16 percent of the steady-state load).

For this analysis, traffic is broken down into classes according to type (e.g. freight, passenger, locomotive) and axle load (e.g. 20-50 tons, 50-70 tons, etc.), with each track class representing a unique set of track characteristics. These are essentially curvature, superelevation and track quality indices, as well as physical rail and track parameters. Within each class there are variations in vehicle parameters. Of these, the most significant is wheel geometry, since a wheel with defective geometry gives rise to considerably higher dynamic load. Figure 3.5 is an example of wheel load distribution for passenger and freight traffic in the North East Corridor. The measurements were taken at a selected track location, hence the variations reflect the non-uniformity of vehicle parameters. At the present time there is insufficient data on the variation in vehicle parameters within each traffic category. Until such data are sufficiently established, the analysis must be based on the nominal characteristics of each traffic type.

3.2.2.2 Model outline

The aim of the vehicle dynamics model is to estimate the response of each traffic class to track geometry variation. Figure 3.6 outlines the structure of the model. The calculations are based on a series of quasi-empirical equations that have been developed from computer simulation runs for a base vehicle, with adjustments made to allow for different vehicle designs.

A description of the equations is given in the following sections, with detailed development outlined in Appendices A and B.

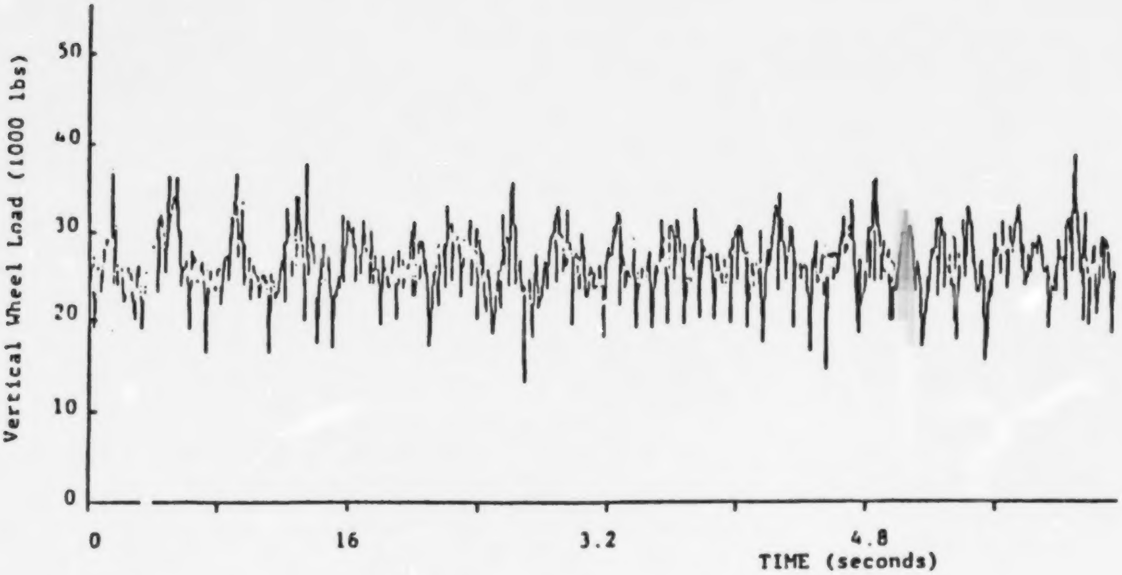

Source: Battelle-Columbus Laboratories [62]

Figure 3.3 Sample vertical wheel force variation of a 100-ton car at 65 mph running over jointed rail track

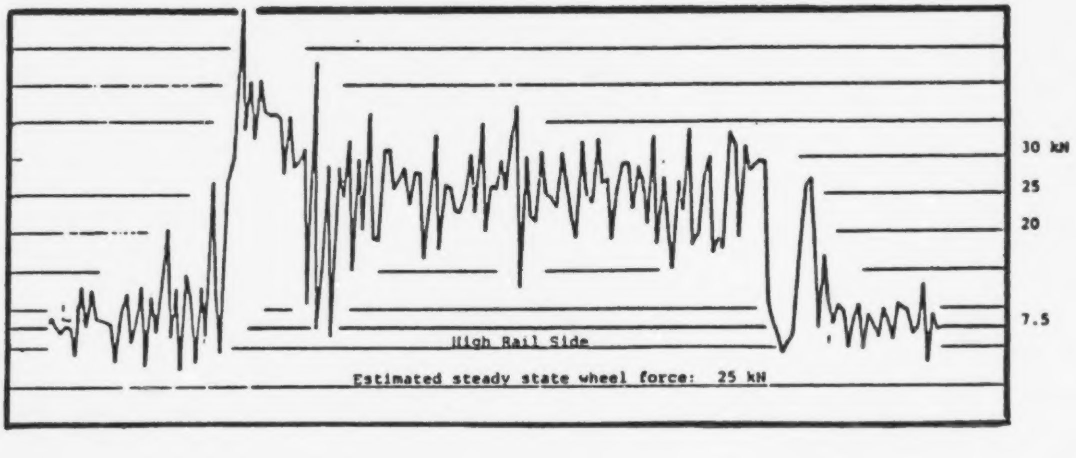

Source: S.T. Lamson [63]

Figure 3.4 Sample lateral wheel force variation of a 100-ton car running through a 1.43 degree curve

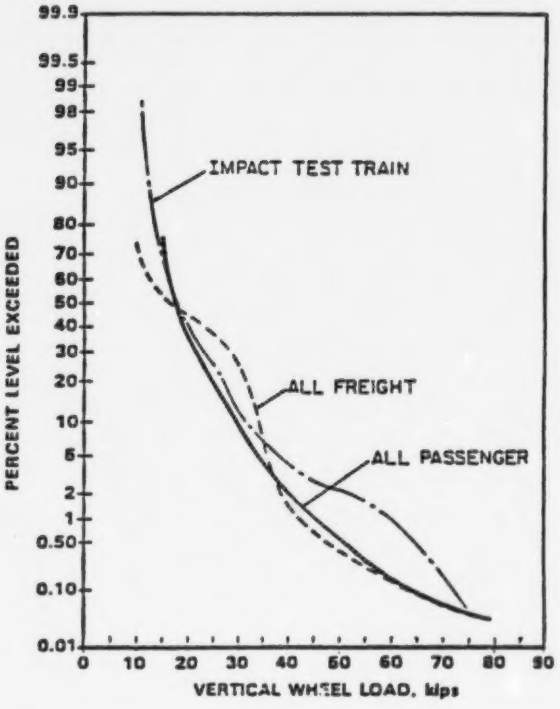

Source:
T. Ferragut,
Federal Railroad
Administration,
personal
communication

Figure 3.5 Sample wheel load distribution for passenger and freight traffic

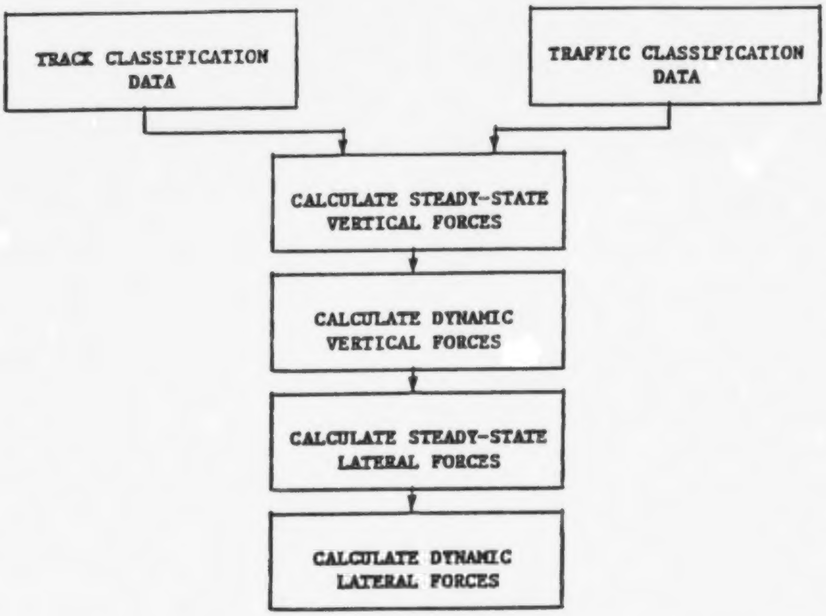
TRACK CLASSIFICATION DATA
TRAFFIC CLASSIFICATION DATA
CALCULATE STEADY-STATE VERTICAL FORCES
CALCULATE DYNAMIC VERTICAL FORCES
CALCULATE STEADY-STATE LATERAL FORCES
CALCULATE DYNAMIC LATERAL FORCES

Figure 3.6 Dynamic Wheel Force Model flowchart

3.2.2.3 Vertical forces

(a) **Steady-state component.** In tangent track, steady-state vertical wheel force is approximately equal to the static wheel load. In curved track it depends on whether the vehicle is travelling at balance speed or not. If, for example, the vehicle speed is higher than the balance speed, some of the vertical load on the low rail is transferred to the high rail. An equation for estimating this load transfer is given below:

$$P_s = 2.788\ P_o\ (1.15 \times 10^{-5}\ V^2\ D - 0.0177\ S)$$

where: P_s = steady-state wheel load (lb/wheel)

P_o = static wheel load (lb/wheel)

V = vehicle speed (mph)

D = degree of curvature (degree)

S = superelevation (inches).

The steady-state wheel forces on high and low rails are $(P_o + P_s)$ and $(P_o - P_s)$, respectively.

(b) **Dynamic Variation Component.** The interaction between the vehicle and random track surface roughness at speed gives rise to dynamic wheel force variation about the steady-state level. This results in maximum and minimum dynamic wheel forces. One standard deviation of the dynamic variation can be estimated using the equation below:

$$P_d = 7.942 \times 10^{-6}\ P_s\ V^{0.68}\ (0.585\ SI^{1.4} + 1.22\ CI)\ (M_u/3156)^{0.5}$$

where: P_d = one standard deviation of the dynamic wheel force variation (lb)

P_s = steady-state wheel load (lb/wheel)

V = vehicle speed (mph)

SI = CN-type surface index

CI = CN-type cross-level index

M_u = unsprung mass of a wheel-set (lb/axle).

This equation is derived from the computer simulation of the dynamic wheel forces of a 100-ton car running over samples of CN track in the Kingston subdivision. The effect of speed (i.e. the power 0.68), as described by this equation, agrees reasonably well with U.S. field data for 100-ton cars and CN test data (see Appendix A). The unsprung mass term is included to take into account the differences in vehicle design.

3.2.2.4 Lateral forces

(a) **Steady-state component.** In tangent track the net steady-state lateral wheel force on track (not on individual rail) is zero. In curved track it depends on whether the vehicle speed is balance or not. If, for example, the vehicle speed is higher than the balance speed, centrifugal force is developed, causing lateral track force. An equation for estimating this force is given below (see Appendix B):

$$L_s = [\ 1668.2\ (D-1)^{.95} + 744.64\ S - 0.494\ V^2\ D\ ]\ (\frac{P_o}{16450})^{2/3}$$

where: L_s = steady-state lateral track force (lb/wheel)

D = degree of curvature (degree)

S = superelevation (inches)

V = vehicle speed (mph)

P_o = static wheel load (lb/wheel).

(b) **Dynamic component.** The interaction between vehicle and track due to random track alignment error gives rise to dynamic lateral wheel forces (see Figure 3.4). One standard deviation of this variation can be estimated using the equation:

$$L_d = 5.15 \times 10^{-5} \times P_o \times V^{1.86}\ (\frac{AI}{100}) \times (\frac{M_u}{3156})^{0.5}$$

where: L_d = dynamic lateral wheel load (lb/wheel) (based on one standard deviation)

P_o = static wheel load (lb/wheel)

V = vehicle speed (mph)

AI = CN-type alignment index

M_u = unsprung mass of a wheel-set (lb/axle).

This equation is derived from computer simulation of the dynamic wheel force of a 100-ton car running at a range of speeds in full-flanging mode (both leading and trailing wheels are assumed to be contacting the high rail and are thus subjected to forced acceleration by the high-rail alignment error). Results of the simulation are shown in Figure 3.7. From this, the effect of speed (i.e. to the power 1.86) is included to take into account the difference in vehicle design.

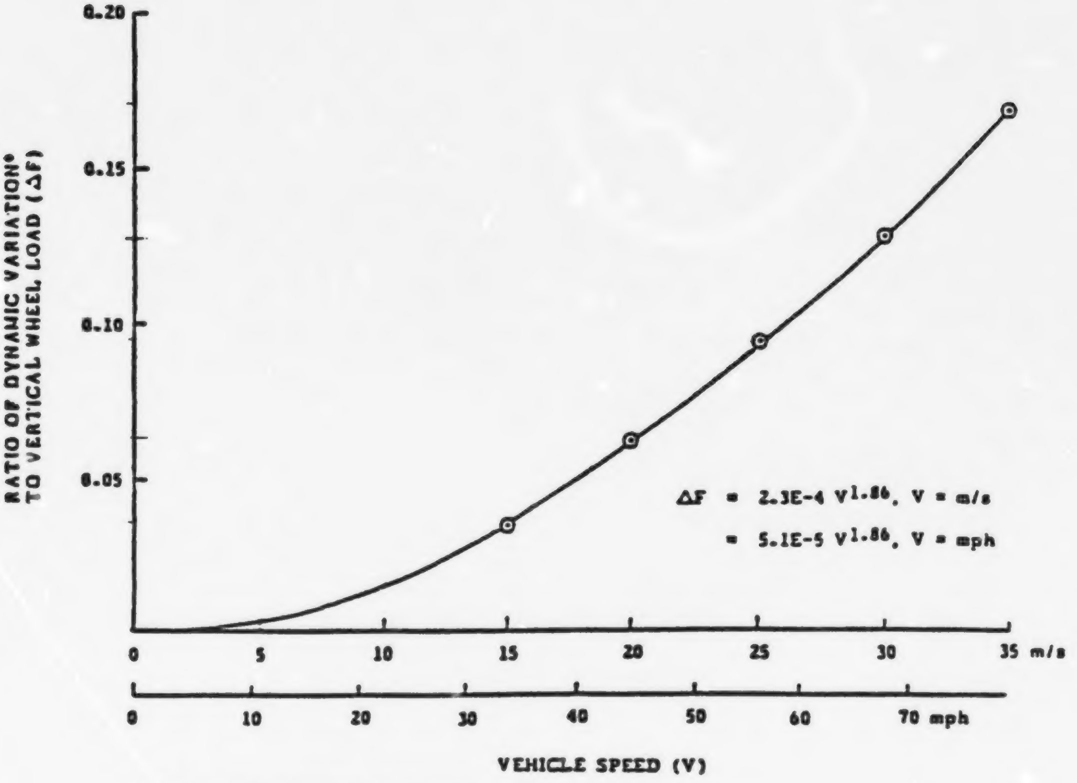

* 1 standard deviation of dynamic lateral wheel force

Figure 3.7 Dynamic lateral load factor versus vehicle speed

3.2.2.5 Track quality indices

Both vertical and lateral dynamic force component equations have been shown to be dependent on track geometry variation. Since there is no standard way of quantifying track geometry variation, the CN-type track geometry index has been used here. It can be described as:

$$I = \sum_{i=1}^{n} \frac{| y_{i+1} - y_i | \times 10^5}{L}$$

where: I = track geometry index

L = reference section length

y_i = track deviation at point i

n = number of points over the reference length of track.

Three track geometry indices are used here:

SI - surface index

XI - cross-level index

AI - alignment index.

3.2.3 Rail Life Model

3.2.3.1 Model Outline

Figure 3.8 describes the conceptual approach of this program. It shows that rail damage and associated costs are basically caused by an accumulation of various wheel loading cycles, each with a different dynamic force, depending on vehicle characteristics, operating conditions, and track quality.

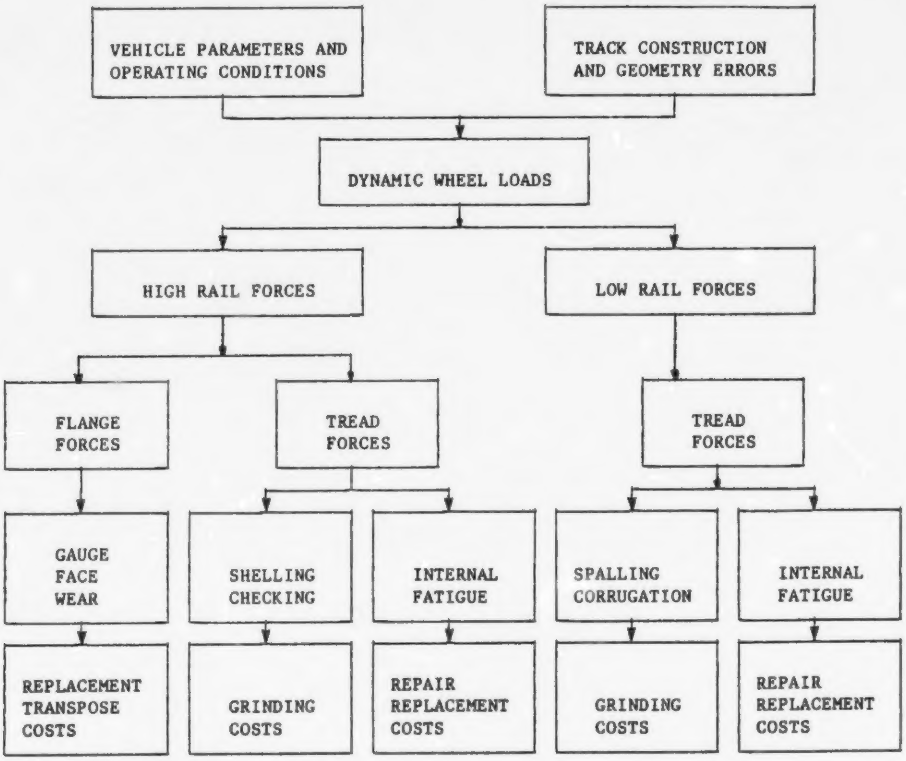
VEHICLE PARAMETERS AND OPERATING CONDITIONS
TRACK CONSTRUCTION AND GEOMETRY ERRORS
DYNAMIC WHEEL LOADS
HIGH RAIL FORCES
LOW RAIL FORCES
FLANGE FORCES
TREAD FORCES
TREAD FORCES
GAUGE FACE WEAR
SHELLING CHECKING
INTERNAL FATIGUE
SPALLING CORRUGATION
INTERNAL FATIGUE
REPLACEMENT TRANSPOSE COSTS
GRINDING COSTS
REPAIR REPLACEMENT COSTS
GRINDING COSTS
REPAIR REPLACEMENT COSTS

Figure 3.8 Concept of rail life/cost model

Generally, if the total cost is known and the accumulated wheel load cycles can be normalized so that each "equivalent cycle" causes equal amounts of damage, then a unit of rail cost per cycle can be established, e.g.:

$$\text{UNIT COST} = \text{TOTAL COST/TOTAL EQUIVALENT CYCLE}$$

If a traffic category such as "passenger train" causes Np equivalent cycles, its share of the rail cost will be:

$$\text{PASSENGER COST} = \text{UNIT COST} \times \text{Np}$$

The key to this approach is to accurately estimate the dynamic force exerted on the rail by each traffic category, and the relative extent of damage the rail sustains when subjected to a cycle of such force. This is explained in more detail in the following section.

3.2.3.2 Working equations

(a) **Estimation of wheel forces.** In the current version of the Rail Life Model, the static wheel force, P_o, is derived from the average loaded vehicle weight. The steady-state force, P_s, is calculated as the load transfer due to unbalanced curving speed. Superelevation is assumed set for 60 mph freight speed.

The dynamic force is calculated through a quasi-empirical equation giving standard deviation of dynamic force fluctuation versus speed. The equation is developed using a full-body dynamic model of a 100-ton car (see Appendix A):

$$\varphi d = 7.94 \times 10^{-6} \times V^{.68} \times (.585 \times SI^{1.4} + 1.22 \times CI)$$

where: φ_d = dynamic load factor

V = vehicle speed

SI = track surface-index

CI = track cross-level index.

As mentioned in Section 3.2.1, the Rail Life Model is still in Lotus spreadsheet format. Some of the equations used for the determination of vertical and lateral wheel forces in this model have since been upgraded to those noted in Sections 3.2.2.3 and 3.2.2.4. Upgrading of the Rail Life Model will be part of ongoing efforts to improve the overall performance of the track system model.

The steady-state lateral tread force is estimated as the average lateral force created by the leading wheel-set on high and low rails. Flange force is twice that.

$$F = (P/35000)^{2/3} \times (3.6\ D^{.552} + 1) \times 10^3$$

where: F = steady-state lateral wheel load (lb)

P = static wheel load (lb)

D = degree of curvature (degree).

(b) **Estimation of rail wear and fatigue.** The rate of gauge face wear on the high rail is proportional to the flange force and friction factor.

$$N_{ew} = N \times [(F_f \times \mu_a)/(F_{ref} \times \mu_{ref})]$$

where: N_{ew} = equivalent cycles for gauge face wear

N = total load cycles (per year)

F_f = high rail flange force

μ_a = friction factor (actual)

F_{ref} = reference force

μ_{ref} = reference friction factor.

The rate of fatigue damage is dependent on the maximum range of octahedral shear stress created by a passage of each wheel.

$$N_{ef} = N \times (So_a/So_{ref})^{3.5}$$

where: N_{ef} = equivalent cycles for fatigue damage

So_a = reference octahedral stress.

A power of 3.5 corresponds to the crack propagation mode. The octahedral shear stress ranges from 0.30 P_o for a tread force of zero, to 0.63 for a tread force equal to 1/3rd of the vertical force.

P_o is given by:

$$P_o = 23452 \times \text{Sum}\,(1/R)^{2/3} \times P1/3$$

where: P_o = maximum contact stress at surface

Sum(1/R) = sum of wheel contact radii

P = impact load.

On low rail, higher contact stress is expected for incidences of false flange contact. It is currently assumed that 10 percent of freight wheels have false flanges and 50 percent of curves have wide gauges, resulting in a false flange contact probability of 5 percent. Passenger wheels are assumed to have no false flange. Maximum stress under the false flange contact condition can be calculated once data on false flange wheels become available. For now it is estimated to be twice the normal contact stress.

3.2.3.3 Procedure to establish rail cost data

(a) **Curved rail replacement cost breakdown.** The following assumptions are used to establish rail replacement cost data:

- survey the location where rails are soon to be replaced
- measure side wear and head wear
- assume that side wear is the main cause of replacement
- assume that transportation of rail is normally carried out
- assume that the total side wear possible is the side wear limit specified in SPC and call this "SWL"
- call the measured side wear "SW".

The proportion of rail replacement cost due to side wear is considered to be as follows:

$$Ks = SW/SWL$$

The remainder of the rail replacement cost is due to surface defects such as shelling, corrugation, etc. Note that the rail replacement cost discussed here (called "R\$net") excludes rail replacement due to a high level of internal fatigue defects (called "R\$if") and the rail change-out for upgrading the track (called "R\$up"). It is assumed here that replaced rails are not relaid elsewhere (however, if this is the case an adjusted rail cost must be applied). The total rail replacement cost shown on the subdivision budget is thus made up as follows:

$$R\$gross = R\$net + R\$if + R\$up$$

R\$net can be separated further, as follows:

$$R\$net = R\$sw + R\$sfH + R\$sfL$$

where: R\$sw = cost of rail side wear

R\$sfH = cost of surface defects on high rail

R\$sfL = cost of surface defects on low rail

and:

$$R\$if = R\$ifH + R\$ifL$$

where: R\$ifH = cost of internal rail fatigue on high rail

R\$ifL = cost of internal rail fatigue on low rail.

R\$ifH and R\$ifL can be determined using records of rail flaw distribution (i.e. percent on rail, percent on low rail, and special rail supply requested due to rail fatigue defects (e.g. miles of rail that must be replaced because the fatigue rate has reached two defects/mile/year) can be made.

R\$sfH and R\$sfL can be determined using rail grinding records. For now, let us call mgH the total miles of grinding because of high rail surface problems, and mgL that for low rail. Assuming regular grinding is sufficient to keep the rail surface in acceptable operating condition (i.e. rail surface problems result in the need for rail replacement due to rail head loss through grinding), the following relationship can be established:

$$R\$sfH = R\$net \times (1-Ks) \times (mgH/(mgH + mgL))$$

$$R\$sfL = R\$net \times (1-Ks) \times (mgL/(mgH + mgL))$$

(b) **Curved rail maintenance cost breakdown**. Rail maintenance cost is made up of:

- internal fatigue defect repair (e.g. plugging) cost (indirect costs such as train delays, derailment, etc., may be included)
- surface defect repair (e.g. grinding) cost.

The breakdown of total rail internal defect costs to high and low rail can be made using instrumented car data.

The breakdown of total rail grinding costs to high and low rail can be made by surveying locations where grinding is required. For each curve one can establish a reason for grinding based on rail surface conditions. For example:

curve #1: 0.3 miles of grinding needed; shelling on high rail

Curve #2: 0.25 miles of grinding needed, shelling on high rail
and corrugation on low rail

For these records the total miles of grinding of high and low rail, mgH and mgL, respectively, can be calculated.

Each component of rail maintenance cost can be added to the respective component of rail replacement cost to derive the following final cost data for use in the "Rail Cost Distribution Model":

- cost of side wear on high rail
- cost of fatigue on high rail
- cost of fatigue on low rail.

Note that for tangent track internal fatigue defects are usually the only problem.

3.2.4 Tie Life Model (Wood)

2.3.4.1 Model outline

Figure 3.9 outlines the structure of the Tie Life Model. The analysis proceeds through a series of logical steps that separate the major components of the model. This approach is taken to allow future upgrading of the individual analysis steps, while keeping the basic structure intact.

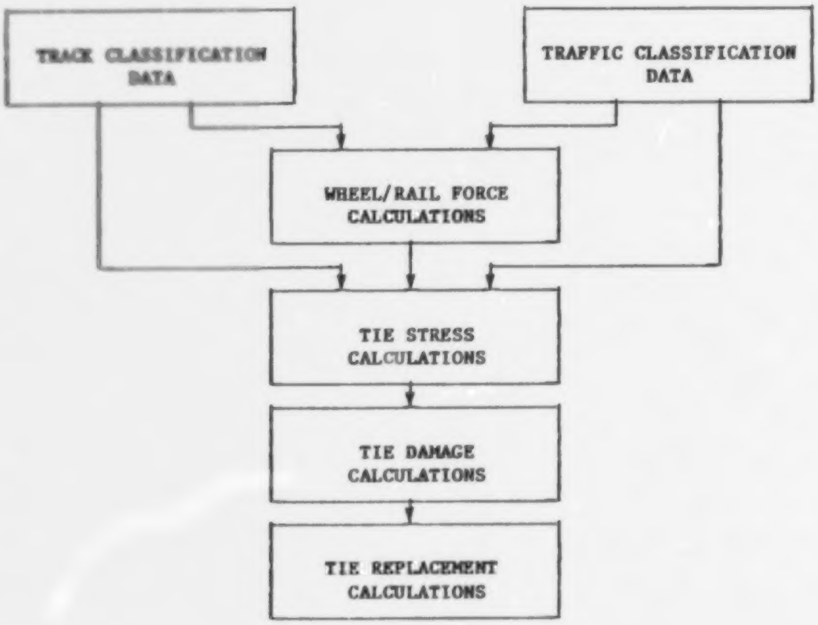
TRACK CLASSIFICATION DATA
TRAFFIC CLASSIFICATION DATA
WHEEL/RAIL FORCE CALCULATIONS
TIE STRESS CALCULATIONS
TIE DAMAGE CALCULATIONS
TIE REPLACEMENT CALCULATIONS

Figure 3.9 Tie Life Model flowchart

The underlying strategy is that a distinct series of track conditions can be identified and grouped into a finite number of classes. Each track class is considered to represent a unique set of track characteristics, as related to tie damage. The total traffic is also broken down into a distinct, finite set of traffic classes, each one representing a unique set of traffic characteristics, as related to tie damage.

The analysis is then carried out by considering the net effect on each track class when subjected to loading by each traffic class. A final summation of tie damage allows the total effect per route to be determined.

In the subsequent sections, details of the individual analysis steps in each module are outlined. The basic analysis modules are:

(a) wheel/rail estimation
(b) tie stress estimation
(c) tie damage estimation
(d) tie replacement estimation.

Initially, the analysis is done on a per track-class, per traffic-class basis, with the final tie replacement requirements being obtained by summation over the track classes.

3.2.4.2 Working equations

(a) **Wheel/rail force calculations**. The Tie Life Model uses the maximum vertical and lateral forces acting on the rail to estimate the tie damage due to loading. These forces are calculated from the steady-state and dynamic forces output from the Vehicle Dynamics Model (see Section 3.2.2).

From the force values calculated in the Vehicle Dynamics Model, the maximum vertical force is calculated as:

$$P_{max_{ij}} = P_{smax_{ij}} \quad P_{dmax_{ij}}$$

where: P_{max} = maximum vertical force (lb/wheel)

P_{smax} = maximum steady-state force (lb/wheel)

P_{dmax} = maximum dynamic force (lb/wheel)

i = track class index

j = traffic class index.

The equation for the maximum lateral force is:

$$L_{max_{ij}} = L_{smax_{ij}} + L_{dmax_{ij}}$$

where: L_{max} = maximum lateral force (lb/wheel)

L_{smax} = maximum steady-state force (lb/wheel)

L_{dmax} = maximum dynamic force (lb/wheel)

i = track class index

j = traffic class index.

(b) Tie stress calculations

Rail seat load. With normal track conditions, only a fraction of a given wheel load is transmitted to the tie. This fraction can be estimated using the following equations which are derived from the beam-on-elastic-foundation theory.

$$\frac{R_{do}}{P} = 1 - e^{-\beta a/2} \cos (\beta a/2)$$

$$\frac{R_d}{P} = \frac{e^{-\beta d}}{2} [\cos \beta d (1-e^{-\beta a} \cos \beta a) + e^{-\beta a} \sin \beta a \sin \beta d]$$

where: P = applied load (lb)

R_{do} = tie reaction below the applied load

R_d = tie reaction at distance d from the applied load

d = distance between axles

a = tie spacing

β = $(U/4EI)^{1/4}$

EI = rail stiffness (lb-in^2)

U = track modulus (lb/in./in.).

For mainline track with 132 or 136 lb/yd rails, EI = 2.7E9 lb-in.^{2} and a = 20 in., typically.

The total rail seat load fraction for a tie due to the wheel load right above it and the two 70 in. (d) adjacent wheel loads (left and right sides) can be estimated for a range of probable track moduli for wood-tie mainline track as given below:

U	1,000	2,000	3,000	4,000
$\frac{R_{do}}{P}$	.1724	.204	.226	.243
$\frac{R_d}{P}$	.084	.041	.016	.001
$\frac{R_{do}}{P} + 2\frac{R_d}{P}$	.340	.286	.258	.245

The result shows that within this range of track modulus, there is not significant change in rail seat load ratio. Therefore, an average ratio of 0.3 was adopted as the typical value to use for wood-tie mainline track. For the lateral direction, it was assumed that the same rail seat load ratio applies. This assumption should be verified in further studies.

Plate Cutting Stress. Tie cutting is the result of tie plate movement. For a given set of climatic conditions, the severity of the cut depends on the compressive stress between the plate and top surface of the tie. This stress is caused by both vertical and lateral rail seat loading onto the tie. An estimate of the stresses is given below:

From vertical load:

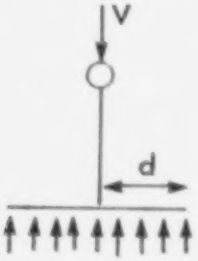

V = vertical force

d = half plate length

w = plate width (not shown)

Average compression stress = V/2dw

From lateral load:

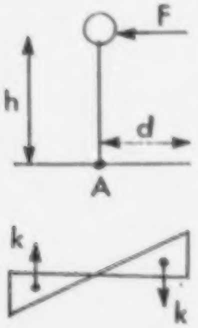

F = lateral force

h = rail height

k = equivalent reaction

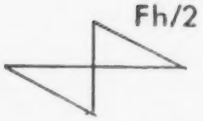

bending moment

Balance of moment at A gives:

$$Fh - \frac{4}{3} dk = 0$$

Therefore: $K = \frac{3\ Fh}{4d}$

If σ_e is the compressive stress at the outer edge, then:

$$\frac{1}{2} \sigma_e \times w \times d = k = \frac{3\ Fh}{4d}$$

Therefore: $\sigma_e = \frac{3\ Fh}{2\ d^2 w}$

Therefore, total cutting stress is given as follows:

$$\sigma_c = \frac{1}{2dw} V + \frac{3\ h}{2\ d^2 w} F$$

End splitting stress. End splitting is the result of both climatic and stress conditions. For a given climatic environment, however, the relative contribution to tie splitting by different wheel loads depends on the severity of the tie stresses which induce splitting. Since tie splitting generally occurs along the wood fibres starting at the spike holes, it was assumed that compressive stress in the fibre direction due to spike pressure and tie bending is the principal factor. An estimate of the stress is given below:

From spike pressure:

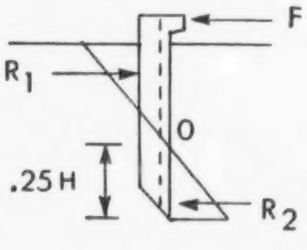

H = spike length

R_1, R_2 = reaction

0 = neutral axis, assumed to be at .25 H.

Balance of forces gives:

$$R_1 = F + R2$$

Taking moments about 0 gives:

$$R_2 \times (.25\ H \times 2/3) + R_1\ (.75\ H \times 2/3) - .75\ H\ F = 0$$

Therefore: $R_2 = .37\ F$; $R_1 = 1.37\ F$.

Splitting stress based on R_1 is:

$$\sigma_1 = \frac{R_1}{NA}$$

$$= \frac{1.37\ F}{NA}$$

where: N = number of spikes

A = contact area of spike (approximately 3 in.^{2})

From tie bending: Tie bearing surface can be estimated to extend 18 inches on each side of the rail. The reaction at tie and ballast interface due to a rail seat load, V, is thus as shown below:

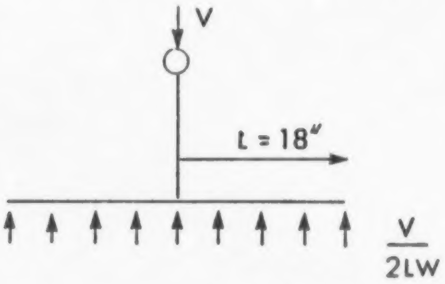

W = tie width

$V/2LW$ = reaction pressure (uniform)

Under this loading configuration, the bending moment under the rail is:

$$M = \frac{VL}{2LW} \times \frac{LW}{2} = \frac{VL}{4}$$

Compressive bending stress on the top fibre under the rail (approximate spike location) is:

$$\sigma_2 = \frac{Mt}{2I}$$

$$= \frac{VLt}{8I}$$

where: t = tie thickness

I = second moment of area

$$x = \frac{Lt}{8I}\ V + \frac{1.37}{NA}\ F$$

Therefore, total splitting stresses are given as follows:

$$\sigma_s = \sigma_2 + \sigma_1$$

(c) **Tie damage calculations:**

Tie damaging stress. The above analysis provides a method for estimating two types of stress to which a tie is subjected for each wheel load cycle. It is assumed that the cutting stress (σ_c) and splitting stress (σ_s) are the two principal stresses that contribute to overall tie damage.

A weighting formula is used to calculate an overall tie damaging stress:

$$\sigma_T = \frac{(R_c\sigma_c + R_s\sigma_s)}{(R_c + R_s)}$$

Use of this formula recognizes the fact that the different stress components have different damaging effects on the ties. In most cases it is difficult to pinpoint exactly what the cause of a tie failure is. Usually a combination of failure modes is responsible for the death and eventual replacement of a tie. However, for a given track section it is possible to determine (e.g. by "cluster sampling") the breakdown of tie failures. These values, in effect, represent the relative contributions of the respective tie damaging stresses to the overall tie damage.

Consider a track section where T ties are replaced over the period in question (usually one year). By survey, it is determined that:

a = percentage of tie failure due to cutting

b = percentage of tie failure due to splitting

c = percentage of ties replaced due to other causes (i.e. decay, derailment).

Thus, the number of ties replaced due to tie stress damage is as follows:

$$T' = T\,(a + b)$$

and of this:

a/a+b = portion of stress-damaged ties replaced due to cutting

b/a+b = portion of stress-damaged ties replaced due to splitting.

Therefore, it may be noted that:

a = R_c = portion of tie damage caused by cutting stresses

b = R_s = portion of tie damage caused by splitting stresses

σ_T = total tie-damaging stress

$$= \frac{R_c \times \sigma_c + R_s\ \sigma_s}{(R_c + R_s)}$$

Stress sensitivity and tie age. Once an overall tie-damaging stress has been established, it is necessary to relate this stress to actual tie damage for each loading cycle. The following relationship is proposed:

$$D_c = t_1\ (\sigma_T d)^{k_1}$$

where: D_c = tie damage per load cycle

t_1 = tie stress index

σ_T = tie-damaging stress

k_1 = tie age index.

(d) Tie age index (k_1). The tie age index implies an assumption that tie damage is stress sensitive, i.e. doubling the tie stress may cause more than double the damage. Within the scope of this study, the appropriate k_1 value could not be estimated. At the lower end, if the damage process is abrasion, such as the problem of gauge face wear of high rail in curved track, then k_1 equals 1. At the upper end, if the damage process is fatigue such as the problem of rail fatigue defects, then k_1 could be up to 6. Since wood ties tend to split naturally as they weather, the splitting failure under traffic loading would be more correctly dealt with as one of crack propagation (or fatigue growth rate). In this case, k_1 would be around 3 to 4 for steel [64]. Furthermore, wood is known to be much tougher (less brittle) than steel. The rate of crack propagation in wood, therefore, should be less sensitive to stress than it is in steel. This may reduce the k_1 value to 2. Since wood loses its strength with time, old ties may be more sensitive to applied stresses than new ties. This effect can be incorporated in the k_1 exponent such that it is small if ties are new and gets larger as ties grow older. Figure 3.10 illustrates this concept.

The solution adopted in this study has been to select a k_1 value of 1.5. This value of k_1 has been found to apply to good quality track. Deteriorating track conditions can be reflected in the model by increasing k_1 values accordingly (see Appendix C on Calibration).

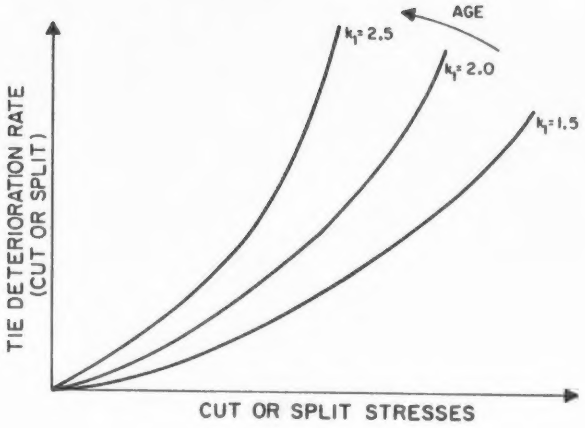

Figure 3.10 Effect of stress and tie age on tie deterioration rate

(e) **Tie stress index (t_1).** The tie stress index indicates a linear relationship between the tie-damaging stress and the actual tie damage. Since the individual components of the tie-damaging stress have been calculated as functions of track and traffic characteristics, it is assumed that relative tie-damaging forces due to different loading characteristics of the different traffic classes have been accounted for.

Tie damage. Now that a level of tie damage per load cycle (D_c) has been estimated, a total level of tie damage per year can be calculated.

Let N_{ij} equal the number of load cycles per year on track class i due to traffic class j. Then:

$$D_{ij} = N_{ij} \times D_{cij}$$

is equal to the total tie damage per year, per tie, for track class i, due to traffic class j. If this value is thought of in terms of ties/year, then the tie life of ties in track class i, subjected to traffic class j, can be considered to be $1/D_{ij}$.

Since the ties of track class i are subjected to the damaging stresses of every traffic class over that route, the total tie damage per year can be calculated as:

$$D_i = \sum_j D_{ij}$$

$$= \sum_j N_{ij} \times D_{cij}$$

and tie life per track class can be estimated as:

$$\text{TIE LIFE} = 1/D_i$$

(f) **Tie replacement**. Given that each track class, i, has an associated length, L_i, the total number of ties per track class i can be calculated as:

$$T_i = \frac{63360 \times L_i}{t}$$

where: T_i = number of ties per track class i

L_i = length of track class i (miles)

t = tie spacing (in.)

63360 = number of inches per mile.

Since the total tie damage per year was determined to be D_i (ties/year), the number of ties to be replaced per year can be established as follows:

$$T_{Ri} = T_i \times D_i$$

and the total number of ties to be replaced per year for the total route can be established as follows:

$$T_R = \sum_i T_{Ri}$$

3.2.4.3 Simplification of stress equations

In order to limit the complexity of the input required to the Tie Life Model, some simplifications were made with regard to the coefficients used in the stress equations. These are listed below.

(a) **Cutting stress**:

$$\sigma_c = \frac{1}{2dw} V + \frac{3h}{2d^2w} F$$

where: σ_c = cutting stress (psi)

V = vertical seat load (lb)

F = lateral seat load (lb)

d = half tie plate length (in.)

w = tie plate width (in.)

h = rail height (in.).

The equation is simplified as follows:

$$\sigma_c = \frac{1}{7.75\ L_1} V + \frac{12\ C}{7.75\ L_1^2} F$$

where: L_1 = tie plate length (in.)

C = rail neutral axis height (in.)

by setting $d = L_1/2$

$w = 7.75$ in.

and assuming $h = 2\ C$.

(b) **Splitting stress**

$$\sigma_s = \frac{Lt}{8I} V + \frac{1.37}{NA} F$$

where: σ_s = splitting stress (psi)

V = vertical seat load (lb)

F = lateral seat load (lb)

L = length of tie bearing surface (18 in.)

t = tie thickness (in.)

I = tie second moment of area

N = number of spikes

A = contact area of spike (in.^{2}).

The equation is simplified as follows:

$$\sigma_s = 0.0612\ V + \frac{0.457}{N} F$$

by setting $I = t^3\ w_1/12$

where w_1 = tie width = 9 in.

L = 18 in.

A = 3 in.^{2}

$t = 7$ in.

3.2.4.4 Model Calibration

(a) **Calibration Indices.** As with any simulation model, this model has several indices which need to be adjusted, or calibrated, so as to tune the model so that it will produce results consistent with actual data.

In the Tie Life Model the calibration indices are:

R_c = percentage of ties replaced due to cutting

R_s = percentage of ties replaced due to splitting

t_1 = tie stress index

k_1 = tie age index.

An initial calibration was done based on CP tie replacement data from the Cascade subdivision (main line, up to 33-ton axle loads, 40-45 MGT per year) between 1965 and 1982.

The resulting indices are as follows (see Appendix C):

$R_c = 36.7$

$R_s = 56.0$

$t_1 = 5.05 \times 10^{-12}$

$k_1 = 1.5.$

(b) **Results and validation.** Predicted tie replacements are shown in Figure 3.11 (• points). This curve corresponds very well with the general trend line on actual tie replacement.

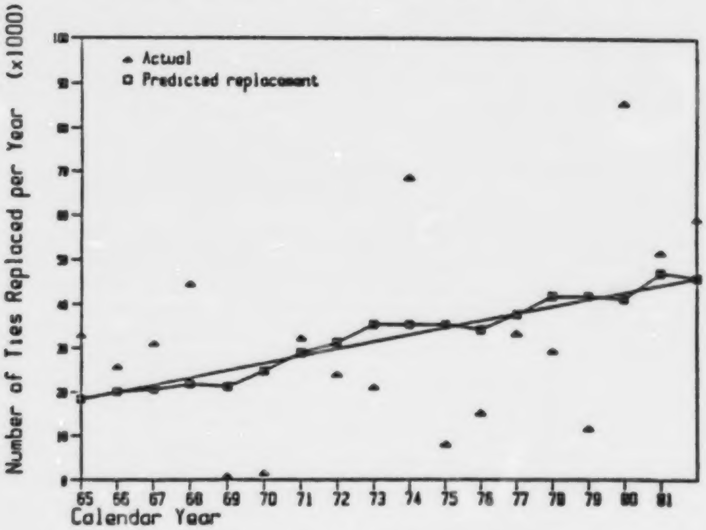

Figure 3.11. Annual tie replacement

(c) **Calibration Procedure.** For detailed calibration procedure of the Tie Life Model, see Appendix C.

3.2.5 Surface Life Model

3.2.5.1 Introductory Remarks

The principal method of correcting track surfacing error is tamping. It is routinely carried out by manual work gangs. Periodically, when track error is beyond the capacity of the local work gangs, mechanized equipment is provided by the region for a systematic reconditioning of track geometry. This is known as a surfacing cycle. Since ballast also degrades under traffic, a small amount of ballast is added at each surfacing cycle to compensate for the degradation. This is known as lifting.

The basic criteria for surfacing work on North American railroads are maximum allowable track geometry error limits. Known as Standard Practice Circular (SPC) limits, these are set for safety reasons and are listed in the Standard Practice Circular. Normally, the magnitude of track errors increases under traffic but their position (i.e. spatial distribution) is unchanged. Consequently, the manual tamping work usually involves inspecting and correcting the usual problem sites.

The relationship between mechanized and manual surfacing work can be described mathematically by considering the track as a long chain of individual elements (see Figure 3.12). Each element would deviate from the ideal geometry by a certain amount called error. Most elements have errors below the safety limit and make up the "good" portion of the track. A few have errors above the safety limit and must be corrected. These make up the "poor" portion of the track. Note that "poor" track is not fully condemnable. Typically, the length of a track error element is 39 feet (i.e. original rail length). A condemnable error at each rail length requires (manual) tamping of approximately three ties (about 5 feet). This is only about 13 percent of the rail length. Thus, for each mile of "poor" track, only 0.13 miles needs repair.

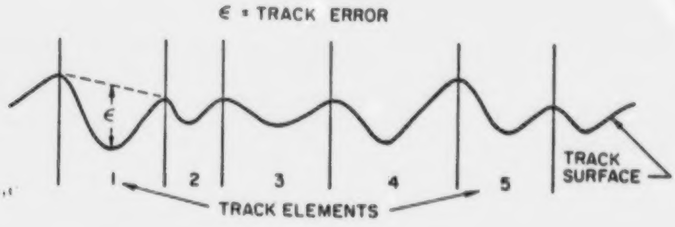

Figure 3.12 Idealized representation of track geometry errors

Assuming that track errors are normally distributed with a mean (x) and standard deviation (s) the relationship between track condition and work load is as follows:

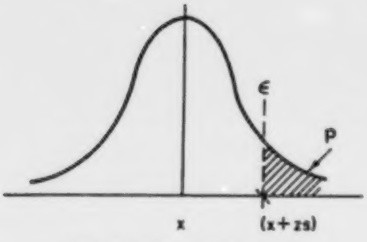

TRACK ERROR DISTRIBUTION

p = percent of "poor" track

$$= f(z) = \int_{-\infty}^{x} \frac{1}{\sqrt{2\pi}} \, e^{-u^2/2} \, du$$

where: $z = (\varepsilon - x)/s$

ε = safety limit.

The distribution of track error can be readily established using a track geometry recording car. From this, the percent of poor track can be calculated for a given set of safety limit criteria.

"Percent of poor track" is a relevant parameter representing overall track geometry quality. It is implicitly used in the current process of surfacing planning on North American railroads. Figure 3.13 summarizes this concept.

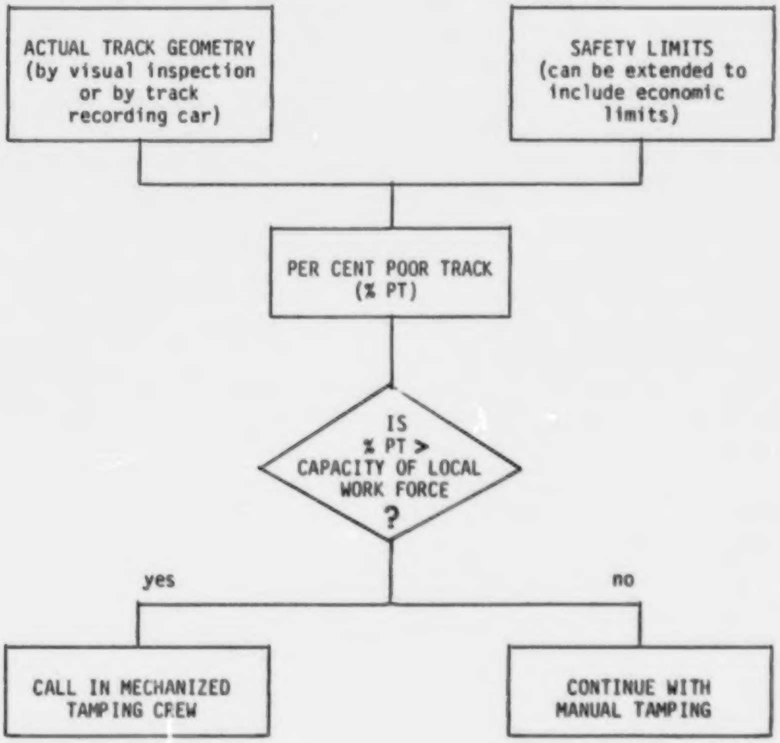
ACTUAL TRACK GEOMETRY (by visual inspection or by track recording car)
SAFETY LIMITS (can be extended to include economic limits)
PER CENT POOR TRACK (% PT)
IS % PT > CAPACITY OF LOCAL WORK FORCE ?
yes
no
CALL IN MECHANIZED TAMPING CREW
CONTINUE WITH MANUAL TAMPING

Figure 3.13 "Percent poor track" as a criterion for mechanized tamping cycle

3.2.5.2 Model outline

Figure 3.14 outlines the structure of the Surface Life Model. As with the Tie Life Model, the analysis has been divided into a series of steps. This structure keeps the analysis simple, while allowing easy upgrading of individual components.

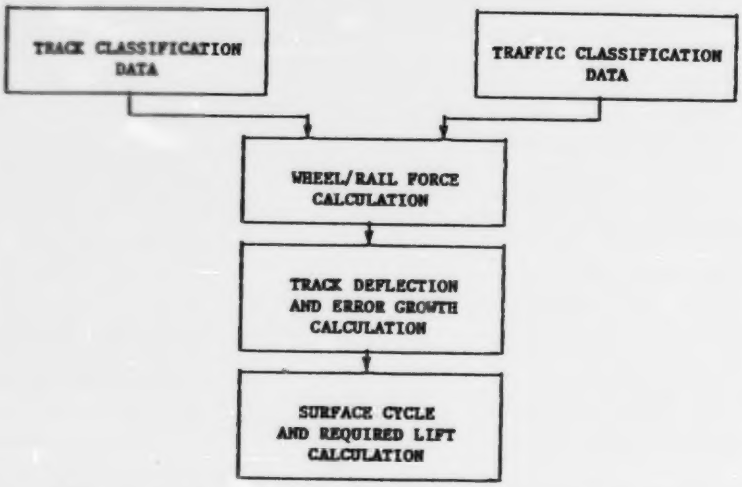
TRACK CLASSIFICATION DATA
TRAFFIC CLASSIFICATION DATA
WHEEL/RAIL FORCE CALCULATION
TRACK DEFLECTION AND ERROR GROWTH CALCULATION
SURFACE CYCLE AND REQUIRED LIFT CALCULATION

Figure 3.14 Surface Life Model flowchart

The analysis is carried out on a per track-class, per traffic-class basis, until a number of normalized wheel load cycles are generated. The normalization standardizes all traffic loading cycles according to their relative significance to track surface degradation. After the total number of normalized wheel load cycles is calculated for a track class, the surfacing cycle and required lift are then estimated.

A detailed outline of the individual analysis steps is presented in the following sections. The basic components of the analysis are:

(a) wheel/rail force calculation
(b) track deflection and error growth calculation
(c) surfacing cycle and required lift calculation.

3.2.5.3 Working equations

The Surface Life Model uses the maximum and minimum vertical wheel forces acting on the high and low rails. These forces are calculated from the steady-state and dynamic force outputs from the Dynamic Wheel Force Model (see Section 3.2.2).

HIGH RAIL MAXIMUM FORCE

$$P_{H_{maxij}} = P_{H_{Sij}} + P_{H_{Dij}}$$

where: $P_{H_{maxij}}$ = high rail maximum force (lb/wheel)

P_{H_S} = high rail steady-state force (lb/wheel)

P_{H_D} = high rail dynamic force (lb/wheel)

i = track class index

j = traffic class index.

HIGH RAIL MINIMUM FORCE

$$P_{H_{minij}} = P_{H_{Sij}} - P_{H_{Dij}}$$

Similarly,

LOW RAIL MAXIMUM FORCE

$$P_{L_{maxij}} = P_{L_{Sij}} - P_{L_{Dij}}$$

LOW RAIL MINIMUM FORCE

$$P_{L_{minij}} = P_{L_{Sij}} - P_{L_{Sij}}$$

(a) **Track deflection and error growth calculations**

Concept. If traffic is uniform (e.g. all unit trains), the relationship between track geometry error growth and wheel loading cycle can be empirically determined by a regression analysis of actual data.

If, however, traffic is not uniform, the actual wheel loading cycle must first be normalized. Normalization converts the actual wheel cycles into the equivalent cycles of the reference traffic type. The normalization must be based on the relative significance of different wheel loads on track geometry degradation. The reference wheel load should be from the main traffic type in a traffic mix.

The current understanding of track degradation under traffic and a corresponding procedure for normalization of the wheel loading cycle are described next.

Outline of track geometry degradation. Research to date on track geometry degradation has indicated that under traffic the amplitude of track errors grows but their positions (i.e. spatial distribution) remain basically unchanged (see Figure 3.15).

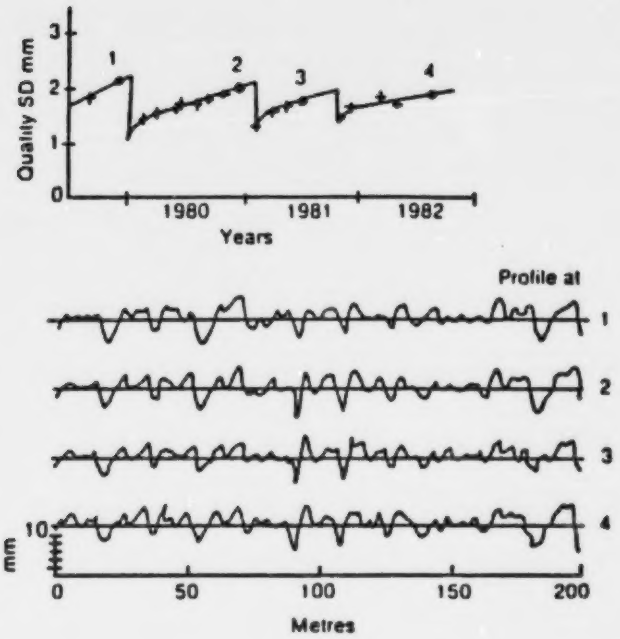

Source: M.J. Shenton [43]

Figure 3.15 The vertical profiles of a section of track towards the end of four maintenance cycles

For a given track location with errors, the trough area receives maximum dynamic load (nominal load plus dynamic increment), while the peak area receives minimum dynamic load (nominal load minus dynamic increment). This happens under each wheel load of the total traffic mix. The trough area, therefore, settles faster than the peak area, resulting in a differential settlement rate which increases track error amplitude (see Section 2.3.1.1). Figure 3.16 shows is process.

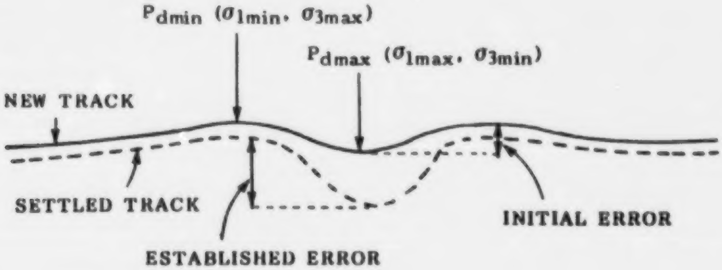
P_{dmin} (σ_{1min}, σ_{3max})
P_{dmax} (σ_{1max}, σ_{3min})
NEW TRACK
SETTLED TRACK
ESTABLISHED ERROR
INITIAL ERROR

Figure 3.16 Track differential settlement and error growth

Given a wheel load, the settlement rate is a function of the following factors:

- stress exerted on the ballast
- number of loading cycles
- compressibility of the subgrade
- ballast quality.

A detailed discussion of these factors was presented in Section 2.3. The factors will only be discussed here on the basis of their direct relationship to the Surface Life Model.

Effect of stress on ballast. For any given track design, different wheel loads create different stresses on the track bed, resulting in different track settlement rates. CN test data (Figures 3.17 and 3.18) has shown that most track settlement occurs within the ballast/ subballast layer. This is expected to be generally true for track which is properly designed and maintained.

Test results from laboratory studies on ballast settlement (small-scale triaxial tests and large-scale ballast box tests, see Section 2.3) have indicated a general increase in track settlement with applied stress. The relationship is not well defined due to the complexity of the ballast medium. In Section 2.3 it was shown that track settlement after a given number of load cycles is proportional to ballast stress raised to a power of 1 to 3 [42,46-51,59], depending on ballast depth and quality and traffic loads.

The relationship between track settlement and ballast stress requires further investigation, especially for typical North American track conditions. For the time being, it may be estimated from recent research findings that the track settlement rate is proportional to the square of ballast stress.

Effect of load cycle accumulation. Data on actual track settlement on CN track, recorded in a four-year test program by the CN Rail Research Centre [58], showed quite consistently that long-term permanent settlement of track increased linearly with time (Figures 3.17 and 3.18). The relationship is agreeable with data from British Rail Research [43] and BHP Melbourne Research Laboratories [59].

The problem of frost heaving (reflected in Figures 3.17 and 3.18) during the winter months affects the settlement rate temporarily. On average, track settlement during the frost heave period, which normally would include several freeze/thaw cycles and an extended period in a frozen-solid state, occurs at approximately the same rate as during the rest of the year.

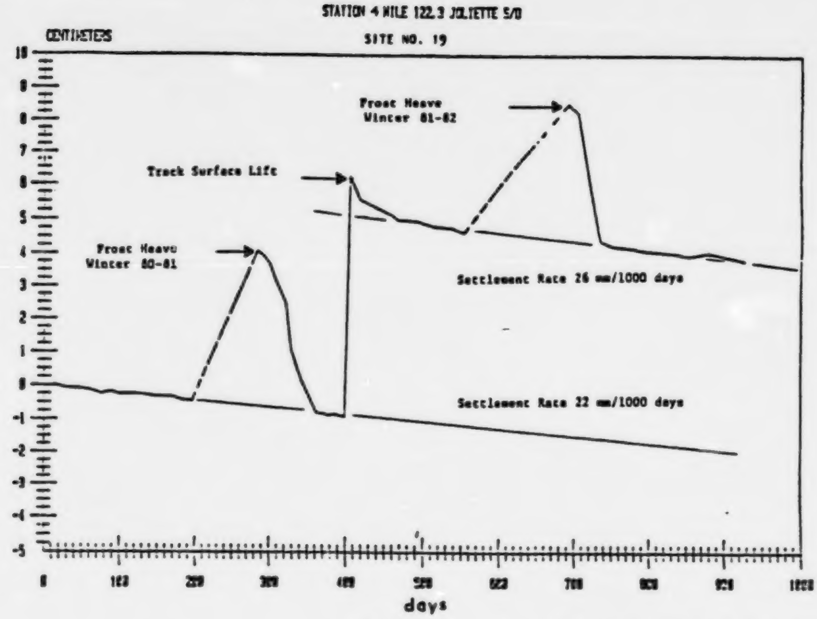

Source: C.J. Dalton and J.F. Scott [58]

Figure 3.17 Total track settlement measured at rail level

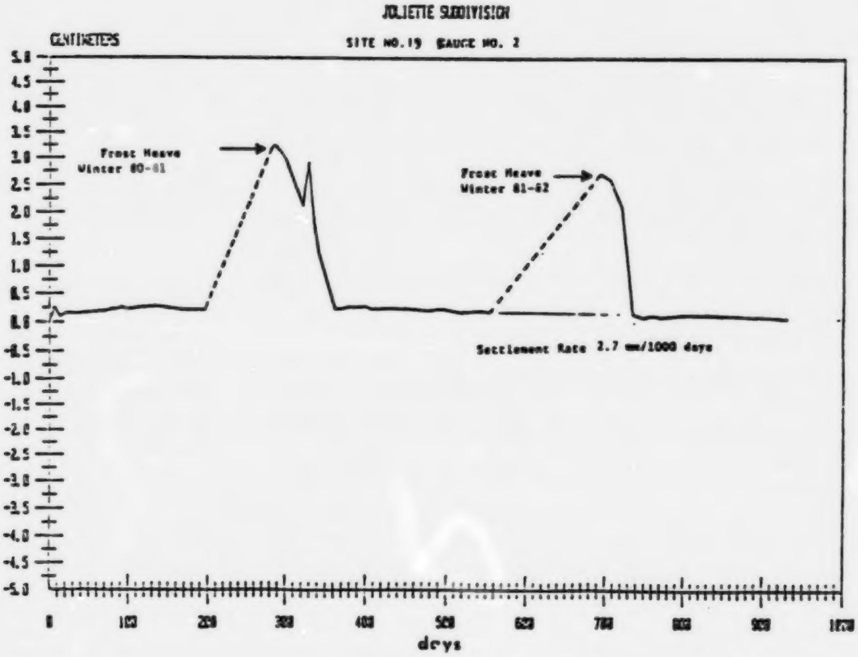

Source: C.J. Dalton and J.F. Scott [58]

Figure 3.18 Subgrade settlement measured at top of subgrade, 20" below base of tie

The effects of a small surface lift (a few inches) is also temporary. There is a period of two to three months following the lift when the track settlement rate is high and decreases rapidly with time. Beyond this period, the track settlement rate becomes constant with time. Depending on the height of the lift and the subgrade conditions, the new track settlement rate may increase slightly after a surface lift.

CN data on traffic density during the test period indicated little change in annual tonnage. Assuming that the traffic mix also did not change much (i.e. no significant increase or decrease in the heavy-axle-load category), the time factor in track settlement measurements could be considered equivalent to the wheel load cycle. Thus, the following can be inferred from the CN test:

(a) long-term permanent track settlement increases linearly with the wheel-loading cycle

(b) frost heaving and small surface lifting have no significant affects on long-term track settlement rate.

As mentioned in Section 2.3.1.1, large surface lifts (e.g. during ballast undercutting and cleaning) rarely occur, while small surface lifts (e.g. during mechanized tamping) occur only infrequently (e.g. every few years). Thus, for most of the remaining time of a surfacing cycle (from two to ten years), a linear relationship prevails. For a practical analysis of track maintenance, the linear relationship will be used and the rapid settlement following a surface lift treated as part of the overall efficiency of the tamping process (i.e. an effective lift equals actual lift minus immediate settlement).

Effect of ballast quality. Ballast breakdown is one of the major contributors to track settlement. The mechanism by which this process takes place was described in Section 2.3.1.2.

The research results outlined in Section 2.3.1.2 indicate a strong relationship between ballast quality and track settlement rate, but do not provide sufficient data for a reliable quantification. Further research into the effect of particle shapes and the percent fines (i.e. degree of fouling) produced by ballast degradation is needed. For the present it is assumed that the track settlement rate is proportional to the aggregate index (I_a).

Effect of subgrade compressibility. It is a well-known fact that track built on a weak subgrade settles at a high rate. Preliminary laboratory tests at Queen's University [60] using a large-scale track section model with various types of subgrade material clearly indicated this trend.

In practice, areas of weak subgrade are given extra granular cover to reduce subgrade stress. The track section, if properly treated, would behave as if the subgrade is the same quality as nearby track built on stronger subgrade. This practice makes it very impractical to characterize actual track with its subgrade compressibility.

Usually, track within a category is designed with the same standard, i.e. same rail and tie. Therefore, if there is any variation in the overall track stiffness (known as track modulus), it is due to the compressibility of the combined ballast/subgrade layer. If the ballast layer is constant (i.e. same aggregate and same thickness), the variation is due to subgrade (hence the problem is reduced to the laboratory test case).

Track modulus can therefore be used as a variable representing track support compressibility in the study of actual track settlement. However, this use is correct only if rail and tie are the same (e.g. a change in track modulus due to the use of concrete ties may not relate to track settlement in the same way).

Combined effect of ballast stress and subgrade compressibility. Both ballast stress and subgrade compressibility contribute to elastic track deflection. Using a beam-on-elastic-foundation model for track support and using wheel load and track modulus to represent ballast stress and subgrade compressibility, respectively, this relationship is formulated as follows [61]:

$$y = \frac{P\beta}{2U} \cdot e^{-\beta x} (\cos \beta x + \sin \beta x)$$

$$\beta = \left(\frac{U}{4EI}\right)^{1/4}$$

where: y = elastic track deflection (in.)

EI = rail section modulus (lb.in.^{2})

P = wheel load (lb)

U = track modulus (lb/in.^{2})

x = wheel position (in.).

The total elastic track deflection is the sum of deflections due to the load from each contributing wheel. Most of the deflection is due to the wheel right above the location ($x = 0$). The rest is from the adjacent wheel on the same truck and the last wheel on the adjacent car. For the current analysis, it is assumed that track elastic deflection is caused by three wheels, one at $x = 0$, and others 70 inches on either side. The total track deflection is therefore:

$$Y = \frac{P\beta}{2U} (1 + 2\, e^{-70\beta} (\cos 70\, \beta + \sin 70\, \beta)$$

Summary. The above equations and discussions can be summarized as follows:

TRACK ERROR

$$\varepsilon \; \alpha \; (S_{max} - S_{min})$$

where: ε = track error amplitude

S_{max} = track settlement under maximum dynamic wheel load (on trough area)

S_{min} = track settlement under minimum dynamic wheel load (on peak area)

TRACK SETTLEMENT

Under uniform traffic, the track settlement rate is proportional to the number of loading cycles, i.e.

$$S \; \alpha \; N$$

The track settlement rate is proportional to the square of elastic track deflection:

$$S \; \alpha \; \text{constant } Y^2$$

where Y is as defined above in Section (vii).

The track settlement rate is proportional to the aggregate index of ballast:

$$S \; \alpha \; I_a$$

The following equation was developed and used in the Surface Life Model to define track settlement per wheel load cycle S (in./cycle).

$$S = k_2 \cdot Y^2 \cdot I_a$$

where: $Y = \frac{P\beta}{2U} (1 + 2 e^{-70\beta} \cdot (\cos 70 \beta + \sin 70 \beta))$

$\beta = (\frac{U}{4EI})^{1/4}$

k_2 = calibration constant

Y = elastic track deflection (in.)

I_a = aggregate index

P = dynamic wheel load (lb)

U = track modulus ($\mathrm{lb/in.}^2$)

EI = rail section modulus ($\mathrm{lb.in.}^2$).

Differential track settlement (i.e. track error growth rate) per wheel loading cycle is given by:

$$\Delta S = \frac{k_2}{2} \left[(S_{Hmax} - S_{Hmin}) + (S_{Lmax} - S_{Lmin}) \right]$$

where: S_{Hmax} = maximum track settlement rate on high rail (calculated with P_{Hmax})

S_{Hmin} = minimum track settlement rate on high rail (calculated with P_{Hmin})

S_{Lmax} = maximum track settlement rate on low rail (calculated with P_{Lmax})

S_{Lmin} = minimum track settlement rate on low rail (calculated with P_{Lmin})

(b) Surfacing cycle and required lift calculations

Surfacing cycle. The track error growth function gives the track geometry error level after each year of traffic accumulation. The corresponding percent of poor track can be calculated using the procedure described in Section 3.2.5.1. By matching this against the allowable average percent poor track in the subdivision, the limit of traffic accumulation can be determined. This is then converted into surfacing cycle (years) for a given traffic density.

Consideration of ballast fouling. A study by CP Rail has produced an empirical relationship between traffic and ballast fouling as shown in Figure 3.19. Traffic is represented by total tonnage (in millions of gross tons). Ballast fouling is represented by the reduction in the depth of the clean, free-draining ballast layer (in inches). Ballast quality is represented by the aggregate index (called abrasion number by CP). An empirical curve is provided for each ballast grading. For grading number 4 (common for a main line), the mathematical expression of the empirical relationship is:

$$d = 3.73\ \mathrm{E}\text{-}5\ (I_a)^{1.54}$$

where: d = ballast fouling rate (inch/MGT)

I_a = aggregate index.

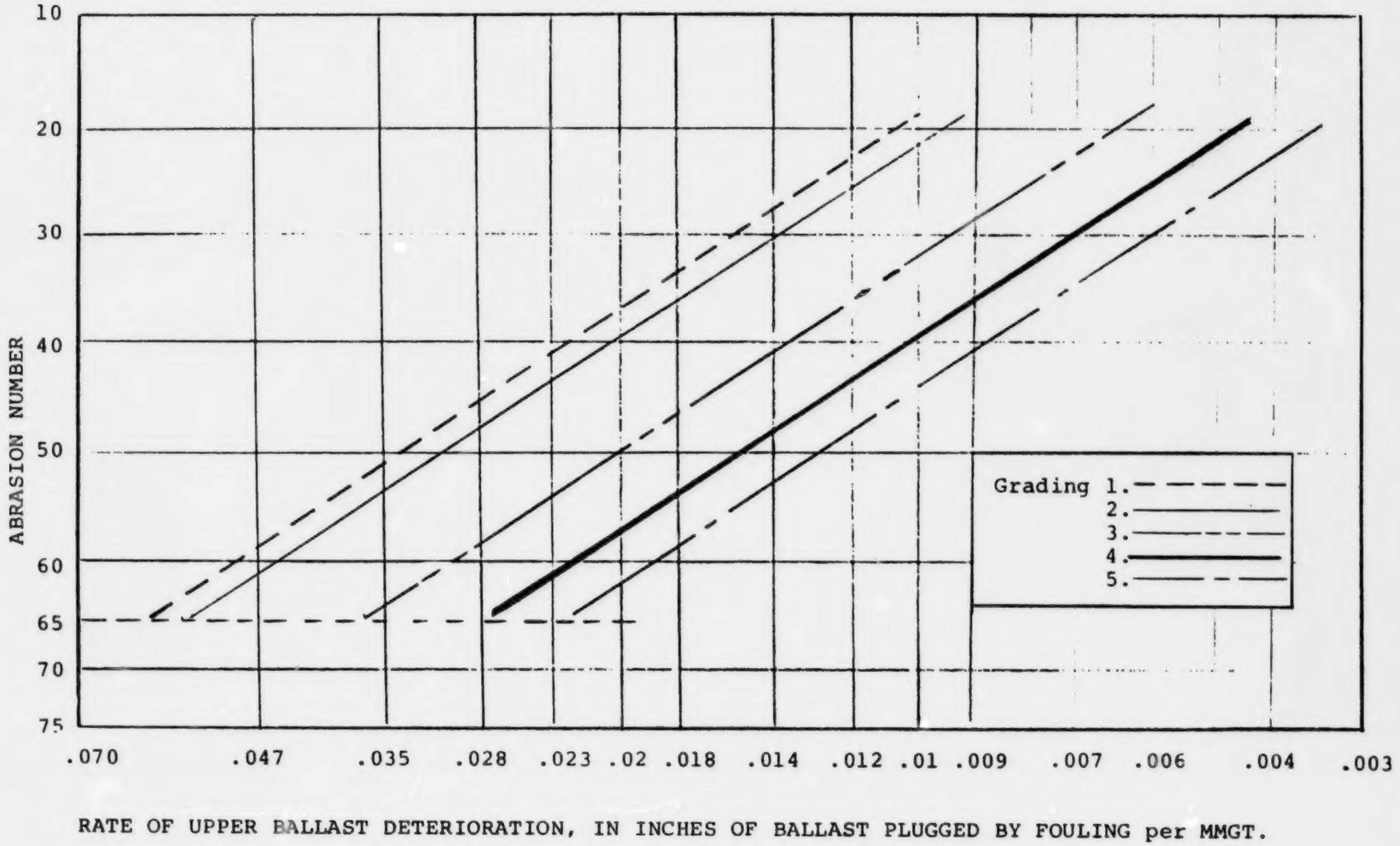

Note: Developed for tangent track with 7 in. of Ballast below tie. A small amount of contamination from outside sources has been taken into consideration.

Caution: Excessive handling of ballast materials in the upper range of Abrasion numbers may generate fines which will reduce applicable cumulative tons of rail traffic.

Figure 3.19 Upper ballast deterioration rate versus abrasion number for different gradations

Height of lift. The following equation was developed and used in the Surface Life Model to estimate the required lift for a given surfacing cycle.

If n (year) is the surfacing cycle, and X (MGT) is the annual tonnage, the depth of fouled ballast is:

$$D_f = 3.37\ \text{E-5}\ (I_a)^{1.54} \times nX\ \text{(in.)}$$

A lift has to be slightly greater than D_f to compensate for the initial track settlement due to compaction. CN data [58] showed that at one test site a lift of 3 inches was followed by an initial track settlement of 0.45 inch. Assuming that the initial settlement is proportional to the height of the lift, the following equation is proposed for the estimation of lift:

$$D_\ell = 1.175\ D_f$$

where: D_ℓ = height of lift (in.)

D_f = depth of fouled ballast (in.).

Limit of surfacing cycle due to ballast fouling. Normally, surfacing maintenance is carried out because of track geometry error. Ballast fouling accelerates track geometry deterioration, and hence indirectly influences the surfacing cycle. The general relationship is therefore:

BALLAST FOULING
↓
TRAFFIC ⟶ ⟷ TRACK GEOMETRY DETERIORATION ⟶ SURFACING CYCLE

Although this relationship is implicitly incorporated in the calibration, the analysis of the surfacing cycle does not formally incorporate the degree of ballast fouling into the track geometry deterioration calculation. This would cause an error if the changes in track, traffic and operating conditions result in a projected new surfacing cycle which is considerably longer than the existing one. This is because the track deterioration rate in later years of the projected cycle would be higher due to a larger degree of ballast fouling compared to the rate calibrated based on data from earlier years. Further research is still needed in this area.

For a track in which the overall ballast condition is not allowed to deteriorate greatly (e.g. 6 to 8 inches of good clean ballast, surfaced every few years with a small lift of 1 to 2 inches), the above flaw in the analysis will not be critical.

3.2.5.4 Surface Life Model calibration

Details of the calibration procedure for the Surface Life Model are given in Appendix C.

3.3 Application of Track System Model to Component Improvement and Maintenance Management

The Track System Model (TSM) can be used effectively to improve track component life and optimize track management decisions.

The model must be calibrated to reflect the current nature of the track system and its condition. It must be at least qualitatively validated to be useful. That is, the trends it produces must match actual system characteristics or at least be agreeable with the experience and/or opinions of track maintenance personnel. There is always a problem with insufficient and/or distorted data. Therefore, engineering and management judgements are always necessary. Despite this, the TSM approach is, in the long run, more objective, rational, orderly and technically superior to any individual track person's opinion. It is a vehicle in which all available knowledge and experience can be incorporated.

To improve track component life, one must first identify the relative contribution to the actual track component replacement by each known deterioration mechanism. For example, rail life is known to be affected by corrugation, shelling, gauge face wear and surface fatigue defects. However, the extent of the contribution to actual rail replacement made by each of these causes varies from case to case. In places where surface fatigue defects are the main cause of premature rail changeout, measures which are effective against this problem can be identified and evaluated using TSM to guide an implementation decision.

TSM can also be used to optimize the frequency and extent of existing maintenance routines to maximize their benefit in terms of component life and/or maintenance cost. One well known example of this is the optimization of rail grinding cycles. The experience of the Australian iron ore railways [66] has shown that an optimal rail grinding cycle can be developed to both increase rail life and reduce rail grinding cost.

Finally, TSM will be a useful tool for management in evaluating the impact of certain proposed decisions. Such evaluation takes into account the complex interaction of various track components with traffic and among themselves, and hence can provide the kind of information which more accurately reflects system behaviour and leads to overall system improvement.

3.4 Recommendations for Further Work on the Track System Model

1. The Track System Model (TSM) requires a detailed sensitivity analysis to establish the relative importance of all input variables in order to prepare for a comprehensive model calibration. The sensitivity analysis and proper model calibration are the keys to achieving reliable predictions of track deterioration.

2. The above work requires that field data be collected and supplied by the railways, at times, a most difficult task. Railways have only recently begun to collect some of the data necessary for prediction of track deterioration. They are still far from having all the required data, or even from having the processes required to collect some of the data. The only way to obtain this data, or at least initiate the process for collecting certain data, is to show the need for it. Models such as TSM are ideal for this purpose. Development of TSM has clearly highlighted some of the shortcomings of the existing data.

3. TSM is currently in spreadsheet format. The Wheel Force, Tie Life and Surface Life modules have been converted to Fortran coding. Rail Life module is yet to be converted. In addition, and perhaps most important, the algorithm used in predicting rail life needs additional work. In the past three or four years, research has added considerably to the knowledge of the mechanisms involved in the process of rail deterioration. In order to have a more reliable tool for predicting rail life, some of the recent findings on the relationships between rail forces and wear and fatigue development must be quantified in a suitable form and incorporated into the Rail Life Model.

4. The Rail Life, Tie Life and Surface Life Models in TSM all use the predicted forces from the Wheel Force Model. The force equations in this model were based on data from 100-ton hopper cars. These equations were applied to various cars with different loads by converting the imposed loads to the unsprung mass. With proper data for additional car types (other than 100-ton hopper cars), the validity of this approach can be investigated further, and if necessary the equations can be revised or upgraded accordingly. The equations developed and used in the other modules may also be upgraded continually as more research findings become available on the degradation process of various track components.

REFERENCES

1. Marich, S., "Research on Railway Metallurgy," Bulletin 663, American Railway Engineering Association, June-July 1977.

2. Sonon, D.C., Pellegrino, J.V., and Wandrisco, J.M., "A Metallurgical Examination of Control-Cooled Carbon-Steel Rails with Service Developed Defects," ASME Symposium on Rail Steels, Denver, November 1976.

3. Marich, S., and Curcio, P., Development of High Strength Alloyed Rail Steels Suitable for Heavy Duty Applications, BHP Melbourne Research Laboratories, Report MRL/083/76/015, Melbourne, Australia, June 1976.

4. Fowler, G.J., and Tetelman, A.S., "The Effect of Grain Boundary Ferrite on Fatigue Crack Propagation in Pearlitic Rail Steels," ASTM Symposium on Rail Steels, Denver, November 1976.

5. Ghonem, H., Kalousek, J., Stone, D.H., and Dibble, D.W., "Observations of Rail Wear on Heavy Haul Railway Lines," Contact Mechanics and Wear of Rail/Wheel Systems, Proceedings of the International Symposium, Vancouver, 1982.

6. King, F.E., and Kalousek, J., "Rail Wear and Corrugation Studies," Bulletin 658, American Railway Engineering Association, 1976.

7. Steele, R.K., and Reiff, R.P., "Rail: Its Behaviour and Relationship to Total System Wear," Proceedings of the Second International Heavy Haul Railway Conference, Colorado Springs, CO., 1982, paper 82-HH-24.

8. Fegredo, D.M., Kalousek, J., Shehata, M.T., and Palmer, A.R., "The Effect of Sulphide and Oxide Inclusions on the Wear Rates of Standard and Alloy Rail Steels," Proceedings of the Third Heavy Haul Railway Conference, Vancouver, B.C., 1986.

9. Kalousek, J., Ghonem, H., and Steele, R.K., 11th Leeds-Lyons Symposium on Tribology, Mixed Lubrication and Lubricated Wear, Mechanical Engineering Publications, 1985.

10. Moucessian, A., Lamson, S.T., and Driscoll, A Review of Rail Steel Cleanliness and its Effects on Rail Performance, Report No. 86-24, Canadian Institute of Guided Ground Transport, Queen's University, Kingston, Ontario, December 1986.

11. Kalousek, J., and Bethune, A.E., "Rail Wear Under Heavy Traffic Conditions," ASTM Symposium on Rail Steels, Denver, November 1976.

12. Clark, R.A.P., "Rail Corrugation -- Recent Theories," Track Technology for the Next Decade, published for the Institution of Civil Engineers by Thomas Telford Limited, London, 1984.

13. Mair, R.I., "Track Design to Prevent Long Pitch Rail Corrugation," Bulletin 692, American Railway Engineering Association, 1983.

14. Bower, A.F., Johnson, K.L., and Kalousek, J., "A Ratcheting Limit for Plastic Deformation of a Quarter-space Under Rolling Contact Loads," Second Symposium of Contact Mechanics, Rhode Island, July 1986.

15. Lamson, S.T., Rail Profile Grinding, Report No. 82-7, Canadian Institute of Guided Ground Transport, Queen's University, Kingston, Ontario, November 1982.

16. Lamson, S.T., Rail Profile Grinding, Phase II Test Report, Report No. 84-14, Canadian Institute of Guided Ground Transport, Queen's University, Kingston, Ontario, February 1985.

17. Stone, D.H., and Steele, R.K., "The Effect of Mechanical Properties Upon the Performance of Railroad Rails," ASTM Symposium on Rail Steels, Denver, November 1976.

18. Lamson, S.T., and Dowdall, B., Tie Life Model, Report No. 84-12, Canadian Institute of Guided Ground Transport, Queen's University, Kingston, Ontario, January 1985.

19. Bowlby, R.E., "The Economics of Wood Ties," Crossties, March 1983.

20. FIP Commission on Prefabrication -- Working Group on Concrete Sleepers, "Concrete Railway Sleepers, A State-of-the-Art Report," second draft, August 1985.

21. Driscoll, M.L., and Lamson, S.T., "Assessment of Steel Railway Ties," Report No. 85-8, Canadian Institute of Guided Ground Transport, Queen's University, Kingston, Ontario, October 1985.

22. Scott, J.F., "Assessing Concrete Ties in Bridges and Turnouts," Railway Track and Structures, August 1986.

23. Buekett, J., "Concrete Sleepers," Railway Industry Association, First Track Sector Course held at Watford, U.K., 1983.

24. Gylltoft, K., "Fatigue Tests of Concrete Sleepers," University of Lulea, Division of Structural Engineering, Research report TULEA 1978:13, Lulea, 1978.

25. Scott, J.F., and McDonald, J.W., Evaluation of Pads and Insulators for Use on Concrete Ties, Transport Canada Report No. TP7174E, October 1985.

26. Brown, J.H., and Skinner, D.H., "The Development of a Steel Sleeper System for Heavy Haul Railways," Proceedings of 1st Heavy Haul Railway Conference, Perth, Western Australia, September 1978.

27. Frost, N.E., March, K.J., and Pook, L.P., Metal Fatigue, Claredon Press, Oxford, 1974.

28. O'Rourke, M.D., Mair, R.I., and Doyle, M., "Towards the Design of Track for Heavy Axle Loads," Proceedings of the 1st Heavy Haul Conference, Perth, Western Australia, September 1978.

29. Brown, J.H., Testing of Steel Sleeper Systems and Recommendations on a Steel Sleeper for Heavy Axle Loads, BHP Melbourne Research Rep., MRL/075/77/008, August 1977.

30. Driscoll, M.L., and Lamson, S.T., Assessment of Steel Railway Ties, Report No. 85-8, Canadian Institute of Guided Ground Transport, Queen's University, Kingston, Ontario, October 1985.

31. Zarembski, A.M., "Performance Characteristics of Wood Ties Fasteners," AREA Bulletin 697, Vol. 85, 1984.

32. Roney, M.D., "Economic Aspect of the Wear of Rail on Canadian Railways," International Symposium on Contact Mechanics and Wear of Rail/Wheel Systems, Vancouver, B.C., July 6-9, 1982.

33. Scott, F., personal correspondence, 1985.

34. Brown, J.H., "Design Refinements Make the Steel Sleeper Viable," Railway Gazette International, October 1979, pp. 902-906.

35. Raymond, G.P., "Session III - Ballast Track Design," AREA Seminar, Railroad Track and Roadbed Engineering Update, 1986.

36. So, W., Martin, G.C., Singh, B., Chang, I.C., and Chang, E.H., Mathematical Models for Track Structures, AAR Report No. R-262, April 1977.

37. Prause, R.H., and Kennedy, J.C., Parametric Study of Track Response, Report No. USDOT FRA/ORD-77/75, December 1977.

38. Kish, A., McConnell, D.P., McCafferty, R.M., Moody, H., and Sluz, A., Track Structures Performance -- Comparative Analysis of Specific Systems and Component Performance, Report No. FRA/ORD-77/29, September 1977.

39. AREA Manual for Railway Engineers, Chapter 22, "Economics of Railway Construction and Maintenance," Subsection 3.2.1(a).

40. Heath, D.C., Shenton, M.J., Sparrow, R.W., and Waters, J.M., "Design of Conventional Rail Track Foundations," Proceedings, Institution of Civil Engineers, Vol. 51, February 1972.

41. Sheeran, D.E., Elmamlouk, H.H., and Faltah, E.A., Prediction of Long-term Track Subgrade Settlement Due to Cyclic Wheel Loading, November 1980.

42. Raymond, G.P., "Design of Railroad Ballast and Subgrade Support," ASCE Journal of Geotechnical Engineering, January 1978.

43. Shenton, M.J., "Ballast Deformation and Track Deterioration," Proceedings, Track Technology for the Next Decade, Nottingham, U.K., July 1984.

44. Ahlf, R.E., Report of the Ballast and Subgrade Subcommittee of the Association of American Railroads, Track Maintenance Planning Committee, October 1985.

45. Scott, J.F., "Granular Depth Requirement for Railroad Track," Transportation Research Record 1006, 1985.

46. Raymond, G.P., Lake, R.W., Boon, C.J., and Roney, M.D., Stresses and Deformations on Railway Track, Volumes I, II and III, CIGGT Reports: 76-11, November 1976; 77-15, November 1977, and 78-16, November 1978.

47. Raymond, G.P., and Bathurst, R.J., "Performance of Large-Scale Model Single Tie/Ballast Systems," TRB, 1987.

48. Adegoke, C.N., Elastic and Inelastic Deformation Response of Track Structure Under Train Loads, Ph.D. Dissertation, Department of Civil Engineering, S.U.N.Y., Buffalo, N.Y., December 1978.

49. Yoo, T.S., and Selig, E.T., "Field Observations of Ballast and Subgrade Deformations in Track, TRB Record No. 733, 1979.

50. Shugu, Z., "Failure of Heavy Haul Track and Its Design," Paper 82-HH-38, Second International Heavy Haul Railway Conference, Colorado Springs, Colorado, September 1982.

51. Stewart, H.E., and Selig, E.T., "Predictions of Track Settlement under Traffic Loading," Paper 82-HH-44A, Second International Heavy Haul Conference, Colorado Springs, Colorado, September 1982.

52. Shenton, M.J., "Deformation of Railway Ballast Under Repeated Loading Conditions," Railroad Track Mechanics and Technology, 1978.

53. Selig, E.G., "Ballast for Heavy-Duty Track," Track Technology for the Next Decade, Nottingham, 1984.

54. Raymond, G.P., Boon, C.J., and Lake, R.W., Ballast Selection and Grading: A Summary Report, CIGGT Report 79-4, April 1979.

55. Raymond, G.P., "Subgrade Requirements for Heavy Haul Railways," lecture notes, September 1986; also base for presentation to the 1987 Annual TRB Meeting A2M01.

56. Raymond, G.P., Purdy, W.J., Gerry, B.S., and Fitzpatrick, C., Geotextiles for Railway Track Rehabilitation Applications, CIGGT Report 81-16, March 1982.

57. Raymond, G.P., Sub-ballast and Geotextiles for Railway Track Support Separation Applications, CIGGT Report 85-12, December 1985.

58. Dalton, C.J., and Scott, J.F., Predicting Requirements for Sub-ballast Thickness, Progress Report No. 3, Transport Canada Report No. TP4350E, 1983.

59. Selig, E.T., and Alva-Hurtado, J.E., "Predicting Effect of Repeated Wheel Loading on Track Settlement," The Second International Heavy Haul Conference, Colorado Springs, CO., September 25-30, 1982.

59. O'Rourke, M.D., and Groehnont, R., The Use of Track Geometry Data for Maintenance Planning.

60. Raymond, G.P., personal communication.

61. Talbot, A.N., "Stresses in Railroad Track," Proceedings of the AREA, First Progress Report, Vol. 19, 1918, pp, 878-1062; ibid, Second Progress Report, Vol. 21, pp. 645-814.

62. Battelle-Columbus Laboratories, Measurements of Wheel/Rail Loads on Class 5 Track, prepared for U.S. Department of Transportation, Federal Railroad Administration, Office of Research and Development, Report No. FRA/ORD-80/19, February 1980.

63. Lamson, S.T., Bogie Curving Model - A Refined Calibration, MRL/CB28/80/003, BHP/MNM/HI/VPC/80/114, September 1980.

64. Ahlbeck, D.R., et al., Measurements of Wheel/Rail Loads on Class 5 Track, FRA/ORD-80/19.

65. Dixon, C.A., and Lamson, S.T., Rail and Fastener Survey, CIGGT Report No. 84.15, February 1985.

66. Longson, B.H., and Lamson, S.T., "Development of Rail Profile Grinding at Hamersley Iron," Proceedings, Second International Heavy Haul Railway Conference, Colorado Springs, Colorado, U.S.A., September 25-30, 1982.

67. Graham, M.D., and Dawley, C.B., "Laboratory Evaluation of Flyash Cement and Lignin Cellulose Cement as Soil Stabilizers," Transport Canada, Report No. TP 5287E and TP 5288E, March 1984.

APPENDIX A

DEVELOPMENT OF AN EMPIRICAL RELATIONSHIP FOR VERTICAL DYNAMIC WHEEL FORCE VARIATION OF A 100-TON CAR AS A FUNCTION OF TRACK ROUGHNESS AND VEHICLE SPEED

A.1 OBJECTIVE

The objective is to derive an equation for the dynamic force variation of a 100-ton car as a function of track roughness and vehicle speed.

$$\Delta Pd = f\ (\text{track roughness, vehicle speed})$$

where ΔPd expresses one standard deviation of the dynamic force.

A.2 CONSTRAINTS

Track roughness has to be expressed as CN surface index (SI) and CN cross-level index (CI) since these are the data currently available for this research work.

A.3 METHOD

At present the most reliable method of estimating the dynamic wheel forces as a vehicle responds to track roughness is by computer simulation. Using a full-body vertical dynamic model, the response of a 100-ton car can be simulated for any track location under a range of vehicle speeds. This procedure is shown in Figure A.1(a).

Computer simulation is, however, very time-consuming, and hence not practical for an economic analysis which requires an estimate of the vehicle dynamic wheel forces over long distances of track. To overcome this problem, a quasi-empirical method is used. It involves regression analysis of data generated by computer simulation. The result is a quasi-empirical equation which produces an estimate of the dynamic wheel forces for a given set of track surface and cross-level errors. This procedure is shown in Figure A.1(b).

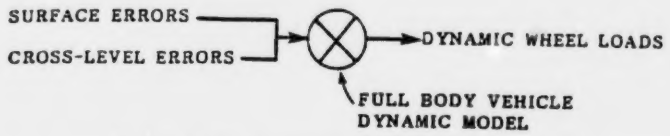

(a) by computer simulation

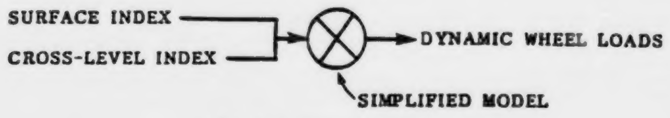

(b) by equation

Figure A.1 Estimation of dynamic wheel loads

The quasi-empirical equation is considered equivalent to the computer simulation for estimating dynamic wheel loads. Note that track roughness input can be represented by CN-type indices. These are readily available for all track; hence the equation is much more versatile than a computer model.

A.4 VEHICLE DYNAMICS COMPUTER MODEL

A.4.1 Description

This model simulates the dynamic response of a four-axle rail vehicle to random surface irregularities as characterized by track coordinates (x,y), rate of change of position (dy/dx), and the second derivation of position (d^2y/dx^2) for both track surface and cross-level conditions. Of prime interest are the dynamic wheel/rail forces. A diagram of the model is shown in Figure A.2.

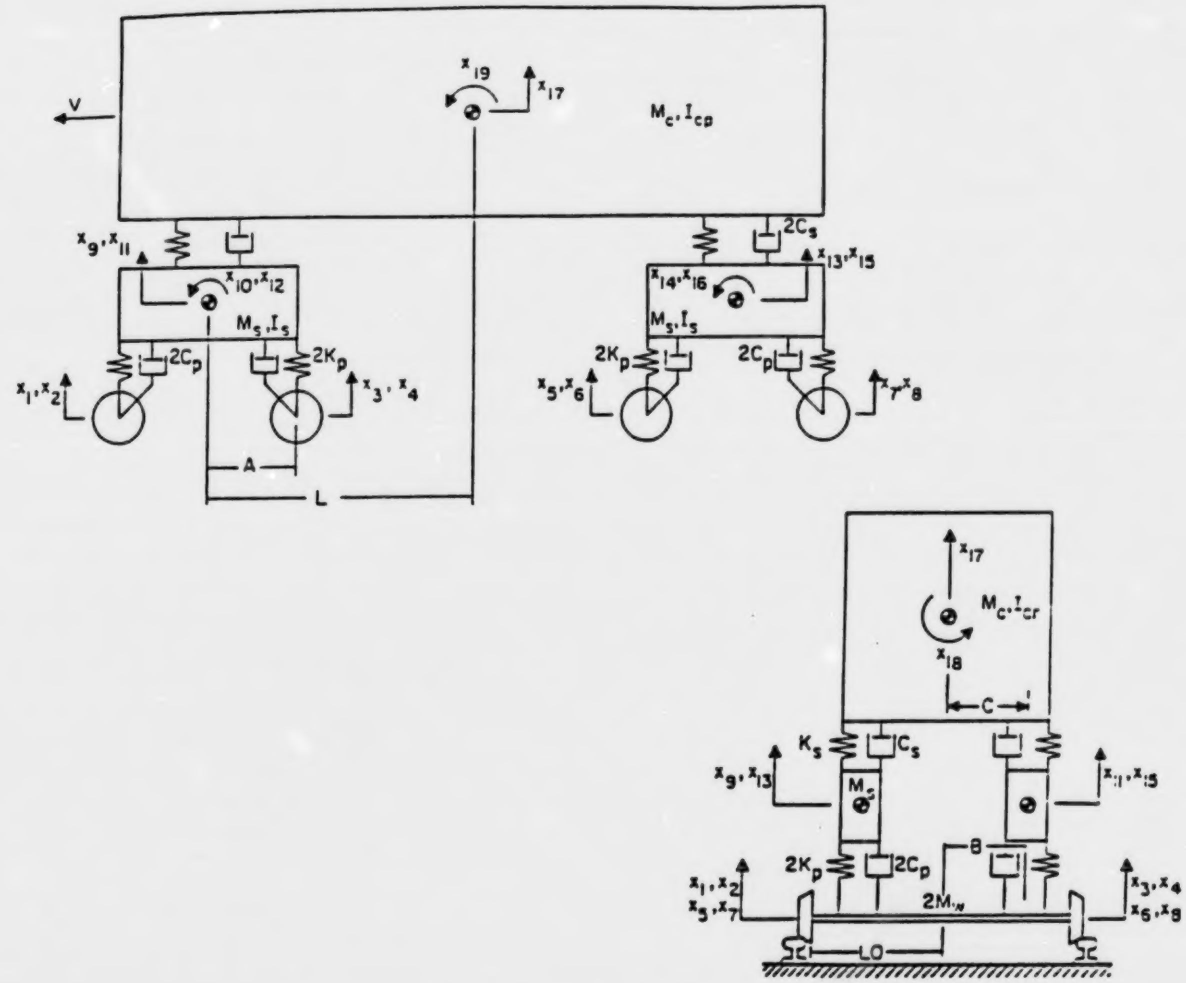
V
x_{19}
x_{17}
M_c, I_{cp}
x_9, x_{11}
x_{10}, x_{12}
M_s, I_s
$2C_p$
$2K_p$
x_1, x_2
x_3, x_4
A
L
$2C_s$
x_{13}, x_{15}
x_{14}, x_{16}
M_s, I_s
$2K_p$
$2C_p$
x_5, x_6
x_7, x_8
x_{17}
M_c, I_{cr}
x_{18}
C
K_s
C_s
x_9, x_{13}
M_s
x_{11}, x_{15}
$2K_p$
$2C_p$
B
x_1, x_2
x_5, x_7
$2M_w$
x_3, x_4
x_6, x_8
LO

Figure A.2 Vertical vehicle dynamic model

The model is a simplified representation of any four-axle vehicle such as a 100-ton car, a four-axle locomotive, etc. It has 19 degrees of freedom:

(a)	wheel heave (8)	$x_1, \ldots x_8$
(b)	sideframe heave (4)	$x_9, x_{11}, x_{13}, x_{15}$
(c)	sideframe pitch (4)	$x_{10}, x_{12}, x_{14}, x_{16}$
(d)	carbody heave	x_{17}
(e)	carbody pitch	x_{19}
(f)	carbody roll	x_{18}

Each wheelset is connected to the sideframes by a primary spring and damper. Each sideframe is connected to the carbody by a secondary spring and damper. If the model is to be applied to another vehicle for which any of these springs or dampers do not exist, their value can be appropriately adjusted.

This model considers three basic assumptions. First, all mass components (namely sideframes, carbody, wheelsets) are assumed to be rigid. Second, all wheelsets are assumed to always be in contact with the rails. Third, all springs and dampers behave linearly.

A.4.2 Vehicle Input Data

A complete list of vehicle data required for vertical dynamic response simulation is given below. The masses, springs and dampers are labeled in Figure A.2.

A_1 = half axle spacing
B = half distance between primary suspension elements
C_o = half distance between secondary suspension elements
L_o = half distance between wheels
L = distance carbody centre-of-gravity to secondary suspension
M_{ax} = mass of wheel and half-axle
M_{sf} = mass of sideframe
M_{bod} = mass of carbody
I_{sf} = sideframe inertia
I_{rot} = carbody rotational inertia
I_{pt} = carbody pitch inertia
K_1, K_2 = primary, secondary spring stiffness
C_1, C_2 = primary, secondary damping coefficients

These input data are stored in computer files which are read by the main program during the simulation runs. Dynamic simulations may be made for any four-axle vehicle operating at any speed by creating a data file with the corresponding parameters. Heavy and light freight cars, passenger coaches and four-axle locomotives can all be represented by this model. A sample data set representing a 100-ton hopper car is shown below.

$A_1 = 0.9$ m
$B = 1.003$ m
$C_o = 1.003$ m
$L_o = 0.7176$ m
$L = 5.5$ m
$M_{ax} = 7.1 \times 10^2$ kg
$M_{sf} = 7.3 \times 10^2$ kg
$M_{bod} = 1.1 \times 10^5$ kg

$I_{sf} = 4.5 \times 10^2$ kg m²
$I_{rot} = 3.6 \times 10^4$ kg m²
$I_{pt} = 1.8 \times 10^6$ kg m²
$K_1 = 2.827 \times 10^7$ N/m
$K_2 = 3.88 \times 10^6$ N/m
$C_1 = 6.2 \times 10^4$ Ns/m
$C_2 = 1.11 \times 10^5$ Ns/m

A.5 TRACK CHARACTERIZATION

The Track Index Program calculates the following characteristics for each sample section of digitized track geometry errors:

- standard deviation (amplitude indication)
- frequency index (an indication of the predominant wave length)
- CN track geometry index (an indication of the product of frequency and amplitude).

The CN index formula is:

$$I = \sum_{i=1}^{n} \frac{| y_{i+1} - y_i | \times 10^5}{L}$$

where: I = track index

L = track section length (m)

y_i = track deviation at point i

n = number of points over L(m) of track

Track surface and cross-level indices are calculated over 50 m sample lengths for 50 m simulation runs, and over 30 m sample lengths for 30 m simulation runs.

A.6 SIMULATION RUNS

Over 100 simulation runs were made with the Vertical Dynamic Model simulating a 100-ton hopper car running at speeds of 5-33 m/s (10-75 mph) over a variety of track sections. Vehicle dynamic force variance (i.e. standard deviation of dynamic force) versus vehicle speed, SI and CI, are shown in Table A.1.

TABLE A.1

SIMULATION DATA

Run #	Vehicle Speed	Surface Index	Cross-Level Index	Standard Deviation for Dynamic Force (kN) from Computer Simulation	Standard Deviation for Dynamic Force (kN) from Empirical Equation
Simulations over 50 m track sections:					
1	33 m/s	129	124	6.473	7.314
2	33 m/s	130	87	6.527	6.889
3	33 m/s	130	124	7.280	7.375
4	33 m/s	130	105	7.053	7.126
5	33 m/s	130	111	6.591	7.204
6	33 m/s	119	87	5.345	6.220
7	30 m/s	115	90	6.023	5.644
8	30 m/s	115	109	5.975	5.878
9	30 m/s	115	130	6.119	6.137
10	30 m/s	115	147	6.856	6.322
11	30 m/s	127	133	6.591	6.850
12	30 m/s	129	124	9.136	6.855
13	30 m/s	130	109	6.460	6.728
14	30 m/s	130	124	6.979	6.913
15	30 m/s	130	90	6.505	6.493
16	30 m/s	130	109	6.460	6.728
17	30 m/s	130	130	6.584	6.986
18	30 m/s	130	147	7.273	7.171
19	30 m/s	144	101	7.832	7.458
20	30 m/s	145	90	7.260	7.383
21	30 m/s	145	109	7.260	7.617
22	30 m/s	145	130	7.337	7.876
23	30 m/s	145	147	7.961	8.061
24	30 m/s	164	105	8.888	8.748
25	30 m/s	165	109*	8.386	8.861
26	30 m/s	165	90	9.152	8.627
27	30 m/s	165	109*	9.128	8.861
28	30 m/s	165	130	9.201	9.120
29	30 m/s	165	147	9.693	9.305
30	25 m/s	115	90	5.594	4.986
31	25 m/s	115	109	5.546	5.193
32	25 m/s	115	130	5.633	5.422
33	25 m/s	115	147	6.047	5.585
34	25 m/s	116	117	6.121	5.329

TABLE A.1 (Cont'd)

SIMULATION DATA

Run #	Vehicle Speed	Surface Index	Cross-Level Index	Standard Deviation for Dynamic Force (kN) from Computer Simulation	Standard Deviation for Dynamic Force (kN) from Empirical Equation
Simulations over 50 m track sections (cont'd):					
35	25 m/s	116	139	6.458	5.569
36	25 m/s	129	124	9.444	6.055
37	25 m/s	130	90	7.024	5.736
38	25 m/s	130	109	6.992	5.943
39	25 m/s	130	124	7.210	6.107
40	25 m/s	130	87	6.923	5.704
41	25 m/s	130	87	6.989	5.704
42	25 m/s	130	109	7.082	5.943
43	25 m/s	130	130	7.054	6.172
44	25 m/s	130	147	7.387	6.335
45	25 m/s	139	98	6.828	6.291
46	25 m/s	139	124	7.085	6.574
47	25 m/s	145	90	7.374	6.522
48	25 m/s	145	109	7.371	6.729
49	25 m/s	145	130	7.426	6.958
50	25 m/s	145	147	7.747	7.121
51	25 m/s	164	124	9.673	7.935
52	25 m/s	164	129	9.561	7.989
53	25 m/s	165	90	9.975	7.621
54	25 m/s	165	109	9.944	7.828
55	25 m/s	165	130	9.980	8.056
56	25 m/s	165	147	10.220	8.220
57	20 m/s	115	90	5.480	4.284
58	20 m/s	115	109	5.417	4.462
59	20 m/s	115	130	5.495	4.658
60	20 m/s	115	147	5.690	4.799
61	20 m/s	130	90	7.247	4.929
62	20 m/s	130	109	7.202	5.106
63	20 m/s	130	124	7.270	5.247
64	20 m/s	130	130	7.262	5.303
65	20 m/s	130	147	7.408	5.443
66	20 m/s	145	90	8.231	5.604
67	20 m/s	145	109	8.193	5.782
68	20 m/s	145	130	8.246	5.978

TABLE A.1 (Cont'd)

SIMULATION DATA

Run #	Vehicle Speed	Surface Index	Cross-Level Index	Standard Deviation for Dynamic Force (kN) from Computer Simulation	Standard Deviation for Dynamic Force (kN) from Empirical Equation
69	20 m/s	145	147	8.375	6.118
70	20 m/s	165	90	8.064	6.548
71	20 m/s	165	109	8.009	6.726
72	20 m/s	165	130	8.077	6.922
73	20 m/s	165	147	8.202	7.063
74	15 m/s	115	90	3.886	3.523
75	15 m/s	115	109	3.790	3.669
76	15 m/s	115	130	3.859	3.831
77	15 m/s	115	147	4.078	3.946
78	15 m/s	119	109	3.598	3.808
79	15 m/s	130	90	4.772	4.053
80	15 m/s	130	109	4.682	4.199
81	15 m/s	130	124	4.729	4.315
82	15 m/s	130	130	4.745	4.361
83	15 m/s	130	147	4.902	4.476
84	15 m/s	129	99	4.418	4.086
85	15 m/s	145	90	4.850	4.608
86	15 m/s	145	109	4.750	4.754
87	15 m/s	145	130	4.816	4.916
88	15 m/s	145	147	4.987	5.031
89	15 m/s	165	90	5.078	5.385
90	15 m/s	165	109	4.968	5.531
91	15 m/s	165	109	5.194	5.531
92	15 m/s	165	117	5.175	5.592
93	15 m/s	165	130	5.059	5.692
94	15 m/s	165	147	5.035	5.808
95	5 m/s	130	124	1.792	2.044
Simulations over 30 m track sections:					
96	40 m/s	129	110	8.925	8.126
97	33 m/s	205	132	9.670	12.605
98	33 m/s	129	109	8.24	7.116
99	33 m/s	105	110	5.60	5.707
100	29 m/s	167	138	8.897	9.133
101	26 m/s	205	132	10.05	10.719

TABLE A.1 (Cont'd)

SIMULATION DATA

Run #	Vehicle Speed	Surface Index	Cross-Level Index	Standard Deviation for Dynamic Force (kN) from Computer Simulation	Standard Deviation for Dynamic Force (kN) from Empirical Equation
102	26 m/s	105	110	5.02	4.853
103	25 m/s	130	104	6.595	5.943
104	20 m/s	147	110	8.14	6.883
105	20 m/s	138	109	4.327	5.463
107	20 m/s	199	149	9.657	8.811
108	20 m/s	199	80	9.456	8.166
109	20 m/s	106	149	4.155	4.465
110	20 m/s	106	104	5.176	4.044
111	20 m/s	125	98	7.698	4.785
112	19 m/s	205	132	11.08	8.660
113	19 m/s	105	110	4.36	3.920
114	20 m/s	147	110	8.14	5.883
115	15 m/s	139	109	5.16	4.529
116	15 m/s	205	132	8.2	7.374
117	15 m/s	105	132	3.5	3.338
118	12 m/s	205	132	6.12	6.336
119	12 m/s	105	110	2.96	2.868
120	5 m/s	205	132	2.24	3.493
121	5 m/s	105	110	1.52	1.582

---

* NOTE: In some instances simulations were made over two separate track sections with identical surface and cross-level indices. Vehicle response to "almost identical" sections were seen to vary slightly.

A.7 EMPIRICAL EQUATION

An empirical equation expressing vehicle dynamic force variation as a function of vehicle speed and track indices as derived from simulation results is shown below.

$$\delta = 10^{-3} V^{.68} (.585 \, SI^{1.4} + 1.22 \, CI)$$

where: δ = one standard deviation of dynamic force variation (kN)

V = vehicle speed (m/s)

SI = CN Surface Index

CI = CN Cross-level Index

The correlation between this equation and simulation results is shown in Figure A.3.

For general applications, the above equation can be generalized to provide a dynamic load factor as follows:

$$\delta_d = \frac{\delta}{145} \times (.44)^{.68} V^{.68} (0.585 \, SI^{1.4} + 1.22 \, CI)$$

$$= 3.97 \, E\text{-}6 \, V^{.68} (0.585 \, SI^{1.4} + 1.22 \, CI)$$

where 145 is the nominal wheel load (in kN) of the 100-ton car and (.44) is the conversion factor for vehicle speed (V) in mph.

A.8 VALIDATION/CALIBRATION

A.8.1 Dynamic Force Increment as a Function of Speed

(a) Battelle-Columbus Data

The effect of speed (i.e. the power .68) in the empirical equation agrees well with U.S. field data for 100-ton cars (i.e. the power .66) shown in Figure A.4.

(b) CN Data

The effect of speed ($V^{.68}$) is further substantiated by CN field data collected on the Wainwright subdivision work train tests. Impact loads were measured at five strain gauge locations for wheels with and without defects. Test speeds were from 2.3 to 55.2 mph. Test data from 13 normal wheels (no defects) are used for this validation.

Data Analysis:

- mean dynamic load was determined for each wheel at each speed from five strain gauge readings

- measured loads at 2.3 mph were consistently higher than at 5.4 mph. Data at 2.3 mph were discarded and measured loads at 5.4 mph were considered steady-state vertical load
- dynamic increment was calculated for each wheel at each speed as:

$$\sigma_{vi} = Fd_{vi} - Fd_o$$

where: σ_{vi} = dynamic increment at speed (vi)

Fd_{vi} = mean dynamic load at speed (vi)

Fd_o = mean steady-state load.

The data obtained were plotted against a family of curves of the form:

$$\sigma = a\ V^{.68}$$

where: σ = dynamic increment (kips)

a = constant representing wheel characteristics.

The results are shown in Figures A.5 through A.16.

Except for wheels 4B and 12A, the data generally indicate that the effect of speed can be reasonably represented by a power of 0.68 (i.e., $V^{0.68}$).

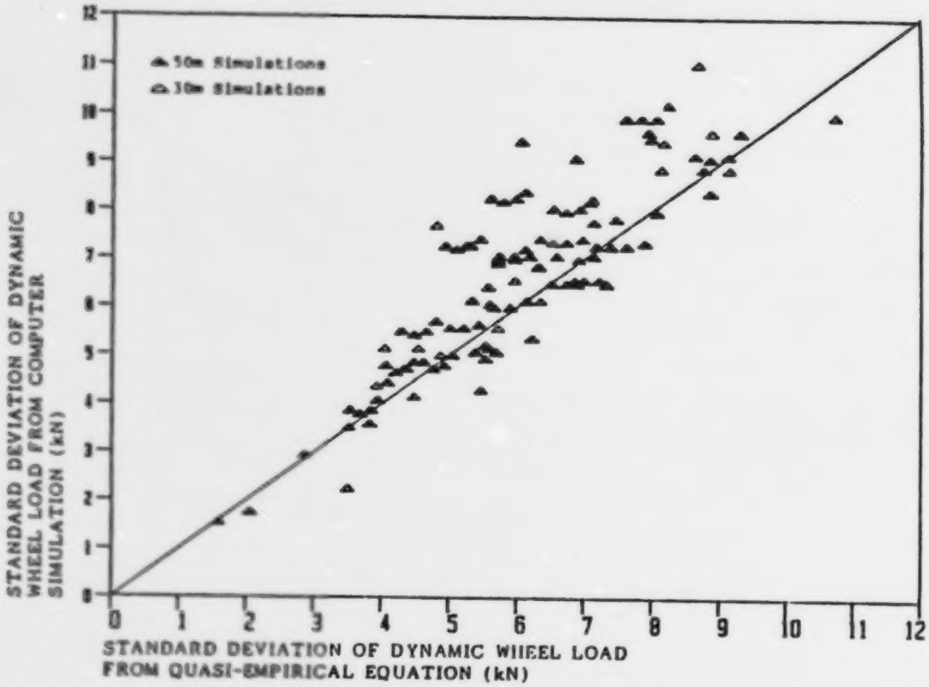

Figure A.3 Correlation between simulated and calculated values of the standard deviation of dynamic wheel load

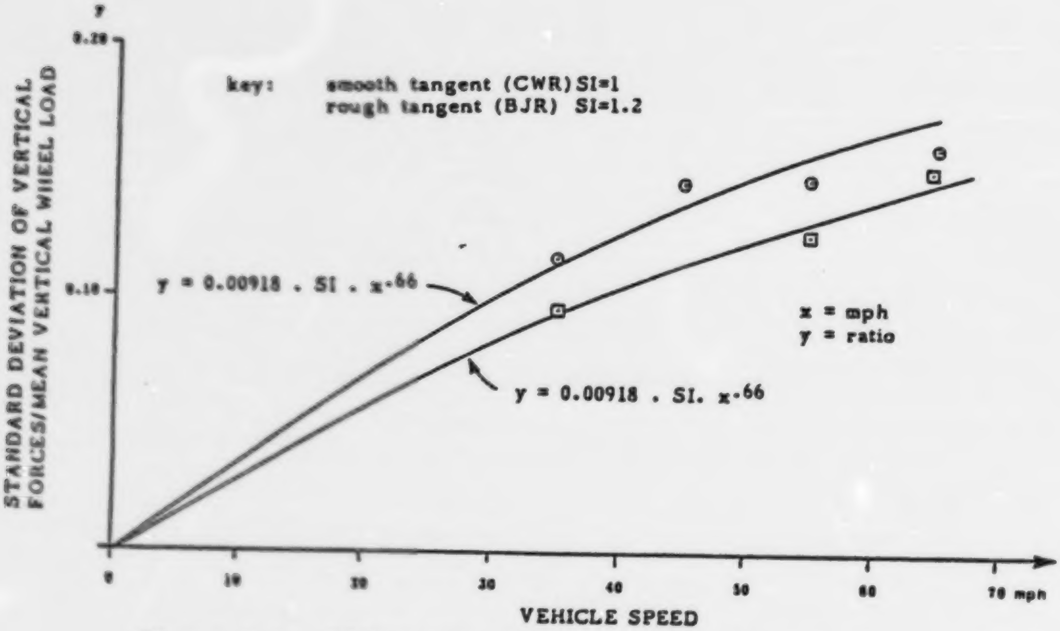

Figure A.4 Effect of speed on dynamic wheel load for a 100-ton car (Ahlbeck)

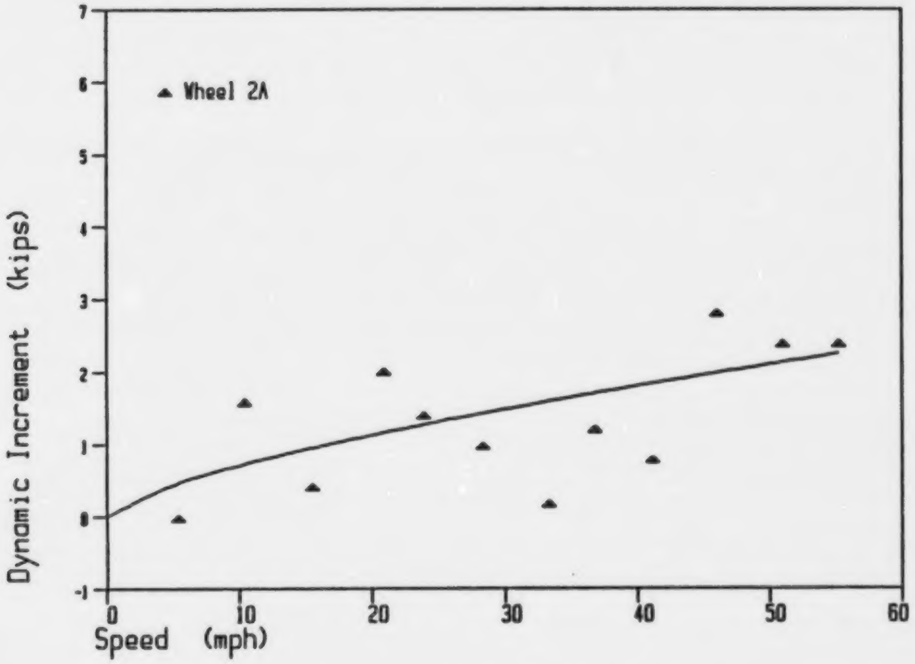

Figure A.5 Dynamic wheel load increment versus speed - Wheel 2A

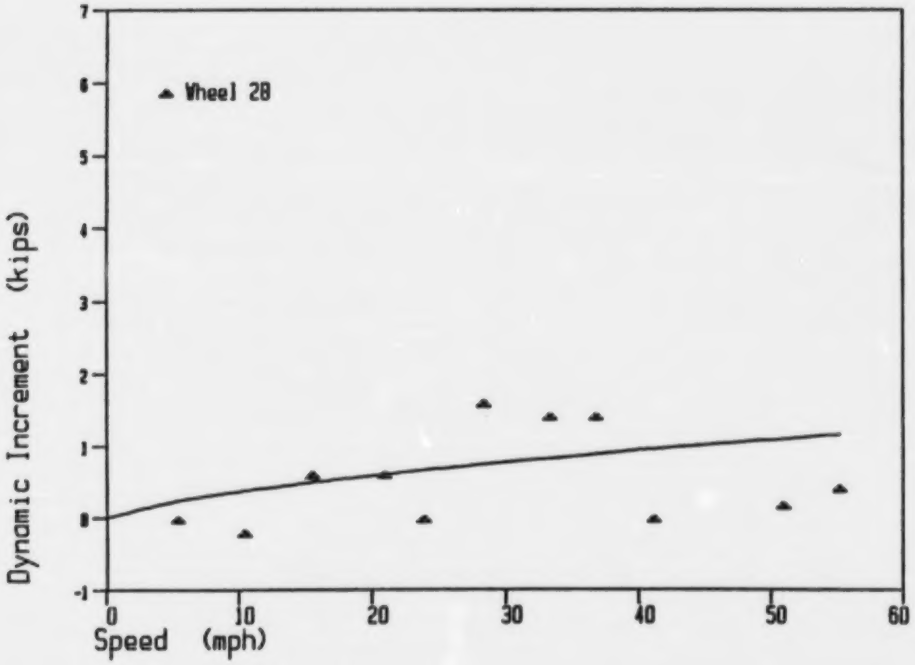

Figure A.6 Dynamic wheel load increment versus speed - Wheel 2B

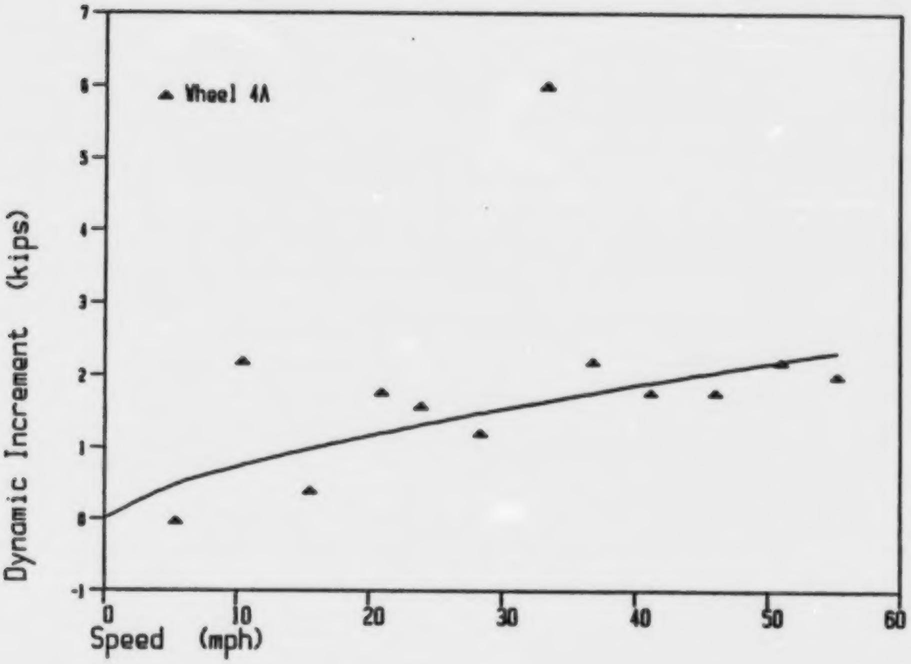

Figure A.7 Dynamic wheel load increment versus speed - Wheel 4A

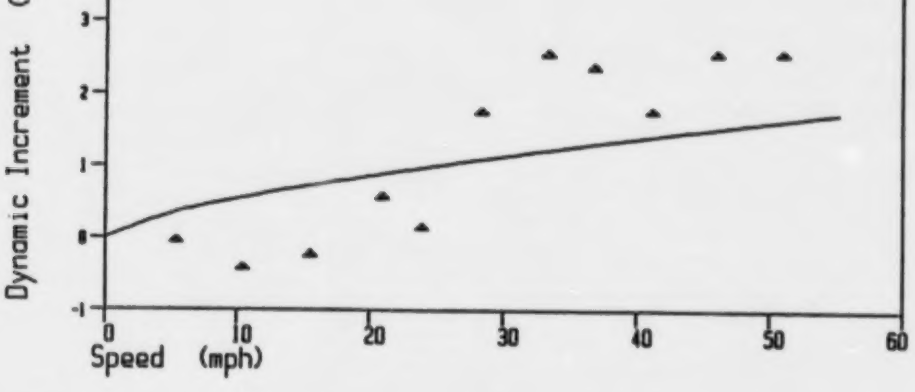

Figure A.8 Dynamic wheel load increment versus speed - Wheel 4B

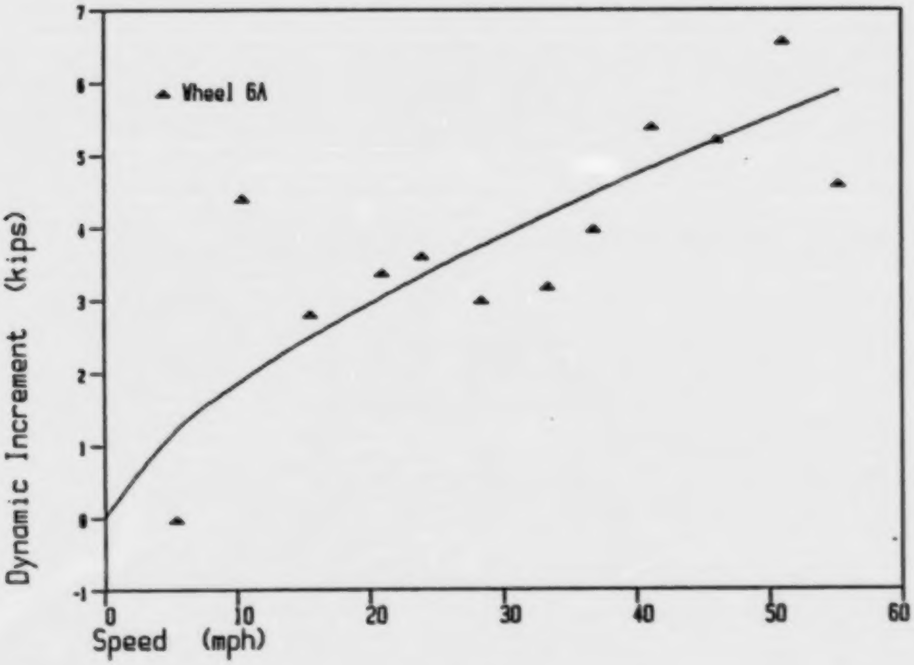

Figure A.9 Dynamic wheel load increment versus speed - Wheel 6A

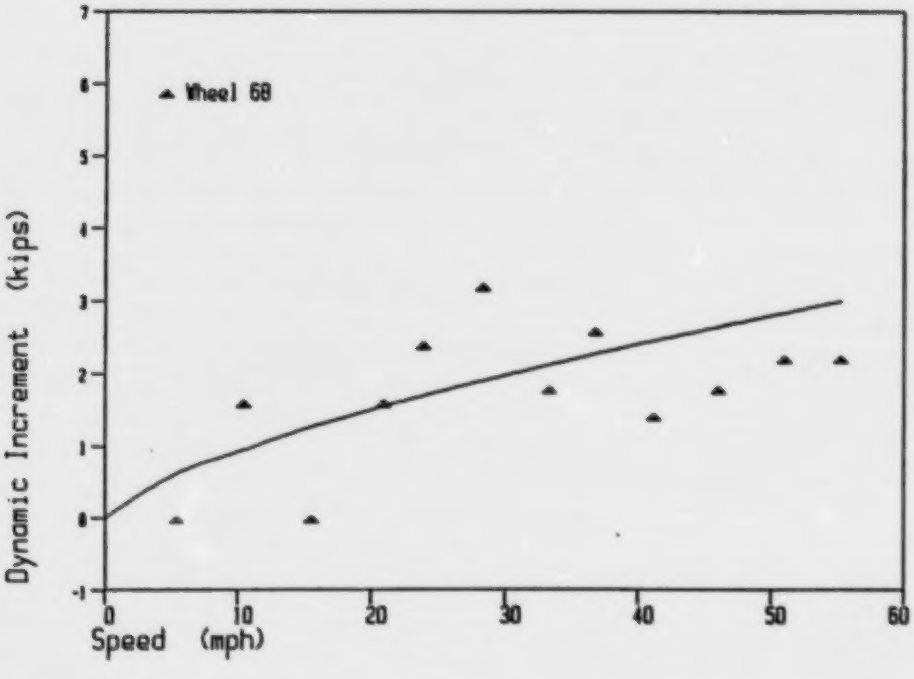

Figure A.10 Dynamic wheel load increment versus speed - Wheel 6B

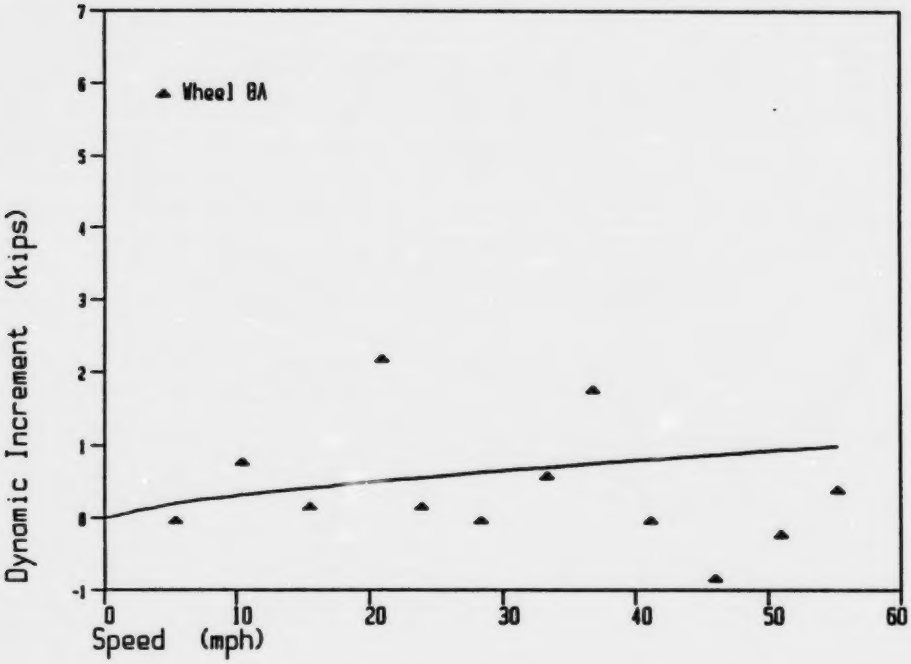

Figure A.11 Dynamic wheel load increment versus speed - Wheel 8A

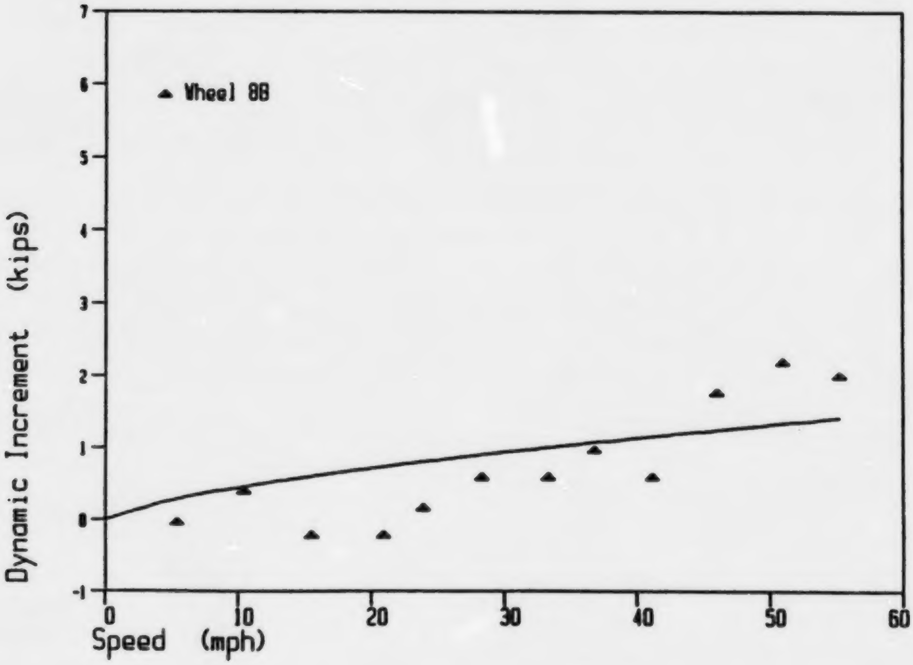

Figure A.12 Dynamic wheel load increment versus speed - Wheel 8B

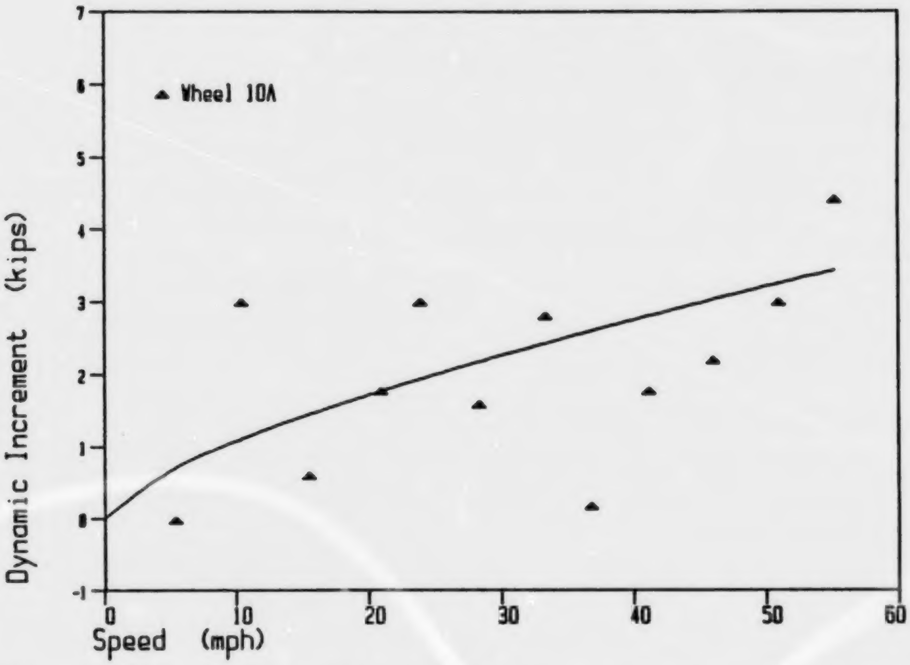

Figure A.13 Dynamic wheel load increment versus speed - Wheel 10A

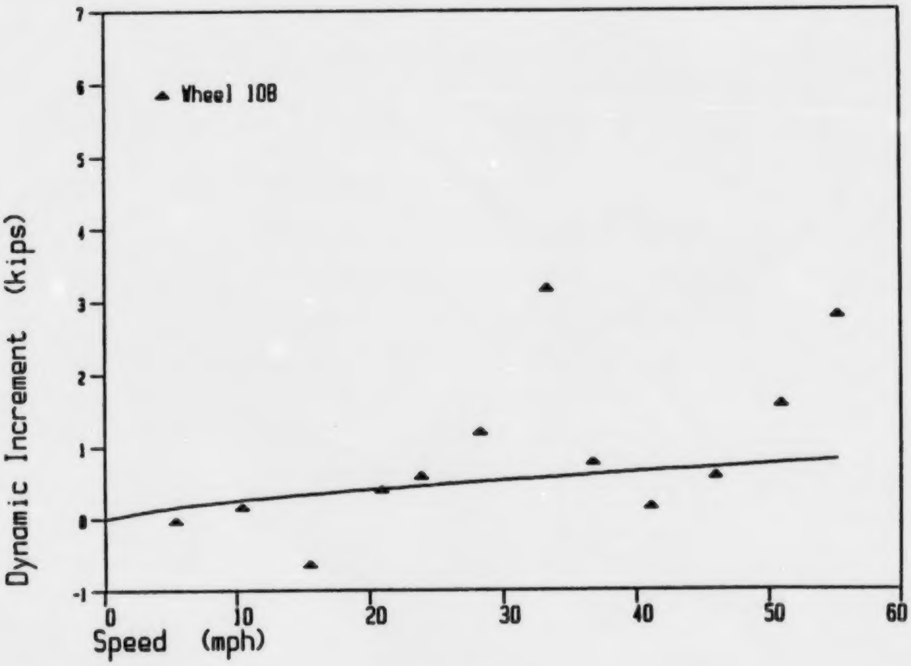

Figure A.14 Dynamic wheel load increment versus speed - Wheel 10B

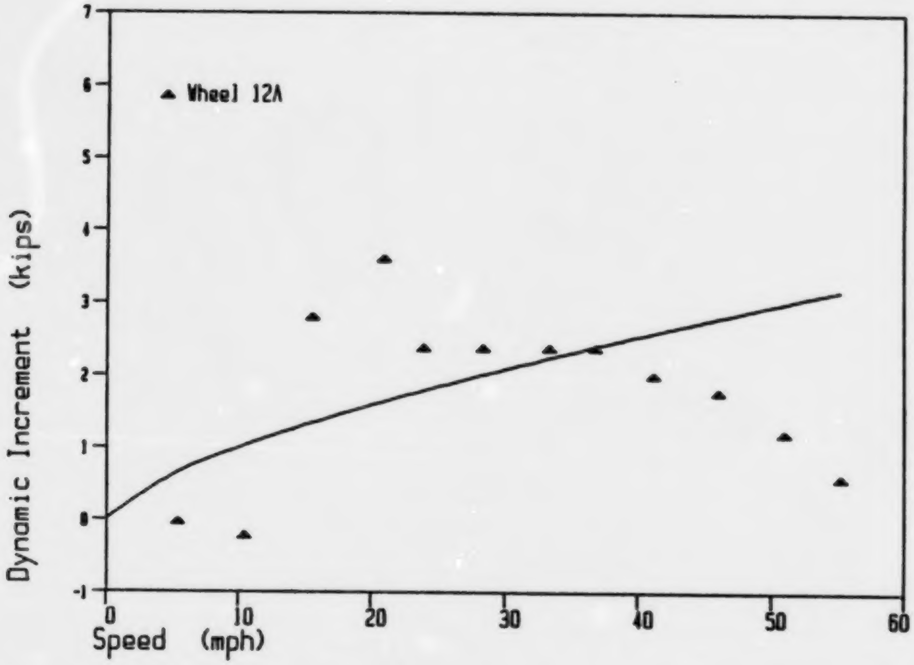

Figure A.15 Dynamic wheel load increment versus speed - Wheel 12A

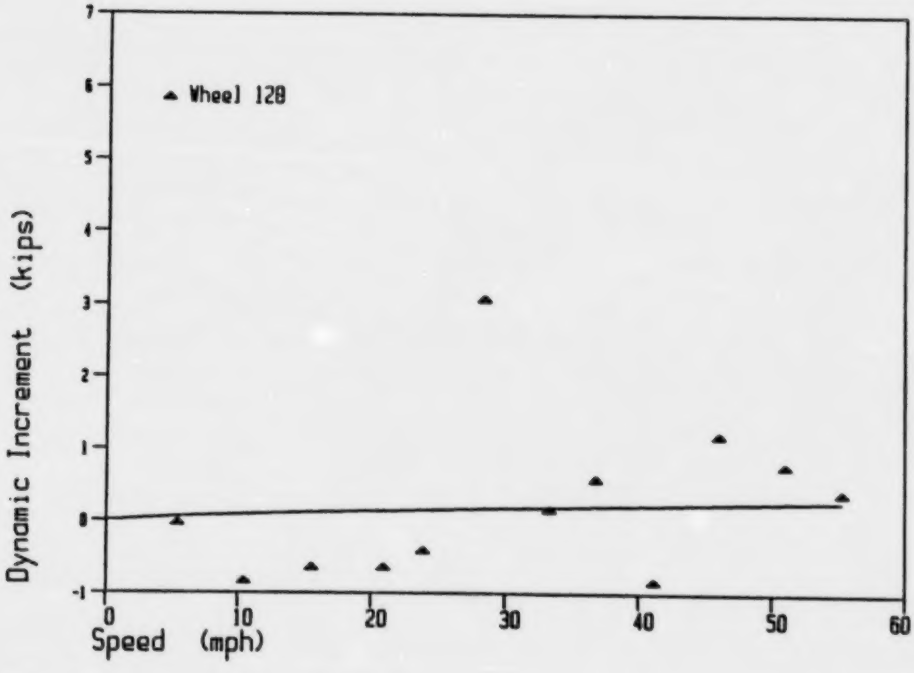

Figure A.16 Dynamic wheel load increment versus speed - Wheel 12B

A.8.2 Calibration

Unfortunately, CN data is not appropriate for direct comparison with the calculated dynamic load factor. Due to the fixed location of the strain gauge system in track, the response of the dynamic wheel load to track geometry error (i.e. different values of surface and cross-level indices) could not be measured. The Battelle-Columbus data shows that the dynamic load factor for CWR and BJR track varies in the range of 0.10 to 0.15, depending on vehicle speed (range 35 to 65 mph). This is roughly twice the dynamic wheel load factor obtained through computer simulation. The discrepancy is likely due to the fact that the track geometry data used in the simulation (obtained by the track recorder car) did not contain shortwave (high frequency) error information. Until this matter is adequately resolved -- perhaps with CN's new track recorder car, a factor of 2 will be used to bring the calculated dynamic load factor to the same range as the Battelle-Columbus data. The dynamic load factor is thus given by:

$$\varphi_d = 7.94\ \text{E-6}\ V^{0.68}\ (0.585\ SI^{1.4} + 1.22\ CI)$$

A.9 DYNAMIC FORCE ESTIMATION FOR OTHER VEHICLES

The empirical equation expressing the dynamic force variation of a 100-ton car to vehicle speed and track indices is expanded to express the dynamic force variation of other vehicles. Of interest are locomotives, passenger coaches, and 50-70 ton freight cars.

Theoretically, each vehicle has its own set of eigen-frequencies which characterize its unique dynamic response to track roughness. Therefore, each type of car must be given a full analysis as was done for the 100-ton car. The lack of data on vehicle parameters for most vehicles (except the 100-ton car), plus the complexity of the analysis, make this option impractical for the present project.

As an approximation, the quasi-empirical equation developed for the 100-ton car is adapted for other cars using a relative unsprung mass term, as follows:

$$P_d = 7.94\ \text{E-6}\ P_s\ V^{0.68}\ (0.585\ SI^{1.4} + 1.22\ CI)\ (M_u/3156)^{0.5}$$

where: P_d = one standard deviation of the dynamic wheel force variation (lbs)

P_s = steady-state wheel load (lbs)

V = vehicle speed (mph)

SI = CN-type surface index

CI = CN-type cross-level index

$\frac{M_u}{3156}$ = ratio of vehicle unsprung mass to that of a 100-ton car.

Research into vehicle dynamics has so far identified unsprung mass as the most significant vehicle parameter to dynamic wheel force increment at high speed. The adaptation, therefore, is considered a reasonable estimate for the present.

APPENDIX B

DEVELOPMENT OF AN EMPIRICAL RELATIONSHIP FOR THE STEADY-STATE LATERAL FORCE OF A 100-TON CAR IN CURVING

B.1 OBJECTIVE

To derive an equation for the steady-state lateral force of a 100-ton car as a function of track curvature, superelevation and vehicle speed:

$$L_s = f\ (\text{track curvature, track superelevation, vehicle speed})$$

B.2 METHOD

The steady-state lateral forces are estimated for a series of curving situations using a Steady-state Truck Curving Model (see Section B.3). From the simulation results, a quasi-empirical equation is formulated. This is done because the computer simulations can be time-consuming and are not practical for use in more complicated problems.

The quasi-empirical equation replaces the computer simulation in subsequent applications (see Figure B.1), speeding up lateral wheel force calculations.

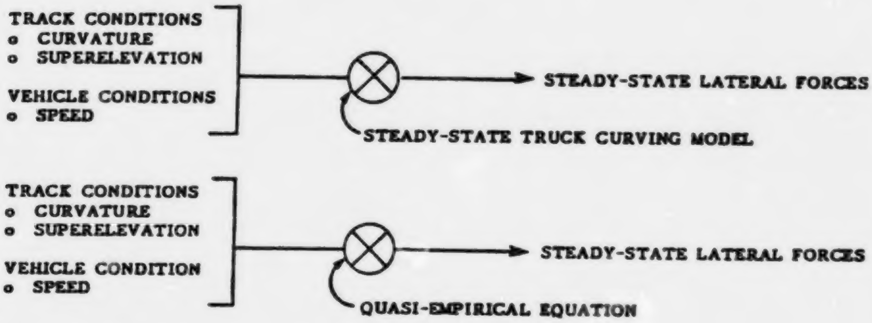
TRACK CONDITIONS
o CURVATURE
o SUPERELEVATION
VEHICLE CONDITIONS
o SPEED
STEADY-STATE LATERAL FORCES
STEADY-STATE TRUCK CURVING MODEL
TRACK CONDITIONS
o CURVATURE
o SUPERELEVATION
VEHICLE CONDITION
o SPEED
STEADY-STATE LATERAL FORCES
QUASI-EMPIRICAL EQUATION

Figure B.1 Estimation of lateral wheel forces

B.3 STEADY-STATE TRUCK CURVING MODEL

This model simulates the steady-state curving behaviour of a three-piece truck under a railway vehicle. A schematic diagram of the model is shown in Figure B.2. Leading and trailing wheel sets are assumed to be parallel. This leaves the model with three degrees of freedom, namely:

- wheelset lateral displacement
- wheelset angle of attack
- truck frame lozenging angle.

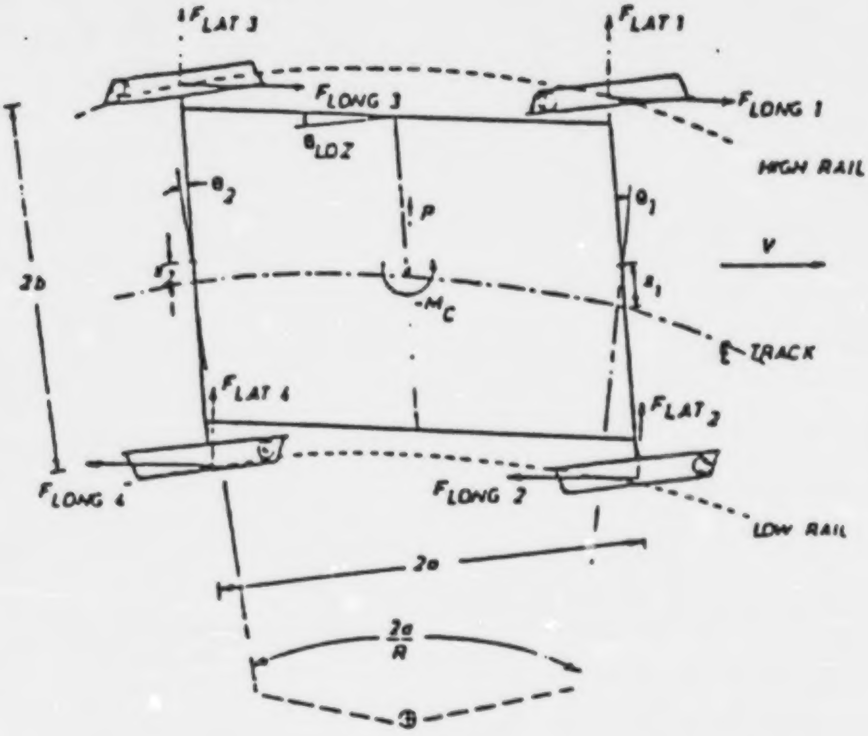
F LAT 3
F LAT 1
F LONG 3
F LONG 1
HIGH RAIL
θ LDZ
θ 2
P
θ 1
V
2b
y 2
y 1
-M C
℄ TRACK
F LAT 4
F LAT 2
F LONG 4
F LONG 2
LOW RAIL
2a
2a/R
③

Figure B.2 Schematic diagram of truck curving model

Two common truck curving modes, non-flanging (in shallow curves) and flanging (in sharp curves), can be simulated, making the model useful for a wide range of curve degrees.

Non-linear interaction characteristics of in-service wheel and rail profiles are incorporated in the simulation, rendering the model suitable for the evaluation of the effect of modifying wheel and rail profiles.

Non-linear creep coefficient and different levels of rail lubrication can be simulated, making the model suitable for the evaluation of the effect of track lubrication.

The model is written in FORTRAN and operates in an interactive mode. A set of default values for track, vehicle and operational parameters is built in for model inputs. Any of these can be modified by the user. A complete list of the model inputs and the default values are given below.

Input		Default Values for Truck on 3° Curve for Two-Point Contact Mode
WBASE	= wheelbase (m)	1.83 m
BCD	= truck centre distance (m)	5.20 m
H	= COG/rail head vertical distance (m)	2.00 m
CLOZ	= lozenging stiffness (kNm/rad)	36,000 kNm/rad
MC	= rotational resistance (kNm)	0.0 kNm
R	= curve radius (m)	582.0 m
GAUGE	= track gauge (m)	1.44 m
SUPEL	= superelevation (m)	0.064 m
VKPH	= vehicle velocity (kph)	57.50 km/m
GWT	= vehicle gross weight (tonne)	125.0 tonnes
MU	= flange friction factor	0.30
MODE	= one- or two-point contact	2.0
C1LON C2LON C3LON C4LAT C5LAT C6LAT	= creep co-efficient equation constants	

Model outputs cover data on track position (lozenging angle), lateral displacement, truck configuration (lozenging angle), wheel/rail interaction forces (creep forces, flanging force, vertical wheel load transfer, etc.) and wheel/rail creepages. Tread and flange wear indices are also provided for wheel and rail wear evaluation. A complete output from the program is shown in Figure B.3.

B.4 SIMULATION RUN

Simulation runs were made for a standard vehicle (a loaded 100-ton hopper car) at speeds ranging from 10 mph (16.09 km/h) to 60 mph (96.54 km/h) through curves ranging from 1 degree to 6 degrees. Both balanced speed and unbalanced speed simulations were carried out. The results of the simulations are listed in Table B.1.

B.5 EMPIRICAL EQUATIONS

From the results of the simulation runs, a set of quasi-empirical equations can be derived that relate steady-state lateral force to the track curvature, track superelevation and vehicle speed. Since the effects on high and low rails are different, an equation for each rail is derived. The equations are derived for the lead axle forces (high rail - FLAT1, low rail - FLAT2), since they are the highest.

```
      CURVE MODEL         RUN NUMBER     3                  02:23:46

                          2POINT CONTACT MODE

LEADING WHEELSET          AAR20.DAT                AAR 1 IN 20 CONE WHEEL
TRAILING WHEELSET         AAR20.DAT                AAR 1 IN 20 CONE WHEEL

VEHICLE                   TRACK                    OPERATION

WBASE        1.830M       R            582.0M      VKPH        57.50KM/H
BCD          5.200M       GAUGE      1.4400M
                                                   GWT       125.00TONNE
H            2.000M       SUPEL     0.06400M       MU        0.30000
PHID       59.789DEG.     FRC1      0.01100M
CLOZ     36000.0KNM/RAD   FRC2     -0.01100M       CENTRIFUGAL FORCE
MC           0.000KNM     FRC3      0.01100M
                          FRC4     -0.01100M       P            -0.156KN

CREEP COEFF EQN CONSTS.   ITERATION CONTROLS       EQUILIB. EQN. ERRORS

C1LON        138.0        DWT          4.000KN     ERLAT   -0.03963KN
C2LON          0.0        DLXX1     0.00050M       ERROT   -0.06978KNM
C3LON          0.1        DTXX2     0.00100M       ERLOZ   -0.06978KNM
C4LAT        138.0        EQERR     0.10000        ERTQL    0.09760KNM
C5LAT      70000.0        EPS     1.000E-06        ERTQT   -0.01407KNM
C6LAT      -1570.0        INTRM           50

WHEEL LOADS               TRUCK CONFIGURATION      CONTACT POINT RADII

W1         153.386KN      X1          0.01100M     R1          0.48550M
WT          81.511KN      X2          0.00752M     RXFC        0.49550M
W2         153.170KN      THTA1  2.812E-03RAD      R2          0.48450M
W3         153.386KN      THTA2 -3.322E-04RAD      R3          0.48533M
W4         153.170KN      THLOZ -6.641E-04RAD      R4          0.48467M

LONG. CREEPAGES           LONG. CREEP CO-EFF       LAT. CREEP CO-EFF

CRL1  -2.401E-03          CL1          -0.201 MU   CT1           0.218MU
CRL2   1.954E-03          CL2           0.180MU    CT2           0.218MU
CRL3  -5.654E-04          CL3          -0.069MU    CT3          -0.043MU
CRL4  -5.654E-04          CL4          -0.069MU    CT4          -0.043MU

GRAVITATIONAL FORCES      LONG. CREEP FORCES       LAT. CREEP FORCES

FG1           4.076KN     FL1         -16.350KN    FT1          17.746KN
FG2           7.658KN     FL2          27.504KN    FT2          33.347KN
FG3           7.669KN     FL3         -10.539KN    FT3          -6.521KN
FG4           7.658KN     FL4         -10.523KN    FT4          -6.512KN

FLANGE FORCES             RESULTANT LONG. FORCES   RESULTANT LAT. FORCES

RF          143.701KN     FLON1        26.761KN    FLAT1      -27.845KN
RFL          43.110KN     FLON2        27.504KN    FLAT2       41.006KN
RFT          41.516KN     FLON3       -10.539KN    FLAT3      -14.171KN
                          FLON4       -10.523KN    FLAT4        1.146KN

WEAR INDICES              ITERATION COUNTERS
                                                   ITXWT            28
WTRD      0.25374         ITAVL           23       I1XX1             0
WFLNG     0.08775         ITAVT            1       ITXX2            15
```

Figure B.3   Sample output, Truck Curving Model

TABLE B.1

SIMULATION AND CALCULATED LATERAL STEADY-STATE FORCES

V (km/hr)	D (Degree)	Sw (m)	TRUCK CURVING MODEL FLAT 1 (KN)	EQUATION FLAT 1 (KN)	TRUCK CURVING MODEL FLAT 2 (KN)	EQUATION FLAT 2 (KN)
48.27	3	0.04524	-13.74	-14.31	18.53	19.64
32.18	3	0.04524	-16.22	-17.60	17.72	18.84
16.09	3	0.04524	-17.73	-19.58	17.24	18.36
64.36	3	0.04524	- 9.67	- 9.70	19.65	20.77
80.45	3	0.04524	- 3.41	- 3.77	21.09	22.21
96.54	3	0.04524	+ 5.24	+ 3.48	22.86	23.98
48.27	1	0.06334	- 8.08	- 6.28	5.83	7.67
48.27	2	0.06334	- 7.19	-11.73	12.12	13.79
48.27	3	0.06334	-15.63	-16.67	17.95	19.07
48.27	4	0.06334	-22.05	-21.43	23.50	23.86
48.27	5	0.06334	-26.66	-26.07	28.84	28.33
48.27	6	0.06334	-30.55	-30.64	34.03	32.55
16.09	3	0.06334	-17.34	-21.94	16.67	17.78
32.18	3	0.06334	-17.62	-19.96	17.15	18.26
48.27	3	0.06334	-15.63	-16.67	17.95	19.07
64.36	3	0.06334	-12.05	-12.06	19.07	20.19
80.45	3	0.06334	- 5.95	- 6.13	20.52	21.64
48.27	4.2	0.06334	-23.14	-22.36	24.58	24.78
48.27	4.2	0.0381	-19.49	-19.07	25.38	25.58
48.27	4.2	0.0508	-21.41	-20.73	24.98	25.18
48.27	4.2	0.0762	-24.70	-24.04	24.17	24.37
48.27	4.2	0.0889	-26.16	-25.70	23.77	23.96
32.18	4.2	0.02815	-23.14	-22.38	24.57	24.77
48.27	4.2	0.06334	-23.14	-22.36	24.58	24.78
64.36	4.2	0.11261	-23.32	-22.33	24.58	24.79
80.45	4.2	0.17595	-23.55	-22.29	24.59	24.80
96.54	4.2	0.25337	-23.76	-22.24	24.60	24.81
48.27	4.2	0.06334	-23.14	-22.36	24.58	24.78
16.09	4.2	0.06334	-28.78	-29.74	22.78	22.98
32.18	4.2	0.06334	-27.00	-26.97	23.46	23.65
64.36	4.2	0.06334	-16.31	-15.91	26.15	26.35
80.45	4.2	0.06334	- 5.62	- 7.61	28.17	28.38
48.27	2	0.03016	- 6.06	- 7.40	13.18	14.85
16.09	2	0.03016	- 8.008	-10.91	12.32	13.99
32.18	2	0.03016	- 7.36	- 9.60	12.64	14.31
64.36	2	0.03016	- 3.73	- 4.33	13.93	15.60
48.27	2	0.0508	- 7.76	-10.09	12.52	14.19
48.27	2	0.04	- 6.88	- 8.68	12.87	14.54
48.27	2	0.02	- 4.86	- 6.08	13.50	15.17
48.27	2	0	- 2.75	- 3.47	14.14	15.81
16.09	2	0.00335	- 6.06	- 7.42	13.18	14.84
80.45	2	0.08377	- 6.06	- 7.37	13.19	14.86
80.45	2	0.03297	0	- 0.74	14.14	16.47
16.09	5	0.0754	- 35.26	-36.43	26.32	25.80
32.18	5	0.0754	- 33.62	-33.13	27.12	26.61
48.27	5	0.0754	- 28.49	-27.65	28.46	27.94
64.36	5	0.0754	- 19.48	-19.96	30.33	29.82
80.45	5	0.0754	- 3.81	-10.08	32.73	32.23
48.27	5	0.0508	- 25.05	-24.40	29.24	28.73
64.36	5	0.0508	- 15.47	-16.71	31.11	30.60
80.45	5	0.0508	- 7.51	- 6.84	33.52	33.01
48.27	6	0.04524	- 27.34	-28.28	34.60	33.13

The resultant equations are shown below.

HIGH RAIL STEADY-STATE LATERAL FORCE

$$L_{S_{HR}} = -[\ 7.42\ (D-1)^{0.95} + 130.4\ S_u - 6.5 \times 10^{-4}\ V^2\ D)\ ]$$

where: $L_{S_{HR}}$ = high rail steady-state lateral force (kN)

D = curvature (deg.)

S_u = superelevation (in.)

V = vehicle speed (km/h)

LOW RAIL STEADY-STATE LATERAL FORCE

$$L_{S_{LR}} = 9.20\ D^{0.69} - 31.79\ (S_u - 6.5 \times 10^{-4}\ V_2\ D)$$

where: $L_{S_{LR}}$ = low rail steady-state lateral force (kN).

Each equation can be seen to consist of two terms. The first term is the result of the centrifugal forces experienced in curving, and is speed independent. The second term is a function of unbalanced speeds while curving.

B.5.1 Speed Independent Term

This term is derived from the simulation results for balanced speed runs, and is assumed to be independent of superelevation and vehicle speed. The calculated terms are for the high rail:

$$L_{HR} = 7.42\ (D-1)^{0.95}$$

and for the low rail:

$$L_{LR} = 9.20\ D^{0.69}$$

Figure B.4 compares the calculated results against the actual simulation results for the high rail. Figure B.5 does the same for the low rail. Figures B.6 and B.7 show the results of the lateral steady-state forces for the high and low rails, respectively, against the simulation results.

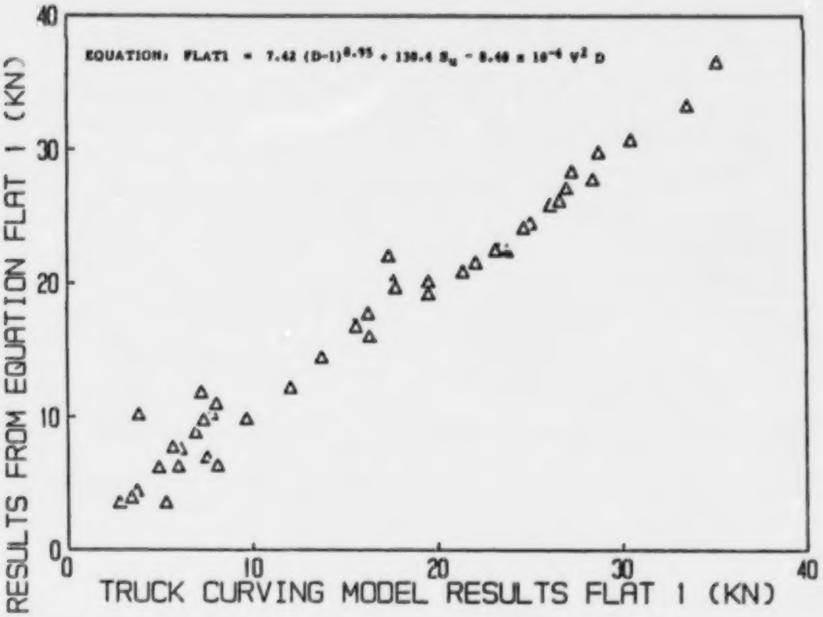

Figure B.4 Speed-independent term for high rail

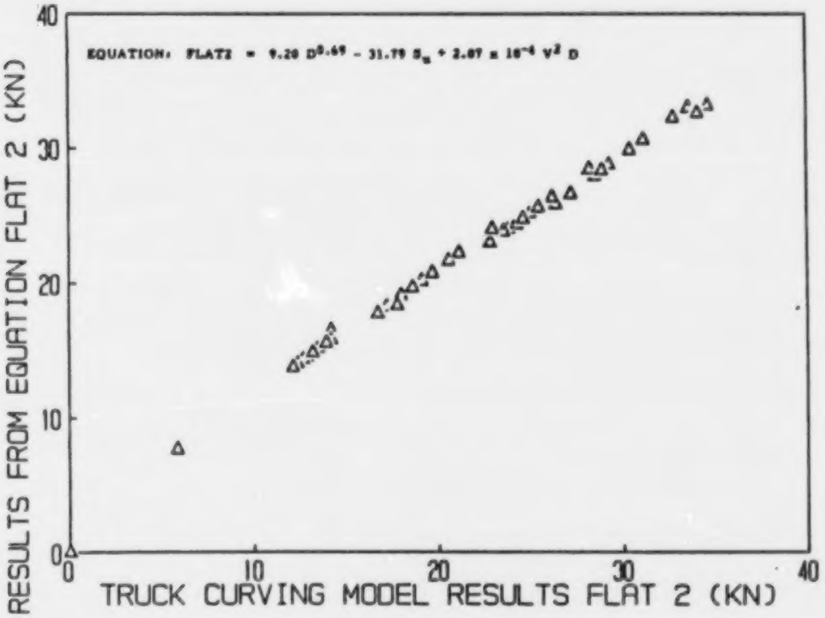

Figure B.5 Speed-independent term for low rail

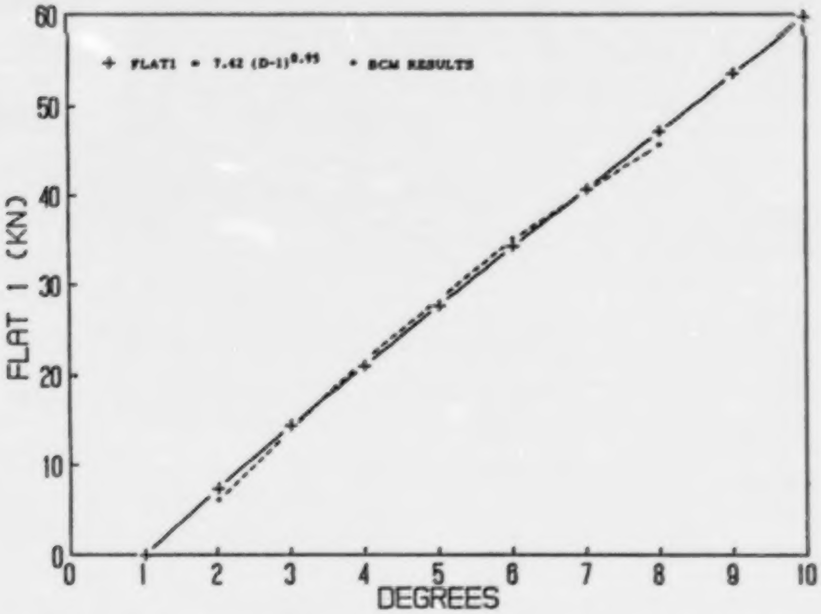

Figure B.6 Correlation between simulated and calculated forces on the high rail

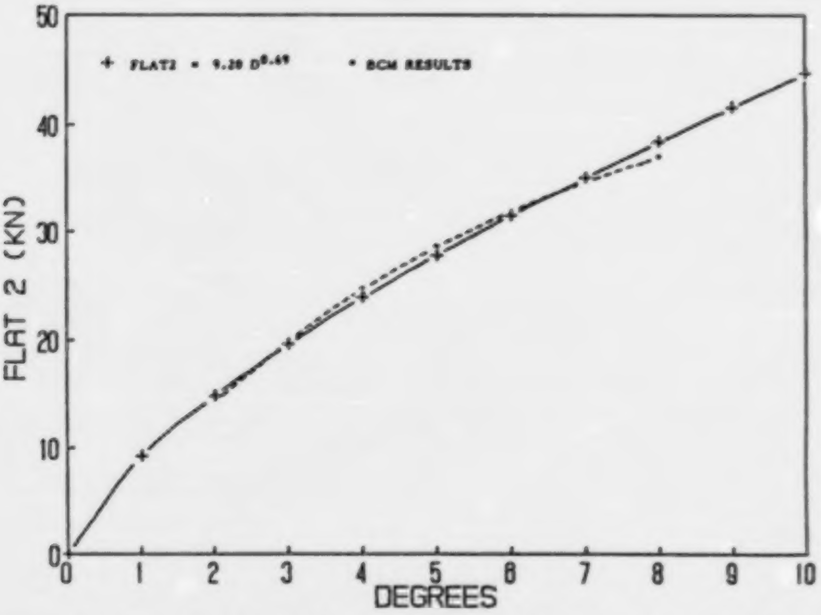

Figure B.7 Correlation between simulated and calculated forces on the low rail

B.6 High Rail Steady-state Force Equation

The equation presented above has been derived for a single vehicle. Since we are interested in modelling several types of vehicles, it can be modified by the addition of a weighting term to account for different vehicle designs. Theoretically, each vehicle has its own set of eigenfrequencies. Therefore, each vehicle design should be subjected to a full analysis. However, as an approximation the estimated force is weighted by the ratio of the static axle loads raised to the power of 2/3. The equation units can also be converted to reflect more conventional units.

In its final form, the high rail steady-state force equation is:

$$L_{S_{HS}} = - [\ 1668.2\ (D-1)^{0.95} + 744.64\ S_u - .494\ V^2\ D\ ]\ (\frac{W}{32.9})^{2/3}$$

where: $L_{S_{HR}}$ = high rail steady-state force (lb)

D = curvature (deg.)

S_u = superelevation (in.)

V = speed (mph)

W = axle weight (tons).

B.7 Low Rail Steady-state Force Equation

As with the high rail equation, the low rail steady-state force equation is modified to allow for different vehicle designs. In its final form, the low rail steady-state force equation is:

$$L_{S_{LR}} = - [\ 2068.4\ D^{0.69} - 181.53\ S_u - .12\ V^2\ S\ ]\ (\frac{W}{32.9})^{2/3}$$

where: $L_{S_{HL}}$ = low rail steady-state force (lb)

D = curvature (deg.)

S_u = superelevation (in.)

V = speed (mph)

W = axle weight (tons).

APPENDIX C

MODEL CALIBRATION REQUIREMENTS AND PROCEDURES

C.1 INTRODUCTION

When using computer models to simulate real events, it is important to note that the model is only a simplification of the system which it is to represent. In order to obtain dependable results from such a model, it must be calibrated and verified against field data. To simplify the calibration, the model should be designed to contain variable factors which can be used to fine-tune the output from the model against additional or improved data as they become available. Simple and flexible calibration procedures are particularly important in the case of the models discussed in this study, since the available data is normally updated and/or improved continuously. Specific calibration requirements and procedures are outlined in the following sections.

C.2 CALIBRATION REQUIREMENTS

Calibration of track maintenance models should be done over a period of time, as well as over different sections of track. By extending the calibration over several years, the effects of anomalous events related to time will be worked out of the calibration. Anomalous events include such effects as economic conditions resulting in a high (or low) level of track maintenance activity. By extending the calibration over several track sections, any effect related to a specific track condition may be identified and incorporated.

In calibrating the system, it is always important to be aware of the validity of the data being used and to be aware of effects which can introduce errors or variations into the model.

C.3 DYNAMIC WHEEL FORCE MODEL CALIBRATION

This model is probably the most difficult to calibrate. At present, the shortage of field data detailing dynamic wheel forces means that the model relies heavily on simulated results. In order to calibrate this model successfully, the required data includes:

- accurate information detailing track geometry quality (including surface level, cross-level, and alignment information)
- accurate records of traffic types, loads and speeds
- measures of the wheel/rail load spectrum (these should be acquired for a series of traffic types and a variety of speeds over different quality tracks)

- valid vehicle characteristic data.

C.4 TIE LIFE MODEL CALIBRATION

Four constants need to be determined in order to calibrate the Tie Life Model:

k_1 - Tie Age Index

R_c - percentage of ties failed or replaced due to cutting failure

R_s - percentage of ties failed or replaced due to splitting failure

t_1 - tie stress index.

These can be determined through the following procedure:

(1) select the calibration track

(2) select a Tie Age Index

(3) determine the tie failure modes and tie replacement numbers

(4) calculate the Tie Stress Index

(5) verify the replacement predictions.

Each step is described in the following sections.

C.4.1 Selection of Calibration Track

The section of track used to calibrate the Tie Life Model must fit the following criteria:

(1) Traffic distribution must be known and must consist of traffic types that can be modelled. This modelling is done using the Dynamic Wheel Force Model.

(2) The maintenance history of the track must be known. It should allow the determination of the number of ties replaced due to tie failure, as well as the percentage breakdown of tie failures.

(3) Although the calibration is actually only done against one year (or other period of interest), it is best if several years of data are available to confirm the trends predicted by the model.

C.4.2 Selection of a Tie Age Index

A Tie Age Index (k_1) represents the overall condition of the ties. It is used as a relative indication of tie quality. As tie quality goes down, it becomes more sensitive to damage compared to a section of good quality tie track under the same loading environment. This is reflected in the model by an increase in the Tie Age Index. Figure C.1 illustrates how the predicted number of ties is affected by the Tie Age Index.

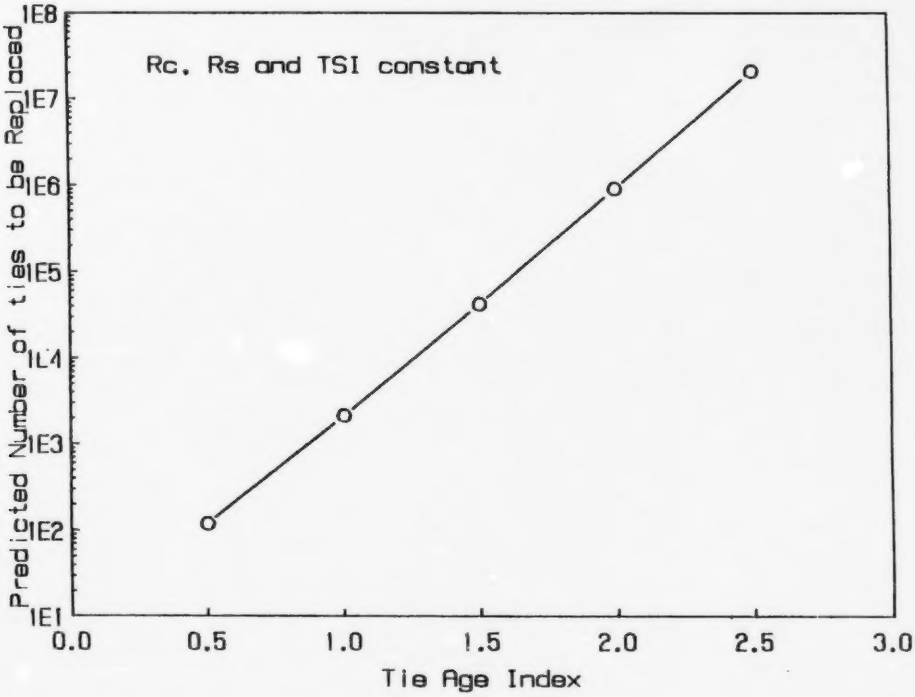

Figure C.1 Tie replacement versus Tie Age Index

The initial selection of k_1 is not important to the calibration of the model. It has been found that a value of 1.5 for good quality track is a reasonable choice.

If the overall quality of the track degrades with time, this can be reflected in the model by increasing k_1. However, more work needs to be done to establish the actual relationship between k_1 and tie quality.

C.4.3 Determining Tie Failure Modes

Tie failure modes, in terms of percentage of total tie failures, needs to be determined from track maintenance records. For the purposes of the Tie Life Model, tie failure modes are grouped into three categories:

- ties failed due to cutting
- ties failed due to splitting
- ties failed due to other reasons.

The model only requires the percentage of ties failed due to cutting (R_c) and the percentage of ties failed due to splitting (R_s). The percentage of ties failed due to other reasons (R_d) is calculated from

$$R_d = 100 - R_c - R_s.$$

Since this type of information is not usually kept in maintenance records, it will be necessary to set up a system to acquire this data. A statistical survey of ties replaced in the calibration section of track would generate the required data. This survey should be done over several years, to ensure that valid results are generated.

The ties included in the survey should only be those replaced because of tie failure. A decision to re-tie a section of track would mean that a large number of ties would be replaced, but many of them may not be near failure. These ties should not be included in the sampling.

It should be noted that variation in R_c, R_s and R_d percentages will not affect the total tie replacement predictions of the model. These percentage values are used internally to allocate tie failures to each traffic class (as a function of the generated loads). If the model is only being used to predict total tie replacement requirements, the specific percentages used are not important. However, once the model is calibrated for a set of R_c, R_s and R_d, these values cannot be changed without recalibration.

C.4.4 Calculating the Tie Stress Index

After the three calibration constants, k_1, R_c and R_s, have been determined, the final factor,

$$t_1 = \text{tie stress index}$$

must be calculated.

A Tie Stress Index (t_1) is a constant that relates the amount of tie damage to each loading cycle. This is done by selecting "t_1" such that the predicted number of ties to be replaced matches the actual number replaced in the calibration case. To do this, the following steps are taken:

(1) Select an initial t_1 (say 0.5×10^{-11}):

$$t_I = 0.5 \times 10^{-11}.$$

(2) Run the model using T_I, the pre-determined calibration constants k_1, R_c and R_s, and the calibration set of track and traffic data. This generates a predicted number of ties to be replaced, say T_I.

(3) From the calibration case data, the actual number of ties replaced is known, say T.

(4) Calculate the correct Track Stress Index from:

$$t_1 = (T/T_I)\ t_I.$$

This formula is based on a linear relationship between T and t_1.

(5) Run the model using t_1 to ensure that the predicted number of ties to be replaced equals the actual number of ties replaced.

It is important to note that t_1 is specific to the set k_1, R_c and R_s used. If these are changed, a new Tie Stress Index must be derived for the calibration data set.

C.4.5 Verification of Tie Replacement Predictions

After the four constants have been determined, run the model for the calibration data set to ensure that the predictions are correct. If possible, run the model for different years of data on the test track to verify that the model is producing results consistent with the actual maintenance history of the track.

If the predicted results differ greatly from actual results, this may be due to:

- an overall change in tie quality, necessitating an adjustment in the Tie Age Index (k_1)
- a change in track geometry which has not been reflected in the track indices.

C.5 SURFACE LIFE MODEL CALIBRATION

The Surface Life Model is calibrated by following the procedure outlined below:

(1) select the calibration track

(2) establish track error growth

(3) calculate the equivalent loading cycles

(4) calculate the calibration constants.

Each step is outlined in the following sections.

C.5.1 Selection of Calibration Track

The section of track used to calibrate the Surface Life Model must meet the following criteria:

(1) Traffic mix must be known and must consist of traffic types that can be modelled. This modelling is done using the Dynamic Wheel Force Model.

(2) The surfacing history of the track must be known. It is necessary to be able to subdivide the track into specific sections as a function of time since last surfacing.

(3) There must be accurate track geometry records for the track.

C.5.2 Establishing Track Error Growth

The track error growth characteristics must be established for the calibration track. This information is usually determined from track geometry car data.

The track length is subdivided into sections of common track since the last tamping cycle. For each track section, the mean and standard deviation of track error is then calculated (see Figure C.2):

Track Error

Years since Surfacing	Mean	Standard Deviation
0	x_o	S_o
1	x_1	S_1
2	x_2	S_2
•	•	•
•	•	•
•	•	•
Q	x_Q	S_Q

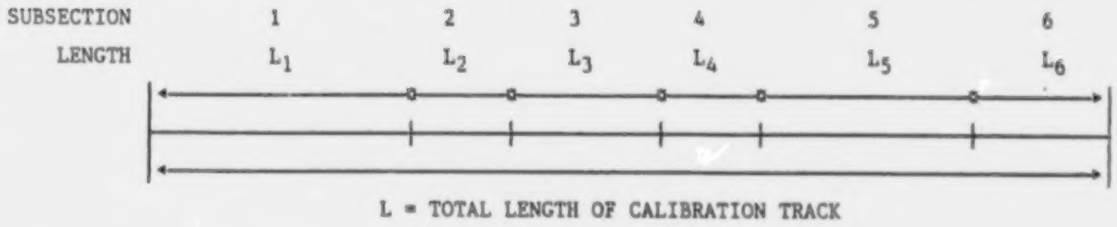
SUBSECTION
1
2
3
4
5
6
LENGTH
L1
L2
L3
L4
L5
L6
L = TOTAL LENGTH OF CALIBRATION TRACK

SUBSECTION	YEARS SINCE TAMPING
1	1
2	2
3	1
4	3
5	2
6	3

YEARS SINCE TAMPING	LENGTH
1	$L_1 + L_3$
2	$L_2 + L_5$
3	$L_4 + L_6$

Figure C.2 Example of subdivision of calibrated track

C.5.3 Calculating the Equivalent Loading Cycle

The number of equivalent loading cycles since the last surfacing cycle is calculated by accumulating the traffic from the time of the last tamping until the present, and running the load cycle calculation routine.

With the traffic mix for each year known, the total traffic since the surfacing cycle, X years ago, is calculated by summing all traffic for the last X years. With this data, the Surface Life Model, which generates the number of equivalent cycles as an intermediate output, is run. This procedure is repeated for each section of track, generating the following information:

Years Since Surfacing	Number of Equivalent Cycles
0	Neq_o
1	Neq_1
2	Neq_2
•	•
•	•
•	•
Q	Neq_Q

Note, however, that since the Surface Life Model has not yet been fully calibrated, the results are only valid up to the number of equivalent cycles output. Output past this point will generate dependable results only after the calibration has been completed.

C.5.4 Calculating the Calibration Constants

The following constants need to be determined in order to calibrate the Surface Life Model:

A, B = relating mean track error to equivalent cycles

C, D = relating standard deviation of track error to equivalent cycles.

These constants are obtained by linear regression of the mean track error versus equivalent load cycles data and standard deviation of track error versus equivalent load cycles data, as shown in Figures C.3 and C.4). The results are equations of the following form:

MEAN ERROR: $\bar{x} = A \times Neq + B$

STANDARD DEVIATION: $s = C \times Neq + D$

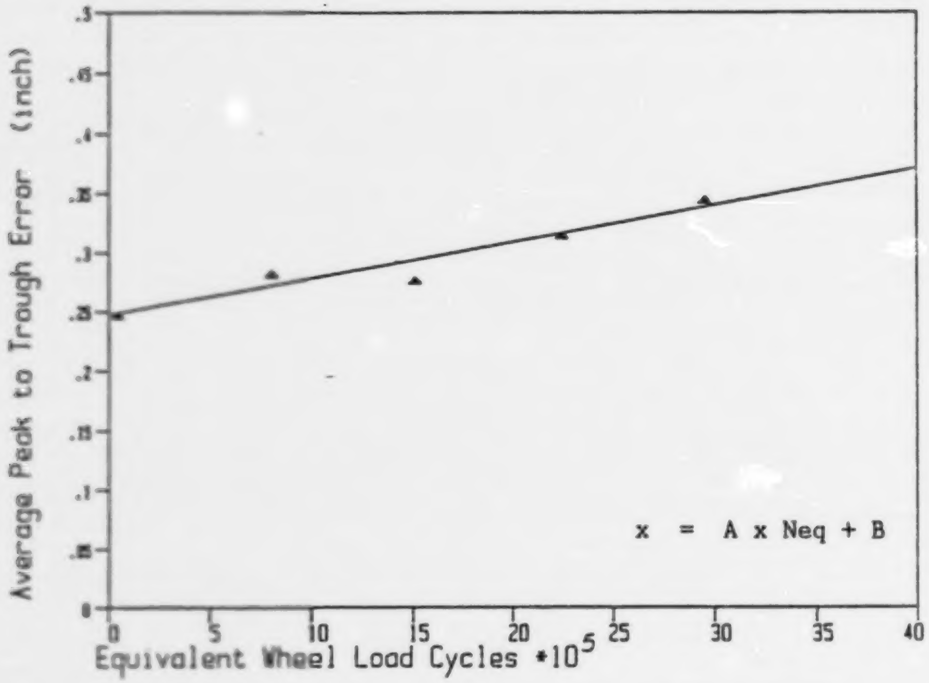

Figure C.3 Average peak to trough error

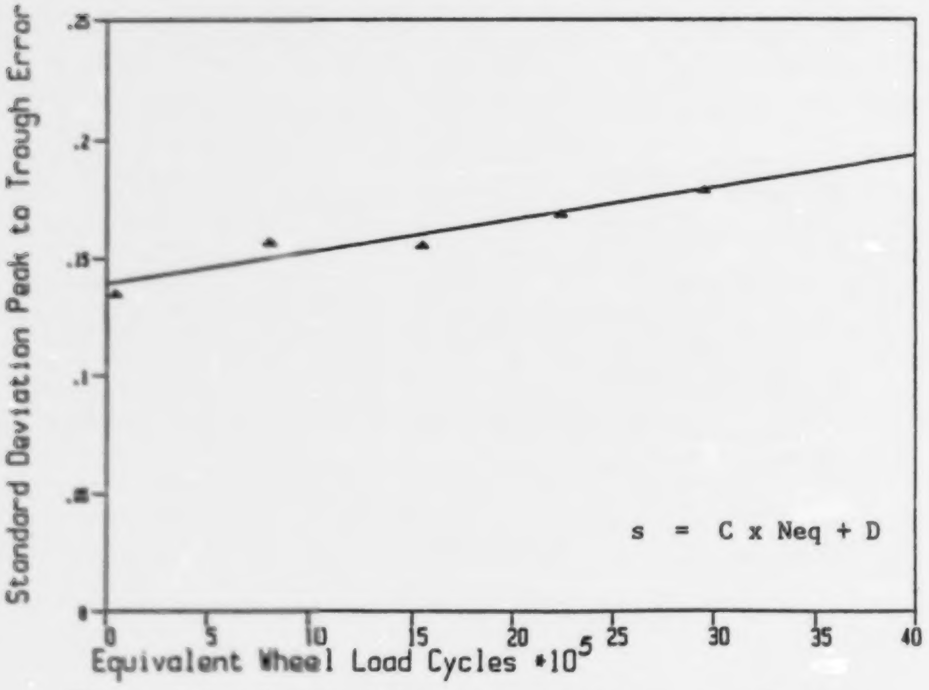

Figure C.4 Standard deviation of peak to trough error

The constants A, B, C and D are then introduced into the Surface Life Model.

C.6 REVIEW OF AVAILABLE DATA FOR CALIBRATION

There are basically four classes of data required for the calibration of the three models:

- track geometry data
- track maintenance data
- traffic make-up data
- wheel/rail force data.

C.6.1 Track Geometry Data

With the growing use of track geometry cars, it is becoming easier to gather valid track geometry data. However, as this data is usually used by track maintenance personnel, the usual means of summarizing track quality is in the form of reports of track quality exceptions (Figure C.5). While this format of data is convenient for planning on-the-spot maintenance work, it does not express the overall track quality needed for use with these models.

What is needed is an index that reflects the overall track quality. The most accurate representation would be the actual rail profile (surface, cross-level and alignment) as recorded by a track geometry car. This would allow the greatest flexibility in subsequent processing.

C.6.2 Track Maintenance Data

In general, the types of detailed maintenance information required for model calibration mean that more stringent maintenance record-keeping methods will have to be enforced.

In terms of tie replacement data, present records simply state the numbers of ties replaced per subdivision. Typically, no records have been kept of tie failure modes. Another factor that makes acquisition of this type of data difficult is that tie replacement work tends to be strongly influenced by outside factors. This means that individual ties are not replaced when they should be, but may be left in place for several years until a large renewal program is carried out.

```
        PRIORITY SUMMARY BETWEEN MILE POST  37 AND  37 ON SOUTH  TRACK            PAGE   1
     EASTERN LINES                          ILLINOIS                          FIRST

DIST TRK    MP      FT    TYPE VALUE   P1#  CV  CL    DATE   TF GA D              COMMENTS
---- ---    --      --    ---- -----   ---  --  --    ----   -- -- -              --------

1101  S     37     128    CVC   3.4      0       2  04/29/86 Y  OK W  ----------------------------
1101  S     37     167     GA   0.9      0  C    2  04/29/86 Y  OK W  ----------------------------
1101  S     37     171     GA   1.0      0  C    2  04/29/86 Y  OK W  ----------------------------
1101  S     37    1838     GA   0.9      0  C    2  04/29/86 Y  OK W  ----------------------------
1101  S     37    1842     GA   1.0      0  C    2  04/29/86 Y  OK W  ----------------------------
1101  S     37    1905     GA   1.2     95  C    2  04/29/86 Y  OK W  ----------------------------
1101  S     37    1907     GA   1.0      0  C    2  04/29/86 Y  OK W  ----------------------------
1101  S     37    1946     GA   0.9      0       2  04/29/86 Y  OK W  ----------------------------
```

Priority #1 Summary Headings

DIST	District Code See Attached List
TRK	Track Tested SG = Single N = North S = South M = Middle 1 = Main Track 1 2 = Main Track 2 3 = Main Track 3 4 = Main Track 4 SX = Siding
MP	Mile Post Number
FT	Plus Feet
TYPE	Type of Defect CVC = Curve Change TW = Twist DIP = Dip NS = North Surface SS = South Surface GA = Gage XLC = Cross Level Change XLV = Excess Super Elevation (more than 6")
VALUE	Defect Value
P1#	Priority #1 Number if = 0 then is a Priority 2 or 3
CV	C = Defect Within Curve
CL	Class that Track was Tested
DATE	Date of Test
TF	Y = Track File Used N = Track File Not Used
GA	OK = Feelers Down NG = Feelers Up
D	E = Track Tested, Car Going East W = Track Tested, Car Going West

Note: Priority #2 headings same as Priority #1, except Priority #2 are not assigned numbers under the P1# column

Figure C.5 Track geometry report

In terms of surfacing work, similar problems apply. The tendency seems to be to carry out surfacing work on a fixed cycle, whether the track needs it or not. This may lead to a very regular cycle for mainline track, resulting in exceptionally good track quality, or a very irregular cycle for spurs and sidings, etc., resulting in generally poor track quality most of the time. Records of track quality between surfacing cycles are required.

C.6.3 Traffic Make-up Data

This data is readily available for model calibration. Usually very accurate records are kept of traffic types and of the individual tonnage. Still, there is the need to represent data for vehicle types accurately in the dynamic models, and this involves the determination of vehicle characteristics. This data is usually quite difficult to ascertain.

C.6.4 Wheel/Rail Force Data

Unfortunately, measured data is not usually directly comparable with calculated forces. Due to the fixed locations of the strain gauge systems in track, the response of wheels to track geometry error cannot be measured. The other alternative, i.e. using instrumented wheelsets, means that the effect of different vehicle designs is not measured.

The accurate measurement of wheel/rail forces for a variety of vehicles on a variety of track structures is therefore an area that needs further work, in order to establish a good base for further developmental work in modelling of track behaviour.

C.7 RECOMMENDED DATA ACQUISITION METHODS

The scope of the data needed for proper calibration is very broad, covering almost every aspect of railroad operation. The calculation of the various calibration constants requires an accurate knowledge of the track deterioration mode which stimulated a maintenance activity, not just information on the nature of the maintenance activity. Extended periods of detailed record-keeping are needed to separate maintenance activity due to good/poor economy, from maintenance due to actual physical track deterioration. Detailed records of traffic, and hence loading environment, are also required.

An ideal environment for collecting the required data would be one where the entire scope of the operation could be monitored. For example, a heavy-haul mining railroad with a captured fleet would provide the best possible situation for examining track deterioration under a single (or at least limited) load type. This would allow the determination of a standardized load cycle.

APPENDIX D

DYNFOR, TIELIF AND SURLIF PROGRAM INTERRELATIONSHIP AND INPUT DATA FORMAT

D.1 WORKING PROCEDURE

Figure D.1 shows the working structure of the latest updated FORTRAN subprograms. All data are kept in a *.DAT file. When DYNFOR is run it picks the required data from the *.DAT file and produces the *.FRC file which contains the necessary wheel forces and stresses. These forces are then used by TIELIF and SURLIF programs in conjunction with the required data from the *.DAT file to produce the tie and surface degradation results.

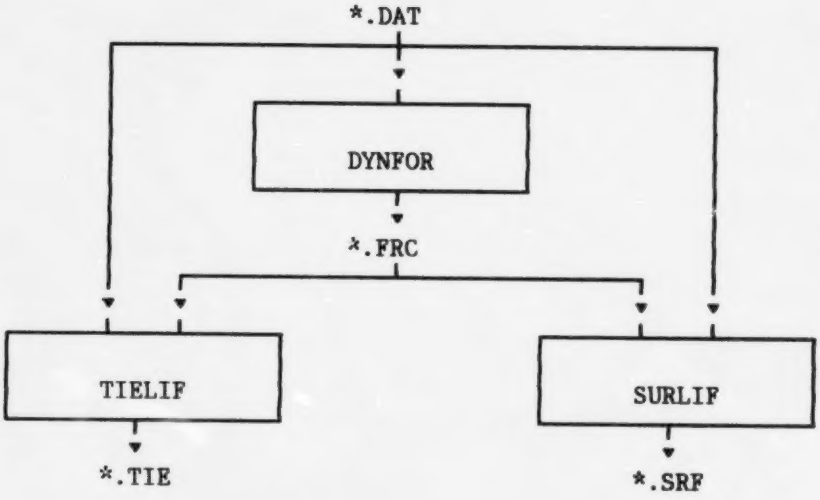

Figure D.1 DYNFOR, TIELIF and SURLIF interrelationship

D.2 INPUT DATA

Sample data for the three programs is given in Figure D.2. Free format is used for the input data. Table D.1 shows the data corresponding to each program, together with the variable names used. A description of the variable names is given in Table D.2.

```
3
 8000. 10.728 2425.
20000. 11.622 2425.
33000. 22.350 3142.
4
44.700  78. 0.0 0.0 152. 152. 152. 20.0 1.5 14.0 2. 3.56 36.7 56.0 .505E-11 2.640e9 2000. 61. 1. .625 16.0
44.700  25. 2.0 1.0 152. 152. 152. 20.0 1.5 14.0 3. 3.56 36.7 56.0 .505E-11 2.640e9 2000. 61. 1. .625 16.0
44.700  37. 5.0 2.0 162. 162. 162. 20.0 1.5 18.0 5. 3.56 36.7 56.0 .505E-11 2.640e9 2000. 61. 1. .625 16.0
44.700  25. 8.0 2.5 162. 162. 162. 20.0 1.5 18.0 5. 3.56 36.7 56.0 .505E-11 2.640e9 2000. 61. 1. .625 16.0
45. 45. 45.
40. 40. 40.
35. 35. 35.
30. 30. 30.
6.214E-8 2.460E-1 2.732E-8 1.390E-1
```

Figure D.2   Sample input data

TABLE D.1

TEST DATA SET FORMAT AND THEIR USE IN DYNFORM, TIELIF AND SURLIF PROGRAMS

Variable Name	Unit	DYNFOR	TIELIF	SURLIF
Record 1: NTRAFF				
Next NTRAFF records:				
Po(j)	(lb/wheel)	x	x	x
XMGT(j)	(MGT/yr)	x	x	x
MU(j)	(lb/axle)	x		
Next record: NTRACK				
Next NTRACK records:				
TMGT(i)	(MGT/yr)		x	x
L(i)	(meter)		x	x
DC(i)	(degree)	x	x	
SE(i)	(in.)	x		
SI(i)		x		
XI(i)		x		
AI(i)		x		
TSPACE	(in.)		x	
TAI			x	
TPLEN	(in.)		x	
SPIKES	(in.)		x	
C			x	
RC			x	
RS			x	
TSI			x	
EI				x
TM				x
BAI				x
BCI				x
SPC				x
PPT				x
Next NTRACK records:				
SPEED(i,j)		x		x
A,B,C,D				x
Next record				

TABLE D.2

DESCRIPTION OF VARIABLES

Variable Name	Description	Units
NTRAFF:		
PO	static wheel load	lb/wheel
XMGT	million tons per year of this traffic type	MGT/yr
MU	unsprung mass	lb/axle
NTRACK:		
TMGT*	million tons per year over track type	MGT/yr
L	length	miles
DC	degree of curvature	degree
SE	superelevation	in.
SI	surface index)	
XI	cross-level index) CN-type indices	
AI	alignment index)	
TSPACE	tie spacing	in.
TAI	tie age index	
TPLEN	tie plate length	
SPIKES	number of spikes per tie plate	
C	half rail height	in.
RC	percent cut ties	
RS	percent split ties	
TSI	tie stress index	
EI	rail modulus	$lb.in.^2$
TM	track modulus	lb.in./in.
BAI	ballast abrasion index	
BCI	ballast condition index	
SPJ	SPC error limit	
PPT	percent allowable poor track	
SPEED	traffic type speed on each track type	mph
A,B,C,D	calibration constants used by SURLIF	

* actually TMGT is calculated internally as:

$$TMGT = \sum_{NTRAFF} XMGT$$

but this is the number echoed in the output file.

APPENDIX E

"DYNFOR" PROGRAM LISTING, INPUT AND OUTPUT

```
C
C $NOFLOATCALLS
C $DEBUG
C
C+++++++++++++++++++++++++++++++++++++++++++++++++++++++++++++++++++++++
C
C     PROGRAM DYNFOR
C
C+++++++++++++++++++++++++++++++++++++++++++++++++++++++++++++++++++++++
C
C     C.I.G.G.T. Wheel-Rail Load Model
C
C
C
C     Program author: J. C. Michaud
C     Date: November 17, 1986
C
C     Input: unit 12 - filename.ext  - supplied by user
C
C     Output: unit 11 - filename.FRC
C
      integer PERIOD
      character*14 INPFIL
      character*1  FILNAM(14)
C
      real    PO(20),MU(20)
      real    DC(20),SE(20),SI(20),XI(20),AI(20)
      real    SPEED(20,20)
C
      real    V
      real    VSTAT(20,20)
      real    HRSSV(20,20),LRSSV(20,20)
      real    HRDV(20,20),LRDV(20,20)
      real    SSLAT(20,20),DLAT(20,20)
      real    SSLT,DLT,LLTF
C
      equivalence ( INPFIL,FILNAM(1) )
C
C+++++++++++++++++++++++++++++++++++++++++++++++++++++++++++++++++++++++
C     Get the files straightened out.
C+++++++++++++++++++++++++++++++++++++++++++++++++++++++++++++++++++++++
C
      write(*,2000)
2000  format(' Enter the input file name: '\)
      read(*,2001) INPFIL
      open ( 12, file=INPFIL, status='old' )
2001  format(a14)
      PERIOD = 0
      do 2 i = 1,14
         if ( FILNAM(i).EQ.'.' ) then
            PERIOD = i
            go to 4
         endif
2     continue
4     FILNAM(PERIOD+1) = 'F'
```

```
      FILNAM(PERIOD+2) = 'R'
      FILNAM(PERIOD+3) = 'C'
      open ( 11, file=INPFIL, status='new' )
C
C+++++++++++++++++++++++++++++++++++++++++++++++++++++++++++++++++++++++
C     Get the data.
C+++++++++++++++++++++++++++++++++++++++++++++++++++++++++++++++++++++++
C
C Read the traffic data
C     NTRAFF = number of traffic classes
C        PO = wheel load (lb/wheel)
C        MU = unsprung mass (lb/axle)
C
      read(12,*) NTRAFF
      do 10 j = 1 , NTRAFF
         read(12,*) PO(j),D1,MU(j)
10    continue
C
C Read the track data
C     NTRACK = number of track classes
C     DC = degree of curvature (deg)
C     SE = superelevation (in)
C     SI = surface index
C     XI = crosslevel index
C     AI = alignment index
C
      read(12,*) NTRACK
      do 20 i = 1, NTRACK
         read(12,*) D1,D2,DC(i),SE(i),SI(i),XI(i),AI(i)
20    continue
C
C Read the speed data
C        SPEED(i,j) = speed (mph) of traffic class j on track class i
C
      do 30 i = 1 , NTRACK
         read(12,*) (SPEED(i,j),j=1,NTRAFF)
30    continue
C
C+++++++++++++++++++++++++++++++++++++++++++++++++++++++++++++++++++++++
C     Calculate the dynamic loads.
C+++++++++++++++++++++++++++++++++++++++++++++++++++++++++++++++++++++++
C
      do 100 i = 1,NTRACK
      do 100 j = 1,NTRAFF
C
C        Select the traffic class speed on this track class
         V = SPEED (i,j)
C
C        Calculate the vertical loads
C
C        Static vertical load (lb/wheel)
         VSTAT(i,j) = PO(j)
C
C        Steady state load transfer factor
         SSLT = 2.788 * (.0000115*V**2.*DC(i)-.0177*SE(i))
```

```
C
C        H.R. steady state vertical load (lb/wheel)
         HRSSV(i,j) = VSTAT(i,j) * (1.+SSLT)
C
C        L.R. steady state vertical load (lb/wheel)
         LRSSV(i,j) = VSTAT(i,j) * (1.-SSLT)
C
C        Dynamic vertical load transfer factor
         DLT = 7.942E-6 * V**.68 * (.585*SI(i)**1.4+1.22*XI(i))
     :       * (MU(j)/3156)**.5
C
C        H.R. dynamic vertical load (lb/wheel)
         HRDV(i,j) = HRSSV(i,j) * DLT
C
C        L.R. dynamic vertical load (lb/wheel)
         LRDV(i,j) = LRSSV(i,j) * DLT
C
C        H.R. steady state lateral force
         if ( DC(i).ge.1.) then
            SSLAT(i,j) = ( 1668.2*(DC(i)-1)**.95
     :                     + 744.64*SE(i) - .494*V**2*DC(i) )
     :                   * ( PO(j)/16450. )**.667
         else
            SSLAT(i,j) = ( 744.64*SE(i) - .494*V**2*DC(i) )
     :                   * ( PO(j)/16450. )**.667
         endif
C
C        Dynamic lateral load transfer factor
         LLTF = 5.1E-5 * (AI(i)/100.) * V**1.86 * (MU(j)/3156)**.5
C
C        Dynamic lateral load (lb/wheel)
         DLAT(i,j) = VSTAT(i,j) * LLTF
C
100   continue
C
C     Output the results
      write(11,3000)
      write(11,*)' '
      do 112 i = 1,NTRACK
         do 110 j = 1,NTRAFF
            write(11,3002) VSTAT(i,j),HRSSV(i,j),LRSSV(i,j),
     :                     HRDV(i,j),LRDV(i,j),
     :                     SSLAT(i,j),DLAT(i,j)
110      continue
         write(11,*)' '
112   continue
3000  format('WHEEL/RAIL LOADS',
     :      /'      st V   ss V HR    ss V LR  dyn V HR',
     :       '  dyn V LR      ss L     dyn L',
     :      /'  (lb/whl)  (lb/whl)   (lb/whl)  (lb/whl)',
     :       '  (lb/whl)  (lb/whl)   (lb/whl)')
3002  format(7(1x,f9.2))
C
C Echo the input data.
      write(11,1140)
      do 40 j = 1,NTRAFF
         write(11,1142) j,PO(j),MU(j)
40    continue
1140  format(//'TRAFFIC DATA',
     :       /' Class     Wheel load    Unsprg mass',
     :       /'     j     (lb/wheel)      (lb/axle)')
1142  format(i6,f15.2,f15.2)
C
      write(11,1150)
      do 50 i = 1,NTRACK
         write(11,1152) i,DC(i),SE(i),SI(i),XI(i),AI(i)
50    continue
1150  format(//'TRACK DATA',
     :/' Class  Curve  S.E. Surf. Xlevl Alig.',
     :/'     i  (deg)  (in) index index index')
1152  format(i6,2(1x,f5.2),3(1x,f5.1))
C
      write(11,1160) (j,j=1,NTRAFF)
      do 60 i = 1 , NTRACK
         write(11,1162) i,(SPEED(i,j),j=1,NTRAFF)
60    continue
1160  format(//'SPEED DATA',
     :       /' Track     Traffic Class (mph)',
     :       /' Class',20i6:)
1162  format(i6,20f6.1:)
C
      stop
      end
```

```
WHEEL/RAIL LOADS
     st V      ss V HR      ss V LR     dyn V HR    dyn V LR        ss L       dyn L
 (lb/whl)    (lb/whl)     (lb/whl)    (lb/whl)    (lb/whl)     (lb/whl)    (lb/whl)

  8000.00     8000.00      8000.00      629.20      629.20          .00      646.05
 20000.00    20000.00     20000.00     1573.00     1573.00          .00     1615.13
 33000.00    33000.00     33000.00     2954.33     2954.33          .00     3033.46

  8000.00     8426.01      7573.99      611.70      549.84       514.43      518.95
 20000.00    21065.02     18934.98     1529.24     1374.61       947.87     1297.37
 33000.00    34757.28     31242.72     2872.15     2581.72      1323.76     2436.65

  8000.00     8781.48      7218.52      632.98      520.32      2899.36      431.45
 20000.00    21953.69     18046.31     1582.46     1300.81      5342.30     1078.62
 33000.00    36223.59     29776.41     2972.10     2443.12      7460.88     2025.82

  8000.00     8859.82      7140.18      575.08      463.46      5502.33      323.90
 20000.00    22149.55     17850.45     1437.69     1158.64     10138.48      809.74
 33000.00    36546.75     29453.25     2700.21     2176.11     14159.07     1520.83


TRAFFIC DATA
 Class        Wheel load      Unsprg mass
     j        (lb/wheel)       (lb/axle)
     1           8000.00         2425.00
     2          20000.00         2425.00
     3          33000.00         3142.00


TRACK DATA
 Class   Curve   S.E.  Surf.  Xlevl  Alig.
     i   (deg)   (in)  index  index  index
     1     .00    .00  152.0  152.0  152.0
     2    2.00   1.00  152.0  152.0  152.0
     3    5.00   2.00  162.0  162.0  162.0
     4    8.00   2.50  162.0  162.0  162.0


SPEED DATA
 Track      Traffic Class (mph)
 Class      1      2      3
     1   45.0   45.0   45.0
     2   40.0   40.0   40.0
     3   35.0   35.0   35.0
     4   30.0   30.0   30.0
```

APPENDIX F

"TIELIF" PROGRAM LISTING, INPUT AND OUTPUT

```
C
C $NOFLOATCALLS
C $DEBUG
C
C+++++++++++++++++++++++++++++++++++++++++++++++++++++++++++++++++++++++
C
C     PROGRAM TIELIF
C
C+++++++++++++++++++++++++++++++++++++++++++++++++++++++++++++++++++++++
C
C     C.I.G.G.T. Tie Life Model
C
C
C
C     Program author: J. C. Michaud
C     Date: November 10, 1986
C
C     Input: unit 12 - filename.ext  - supplied by user
C            unit 14 - filename.FRC  - force data calcualted by DYNFOR
C
C     Output: unit 11 - filename.TIE
C
      integer PERIOD
      character*14 INPFIL
      character*1  FILNAM(14)
C
      real    PO(20),XMGT(20)
      real    TMGT(20),L(20),DC(20),TSPACE(20),TAI(20)
      real    TPLEN(20),SPIKES(20),C(20),RC(20),RS(20),TSI(20)
C
      real    VSTAT(20,20)
      real    HRSSV(20,20),LRSSV(20,20)
      real    HRDV(20,20),LRDV(20,20)
      real    SSLAT(20,20),DLAT(20,20)
C
      real    LDCYC(20)
      real    SSVL(20,20),DVL(20,20)
      real    SSLL(20,20),DLL(20,20)
      real    LL
      real    DVSL(20,20),DLSL(20,20)
      real    CS(20,20),SS(20,20)
      real    TWPC(20,20),TWPY(20,20)
      real    TWTRA(20,20),TWTCK(20)
      real    TRAFTL(20,20),TRCKTL(20)
      real    PTRAF(20,20),PTRCK(20)
      real    TIEPYR(20)
C
      equivalence ( INPFIL,FILNAM(1) )
C
C+++++++++++++++++++++++++++++++++++++++++++++++++++++++++++++++++++++++
C     Get the files straightened out.
C+++++++++++++++++++++++++++++++++++++++++++++++++++++++++++++++++++++++
C
      write(*,2000)
2000  format(' Enter the input file name: '\)
```

```
      read(*,2001) INPFIL
      open ( 12, file=INPFIL, status='old' )
2001  format(a14)
      PERIOD = 0
      do 2 i = 1,14
         if ( FILNAM(i).EQ.'.' ) then
            PERIOD = i
            go to 4
         endif
2     continue
4     FILNAM(PERIOD+1) = 'T'
      FILNAM(PERIOD+2) = 'I'
      FILNAM(PERIOD+3) = 'E'
      open ( 11, file=INPFIL, status='new' )
      FILNAM(PERIOD+1) = 'F'
      FILNAM(PERIOD+2) = 'R'
      FILNAM(PERIOD+3) = 'C'
      open ( 14, file=INPFIL, status='old' )
C
C++++++++++++++++++++++++++++++++++++++++++++++++++++++++++++++++++++++++++
C     Get the data.
C++++++++++++++++++++++++++++++++++++++++++++++++++++++++++++++++++++++++++
C
C Read the traffic data
C     NTRAFF = number of traffic classes
C        PO     = wheel load (lb/wheel)
C        XMGT   = annual tonnage (million tons/yr)
C
      read(12,*) NTRAFF
      do 10 j = 1 , NTRAFF
         read(12,*) PO(j),XMGT(j)
10    continue
C
C Read the track data
C     NTRACK = number of track classes
C        TMGT   = total tonnage (million tons/yr)
C        L      = length (miles)
C        DC     = degree of curvature (deg)
C        TSPACE = tie spacing (in)
C        TAI    = tie age index
C        TPLEN  = tie plate length (in)
C        SPIKES = number of spikes per tie plate
C        C      = half rail height (in)
C        RC     = % ties replaced due to cutting
C        RS     = % ties replaced due to splitting
C        TSI    = tie stress index
C
      read(12,*) NTRACK
      do 20 i = 1, NTRACK
         read(12,*) TMGT(i),L(i),DC(i),D1,D2,D3,D4,
     :              TSPACE(i),TAI(i),TPLEN(i),SPIKES(i),
     :              C(i),RC(i),RS(i),TSI(i)
20    continue
C
C Read the precalculated force data
```

```
         read(14,36)
         read(14,36)
         read(14,36)
         read(14,36)
         do 35 i = 1,NTRACK
            do 34 j = 1,NTRAFF
               read(14,*) VSTAT(i,j),HRSSV(i,j),LRSSV(i,j),
     :                    HRDV(i,j),LRDV(i,j),
     :                    SSLAT(i,j),DLAT(i,j)
 34         continue
            read(14,36)
 36         format(1x)
 35      continue
C
C Echo the input data.
         write(11,1140)
         do 40 j = 1,NTRAFF
            write(11,1142) j,PO(j),XMGT(j)
 40      continue
 1140    format(//'TRAFFIC DATA',
     :          /'Class     Wheel load        Ann. ton.',
     :          /'   j      (lb/wheel)         (mgt/yr)')
 1142    format(i5,f15.2,f15.3)
C
         write(11,1150)
         do 50 i = 1,NTRACK
            write(11,1152) i,TMGT(i),L(i),DC(i),
     :                     TSPACE(i),TAI(i),TPLEN(i),SPIKES(i),
     :                     C(i),RC(i),RS(i),TSI(i)
 50      continue
 1150    format(//'TRACK DATA',
     :          /'Class TotTon Length  Curve TieSp   Tie PltLn   no.',
     :           ' H.hgt    RC     RS           TSI',
     :          /'    i per yr (mile)  (deg)  (in) index  (in) spike',
     :           '  (in)                                         ')
 1152    format(i5,1x,f6.3,2(1x,f6.2),7(1x,f5.2),1x,e10.5)
C
C        Calculate the total track length
         TLEN = 0.0
         do 70  i = 1,NTRACK
 70         TLEN = TLEN + L(i)
C
C        Initialize the total tonnage
         TTON = 0.0
C
C+++++++++++++++++++++++++++++++++++++++++++++++++++++++++++++++++++++
C        Calculate the dynamic loads.
C+++++++++++++++++++++++++++++++++++++++++++++++++++++++++++++++++++++
C
         do 100 j = 1,NTRAFF
C
C           Total ton/yr for each track cat. (ton/yr)
            TTON = TTON + XMGT(j)*1.0e6
C
C           Load cycles per year for each traffic category
```

```
         LDCYC(j)  = 1.0e9*XMGT(j) / PO(j)
C
         do 100 i = 1,NTRACK
C
C           Maximum steady state vertical load
            SSVL(i,j) = HRSSV(i,j)
C
C           Maximum vertical load
            DVL(i,j)  = HRSSV(i,j)+ HRDV(i,j)
C
C           Steady state lateral load
            SSLL(i,j) = SSLAT(i,j)
C
C           Maximum lateral load
            DLL(i,j) = SSLAT(i,j) + DLAT(i,j)
C
100   continue
      write(11,3000)
      do 112 i = 1,NTRACK
         do 110 j = 1,NTRAFF
            write(11,3002) LDCYC(j),PO(j),
     :                     SSVL(i,j),DVL(i,j),SSLL(i,j),DLL(i,j)
110      continue
         write(11,*)' '
112   continue
3000  format(//'DYNAMIC LOADS',
     :        /' ld cycles  stat vert  s.s. vert',
     :         '   dyn vert  s..s. lat    dyn lat',
     :        /'  (cyc/yr)  load (lb)  load (lb)',
     :         '  load (lb)  load (lb)  load (lb)')
3002  format(f10.0,5(1x,f10.2))
C
C+++++++++++++++++++++++++++++++++++++++++++++++++++++++++++++++++++++++
C     Calculate the stresses.
C+++++++++++++++++++++++++++++++++++++++++++++++++++++++++++++++++++++++
C
      do 200 i = 1,NTRACK
C
C     Calculate the stress equations coefficients
      CS1 = 1. / ( 7.75 * TPLEN(i) )
      CS2 = ( 12. * C(i) ) / ( 7.75 * TPLEN(i)**2 )
      SS1 = 0.0612
      SS2 = 0.457 / SPIKES(i)
C
      do 200 j = 1,NTRAFF
C
C        Dynamic vertical seat load
         DVSL(i,j) = 0.3*DVL(i,j)
C
C        Dynamic lateral seat load
         DLSL(i,j) = 0.3*DLL(i,j)
C
C        Cut stress
         CS(i,j) = CS1 * DVSL(i,j) + CS2 * DLSL(i,j)
C
```

```
C        Split stress
         SS(i,j) = SS1 * DVSL(i,j) + SS2 * DLSL(i,j)
C
200   continue
      write(11,2450)
      do 250 i = 1,NTRACK
         write(11,*)' '
         do 250 j = 1,NTRAFF
250         write(11,2500) DVSL(i,j),DLSL(i,j),CS(i,j),SS(i,j)
2450  format(//'STRESS LEVELS',
     :        /'  v rail st  l rail st    cut str  split str',
     :        /'  load (lb)  load (lb)     (psi)      (psi)')
2500  format(4(1x,f10.2))
C
C++++++++++++++++++++++++++++++++++++++++++++++++++++++++++++++++++++++++
C     Calculate the tie damage.
C++++++++++++++++++++++++++++++++++++++++++++++++++++++++++++++++++++++++
C
      TTWPY = 0.0
      do 302 i = 1,NTRACK
302      TWTCK(i)   = 0.0
C
      do 300 j = 1,NTRAFF
         do 300 i = 1,NTRACK
            TWPC(i,j)  = TSI(i)
     :                     *( (RC(i)*CS(i,j)+RS(i)*SS(i,j))
     :                             / (RC(i)+RS(i))          )**TAI(i)
            TWPY(i,j)  = LDCYC(j)*TWPC(i,j)
            TWTCK(i)   = TWTCK(i) + TWPY(i,j)
            TWTRA(i,j) = TWPY(i,j)
            TTWPY      = TTWPY + TWPY(i,j)
300   continue
C
      do 310 i = 1,NTRACK
      do 310 j = 1,NTRAFF
         if ( XMGT(j).ne.0.0 ) then
            TRAFTL(i,j) = 1./TWTRA(i,j)
         else
            TRAFTL(i,j) = 0.0
         endif
310      PTRAF(i,j) = TWTRA(i,j)/TWTCK(i)*100.
C
      do 315 i = 1,NTRACK
         TRCKTL(i) = 1./TWTCK(i)
315      PTRCK(i) = TWTCK(i)/TTWPY*100.
C
C     Output the estimated tie lives.
C
      write(11,3500)
      do 350 i = 1,NTRACK
         write(11,*)' '
         do 350 j = 1,NTRAFF
            if ( j.eq.1 ) then
               write(11,3501) TWPC(i,j),TWPY(i,j),
     :                        TWTRA(i,j),PTRAF(i,j),TRAFTL(i,j),
     :                        TWTCK(i),PTRCK(i),TRCKTL(i)
            else
               write(11,3502) TWPC(i,j),TWPY(i,j),
     :                        TWTRA(i,j),PTRAF(i,j),TRAFTL(i,j)
            endif
350   continue
3500  format(//'ESTIMATED TIE LIFE',
     :       /'  wear rate  wear rate  wr/tracat    %',
     :         '   est life/  wr/tckcat   %    est life/',
     :       /'  (tie/cyc)   (tie/yr)   (tie/yr)    ',
     :         '     trafcat  (tie/yr)          trckcat')
3501  format(2(1x,e10.5),2(1x,e10.5,1x,f5.2,1x,f10.2))
3502  format(2(1x,e10.5),1x,e10.5,1x,f5.2,1x,f10.2)
3503  format(2(1x,e10.5),28x,1x,e10.5,1x,f5.2,1x,f10.2)
3504  format(2(1x,e10.5))
C
C+++++++++++++++++++++++++++++++++++++++++++++++++++++++++++++++++++++++
C     Calculate the number of ties lost per year.
C+++++++++++++++++++++++++++++++++++++++++++++++++++++++++++++++++++++++
C
      TIEMEC = 0.0
      write(11,3615)
      do 360 i = 1,NTRACK
         TIEPMI = 63360.0/TSPACE(i)
         TIEPYR(i) = TWTCK(i)*TIEPMI*L(i)
         TIEMEC = TIEMEC + TIEPYR(i)
         write(11,3610) i,TIEPYR(i)
360   continue
3615  format(//'    Tie loss per track category',
     :       /'         i      Ties')
3610  format(5x,i5,f10.2)
C     TIEMEC = TTWPY*TIEPMI*TLEN
      TIEDEC = TIEMEC*(100-RC(1)-RS(1))/(RC(1)+RS(1))
      TIETOT = TIEMEC+TIEDEC
      write(11,3600) TIEMEC,TIEDEC,TIETOT
3600  format(//'    Mechanical tie loss = ',f10.0,
     :       /'           Other tie loss = ',f10.0,
     :       /'           Total tie loss = ',f10.0)
C
C+++++++++++++++++++++++++++++++++++++++++++++++++++++++++++++++++++++++
C     End of routine.
C
      stop
      end
```

```
TRAFFIC DATA
Class     Wheel load       Ann. ton.
    j     (lb/wheel)        (mgt/yr)
    1        8000.00          10.728
    2       20000.00          11.622
    3       33000.00          22.350


TRACK DATA
Class TotTon Length   Curve TieSp    Tie PltLn    no. H.hgt     RC     RS         TSI
    i per yr (mile)   (deg)  (in)  index  (in)  spike  (in)
    1 44.700  78.00     .00 20.00   1.50 14.00   2.00  3.56  36.70  56.00  .50500E-11
    2 44.700  25.00    2.00 20.00   1.50 14.00   3.00  3.56  36.70  56.00  .50500E-11
    3 44.700  37.00    5.00 20.00   1.50 18.00   5.00  3.56  36.70  56.00  .50500E-11
    4 44.700  25.00    8.00 20.00   1.50 18.00   5.00  3.56  36.70  56.00  .50500E-11


DYNAMIC LOADS
 ld cycles  stat vert  s.s. vert   dyn vert   s..s. lat    dyn lat
 (cyc/yr)   load (lb)  load (lb)  load (lb)   load (lb)  load (lb)
  1341000.    8000.00    8000.00    8629.20         .00     646.05
   581100.   20000.00   20000.00   21573.00         .00    1615.13
   677273.   33000.00   33000.00   35954.33         .00    3033.46

  1341000.    8000.00    8426.01    9037.71      514.43    1033.38
   581100.   20000.00   21065.02   22594.26      947.87    2245.24
   677273.   33000.00   34757.28   37629.43     1323.76    3760.41

  1341000.    8000.00    8781.48    9414.46     2899.36    3330.81
   581100.   20000.00   21953.69   23536.15     5342.30    6420.92
   677273.   33000.00   36223.59   39195.69     7460.88    9486.70

  1341000.    8000.00    8859.82    9434.90     5502.33    5826.23
   581100.   20000.00   22149.55   23587.24    10138.48   10948.22
   677273.   33000.00   36546.75   39246.96    14159.07   15679.90


STRESS LEVELS
  v rail st  l rail st    cut str  split str
  load (lb)  load (lb)      (psi)      (psi)

    2588.76     193.82      29.31     202.72
    6471.90     484.54      73.28     506.80
   10786.30     910.04     125.01     868.07

    2711.31     310.01      33.71     213.16
    6778.28     673.57      81.42     517.44
   11288.83    1128.12     135.77     862.73

    2824.34     999.24      37.25     264.18
    7060.84    1926.28      83.39     608.19
   11758.71    2846.01     132.71     979.76
   2830.47     1747.87       50.03      332.98
   7076.17     3284.47      106.60      733.26
  11774.09     4703.97      164.43     1150.52


ESTIMATED TIE LIFE
  wear rate   wear rate   wr/tracat     %      est life/  wr/tckcat    %      est life/
  (tie/cyc)     (tie/yr)  (tie/yr)               trafcat  (tie/yr)             trckcat

 .78392E-08 .10512E-01 .10512E-01 13.92         95.13 .75540E-01 20.24         13.24
 .30987E-07 .18007E-01 .18007E-01 23.84         55.54
 .69428E-07 .47021E-01 .47021E-01 62.25         21.27

 .85555E-08 .11473E-01 .11473E-01 14.82         87.16 .77412E-01 20.74         12.92
 .32335E-07 .18790E-01 .18790E-01 24.27         53.22
 .69616E-07 .47149E-01 .47149E-01 60.91         21.21

 .11625E-07 .15589E-01 .15589E-01 16.40         64.15 .95052E-01 25.46         10.52
 .40463E-07 .23513E-01 .23513E-01 24.74         42.53
 .82611E-07 .55950E-01 .55950E-01 58.86         17.87

 .16587E-07 .22243E-01 .22243E-01 17.75         44.96 .12528E+00 33.56          7.98
 .53967E-07 .31360E-01 .31360E-01 25.03         31.89
 .10583E-06 .71677E-01 .71677E-01 57.21         13.95


     Tie loss per track category
         i       Ties
         1   18666.32
         2    6131.01
         3   11141.58
         4    9922.21


     Mechanical tie loss =       45861.
          Other tie loss =        3612.
          Total tie loss =       49473.
```

APPENDIX G

"SURLIF" PROGRAM LISTING, INPUT AND OUTPUT

```
C
C $NOFLOATCALLS
C $DEBUG
C
C+++++++++++++++++++++++++++++++++++++++++++++++++++++++++++++++++++++++
C
C     PROGRAM SURLIF
C
C+++++++++++++++++++++++++++++++++++++++++++++++++++++++++++++++++++++++
C
C     C.I.G.G.T. Surface Life Model
C
C
C
C     Program author: J. C. Michaud
C     Date: November 10, 1986
C
C     Input: unit 12 - filename.ext  - supplied by user
C            unit 14 - filename.FRC  - force data calcualted by DYNFOR
C
C     Output: unit 11 - filename.SRF
C
      integer PERIOD
      character*14 INPFIL
      character*1  FILNAM(14)
C
      real    PO(20),XMGT(20)
      real    TMGT(20),L(20),TON(20)
      real    EI(20),TM(20),BAI(20),BCI(20),SPC(20),PPT(20)
      real    SPEED(20,20)
      real    VSTAT(20,20)
      real    HRSSV(20,20),LRSSV(20,20)
      real    HRDV(20,20),LRDV(20,20)
      real    SSLAT(20,20),DLAT(20,20)
C
      real    LDCYC(20)
      real    TCYC(20,20)
      real    HRMIN(20,20),HRMAX(20,20)
      real    LRMIN(20,20),LRMAX(20,20)
      real    LAMBDA(20)
      real    TD(20)
      real    HRMIND(20,20),HRMAXD(20,20),HREGF(20,20)
      real    LRMIND(20,20),LRMAXD(20,20),LREGF(20,20)
      real    AEGF(20,20)
      real    ECYC(20,20)
      real    LIFT(20),SCYCL(20),BFR(20),CYCLES(20)
C
      equivalence ( INPFIL,FILNAM(1) )
C
C+++++++++++++++++++++++++++++++++++++++++++++++++++++++++++++++++++++++
C     Get the files straightened out.
C+++++++++++++++++++++++++++++++++++++++++++++++++++++++++++++++++++++++
C
      write(*,2000)
2000  format(' Enter the input file name: '\)
```

```
      read(*,2001) INPFIL
      open ( 12, file=INPFIL, status='old' )
2001  format(a14)
      PERIOD = 0
      do 2 i = 1,14
         if ( FILNAM(i).EQ.'.' ) then
            PERIOD = i
            go to 4
         endif
2     continue
4     FILNAM(PERIOD+1) = 'S'
      FILNAM(PERIOD+2) = 'R'
      FILNAM(PERIOD+3) = 'F'
      open ( 11, file=INPFIL, status='new' )
      FILNAM(PERIOD+1) = 'F'
      FILNAM(PERIOD+2) = 'R'
      FILNAM(PERIOD+3) = 'C'
      open ( 14, file=INPFIL, status='old' )
C
C+++++++++++++++++++++++++++++++++++++++++++++++++++++++++++++++++++++
C     Get the data.
C+++++++++++++++++++++++++++++++++++++++++++++++++++++++++++++++++++++
C
C Read the traffic data
C     NTRAFF = number of traffic classes
C        PO     = wheel load (lb/wheel)
C        XMGT   = annual tonnage (million tons/yr)
C
      read(12,*) NTRAFF
      do 10 j = 1 , NTRAFF
         read(12,*) PO(j),XMGT(j)
10    continue
C
C Read the track data
C     NTRACK = number of track classes
C        TMGT   = total tonnage (million tons/yr)
C        L      = length (miles)
C        EI     = rail EI
C        TM     = track modulus (lb/in/in)
C        BAI    = ballast abraision index
C        BCI    = ballast condition index
C        SPC    = effective SPC limit (in)
C        PPT    = allowable percantage of poor track
C
      read(12,*) NTRACK
      do 20 i = 1, NTRACK
         read(12,*) TMGT(i),L(i),
     :                 D1,D2,D3,D4,D5,D6,D7,D8,D9,D10,D11,D12,D13,
     :                 EI(i),TM(i),BAI(i),BCI(i),SPC(i),PPT(i)
20    continue
C
C Read the speed data
C        SPEED(i,j) = speed (mph) of traffic class j on track class i
C
      do 30 i = 1 , NTRACK
```

```
         read(12,*) (SPEED(i,j),j=1,NTRAFF)
 30   continue
 C
 C Read the model calibration data
      read(12,*) A,B,C,D
 C
 C Read the precalculated force data
      read(14,36)
      read(14,36)
      read(14,36)
      read(14,36)
      do 35 i = 1,NTRACK
         do 34 j = 1,NTRAFF
            read(14,*) VSTAT(i,j),HRSSV(i,j),LRSSV(i,j),
     :                 HRDV(i,j),LRDV(i,j),
     :                 SSLAT(i,j),DLAT(i,j)
 34      continue
         read(14,36)
 36      format(1x)
 35   continue
 C
 C Echo the input data.
      write(11,1140)
      do 40 j = 1,NTRAFF
         write(11,1142) j,PO(j),XMGT(j)
 40   continue
 1140 format(//'TRAFFIC DATA',
     :        /'Class     Wheel load      Ann. ton.',
     :        /'    j     (lb/wheel)       (mgt/yr)')
 1142 format(i5,f15.2,f15.3)
 C
      write(11,1150)
      do 50 i = 1,NTRACK
         write(11,1152) i,TMGT(i),L(i),
     :                  EI(i),TM(i),BAI(i),BCI(i),SPC(i),PPT(i)
 50   continue
 1150 format(//'TRACK DATA',
     :        /'Class TotTon Length           EI TrkMod',
     :         '   BAI   BCI   SPC   PPT',
     :        /'     i per yr (mile)   lb*in**2 lb.in/in')
 1152 format(i5,1x,f6.3,1x,f6.2,1x,e10.4,1x,f6.1,4(1x,f5.2))
 C
      write(11,1160) (j,j=1,NTRAFF)
      do 60 i = 1 , NTRACK
         write(11,1162) i,(SPEED(i,j),j=1,NTRAFF)
 60   continue
 1160 format(//'SPEED DATA',
     :       /' Track      Traffic Class (mph)',
     :       /' Class',20i6:)
 1162 format(i6,20f6.0:)
 C
      write(11,1170)
      write(11,1173) A,B,C,D
 1170 format(//'CALIBRATION DATA')
 1173 format(' A =',e9.3,1x,'B =',e9.3,1x,'C =',e9.3,1x,'D =',e9.3)
```

```
C
C     Set the system wide parameters
      ITOT = NTRACK + 1
C
C     Calculate the total track length
      L(ITOT) = 0.0
      do 70  i = 1,NTRACK
70       L(ITOT) = L(ITOT) + L(i)
C
C     Initialize the total tonnage
      TON(ITOT) = 0.0
C
C     Set these values (assumed same for all trcak classes)
      BAI(ITOT) = BAI(1)
      BCI(ITOT) = BCI(1)
      SPC(ITOT) = SPC(1)
      PPT(ITOT) = PPT(1)
C
C++++++++++++++++++++++++++++++++++++++++++++++++++++++++++++++++++++++++
C     Calculate the dynamic loads.
C++++++++++++++++++++++++++++++++++++++++++++++++++++++++++++++++++++++++
C
      do 100 j = 1,NTRAFF
C
C        Total ton/yr for each track cat. (ton/yr)
         TON(ITOT) = TON(ITOT) + XMGT(j)*1.0e6
C
C        Load cycles per year for each traffic category
         LDCYC(j)  = 1.0e9*XMGT(j) / PO(j)
C
         do 100 i = 1,NTRACK
C
C           H.R. minimum load (lb)
            HRMIN(i,j) = HRSSV(i,j) - HRDV(i,j)
C
C           H.R. maximum load (lb)
            HRMAX(i,j) = HRSSV(i,j) + HRDV(i,j)
C
C           L.R. minimum load (lb)
            LRMIN(i,j) = LRSSV(i,j) - LRDV(i,j)
C
C           L.R. maximum load (lb)
            LRMAX(i,j) = LRSSV(i,j) + LRDV(i,j)
C
100   continue
      write(11,3000)
      do 112 i = 1,NTRACK
         do 110 j = 1,NTRAFF
            write(11,3002) LDCYC(j),PO(j),
     :                     HRMIN(i,j),HRMAX(i,j),LRMIN(i,j),LRMAX(i,j)
110      continue
         write(11,*)' '
112   continue
3000  format(//'DYNAMIC LOADS',
     :       /' Load cycl  Static V  HR min D  HR max D',
     :          '  LR min D  LR max D',
     :        /'  per year   ld (lb)   ld (lb)   ld (lb)',
     :          '   ld (lb)   ld (lb)',/)
3002  format(1x,f9.0,1x,f9.0,4(1x,f9.2))
C
C++++++++++++++++++++++++++++++++++++++++++++++++++++++++++++++++++++++++
C     Calculate the error growth factors
C++++++++++++++++++++++++++++++++++++++++++++++++++++++++++++++++++++++++
C
C     Initialize the total number of equivalent load cycles
      CYCLES(ITOT) = 0.0
C
      do 210 i = 1,NTRACK
C
C        Tonnage per track class equals the total tonnage
         TON(i) = TON(ITOT)
C
C        Initialize the total number of equivalent load cycles for
C        this track class
         CYCLES(i) = 0.0
C
C        Lambda
         LAMBDA(i) = (TM(i)/(4.*EI(i)))**.25
C
C        Track deflection per unit P
         TD(i) = LAMBDA(i)
     :              *(1.+2.*exp(-70.*LAMBDA(i))
     :              *(cos(70.*LAMBDA(i))+sin(70.*LAMBDA(i))))
     :              /(2.*TM(i))
C
         do 200 j = 1,NTRAFF
C
C           H.R. minimum track deflection (in)
            HRMIND(i,j) = TD(i)*HRMIN(i,j)
C
C           H.R. maximim track deflection (in)
            HRMAXD(i,j) = TD(i)*HRMAX(i,j)
C
C           H.R. track error growth factor
            HREGF(i,j) = (HRMAXD(i,j)**2-HRMIND(i,j)**2)*BCI(i)*BAI(i)
C
C           L.R. minimum track deflection (in)
            LRMIND(i,j) = TD(i)*LRMIN(i,j)
C
C           L.R. maximum track deflection (in)
            LRMAXD(i,j) = TD(i)*LRMAX(i,j)
C
C           L.R. track error growth factor
            LREGF(i,j) = (LRMAXD(i,j)**2-LRMIND(i,j)**2)*BCI(i)*BAI(i)
C
C           Average track error growth factor
            AEGF(i,j) = (HREGF(i,j)+LREGF(i,j))/2.
C
C           Equivalent cycles
            ECYC(i,j) = LDCYC(j)*(AEGF(i,j)/.79)
```

```
C
C           Annual equivalent cycles per class
            TCYC(i,j) = ECYC(i,j)*L(i)
C
C           Number of equivalent load cycles
            CYCLES(i) = CYCLES(i) + TCYC(i,j)
            CYCLES(ITOT) = CYCLES(ITOT) + TCYC(i,j)
200      continue
C
C        Number of equivalent load cycles
         CYCLES(i) = CYCLES(i)/L(i)
C
210   continue
C
C     Number of equivalent load cycles
      CYCLES(ITOT) = CYCLES(ITOT)/L(ITOT)
C
C     Output the results so far
C
      write(11,3100)
      do 253 i = 1,NTRACK
         do 252 j = 1,NTRAFF
            write(11,3102) LAMBDA(i),TD(i),
     :                       HRMIND(i,j),HRMAXD(i,j),HREGF(i,j),
     :                       LRMIND(i,j),LRMAXD(i,j),LREGF(i,j)
252      continue
         write(11,*)' '
253   continue
      write(11,3104)
      do 255 i = 1,NTRACK
         do 254 j = 1,NTRAFF
            write(11,3106) AEGF(i,j),ECYC(i,j)
254      continue
         write(11,*)' '
255   continue
3100  format(//' LMBDA  trk def.     HR min    HR max    HR trk',
     :         '    LR min    LR max    LR trk',
     :        /'        / unit P   trk def   trk def       EGF',
     :         '   trk def   trk def       EGF',/)
3102  format(1x,f5.3,1x,e9.3,6(1x,e9.2))
3104  format(//'   avg trk    equiv.',
     :        /'      EGF    cycles',/)
3106  format(1x,e9.2,1x,f9.0)
C
C
      do 410 i = 1,ITOT
C
C        Iterative calculation to calculate surfacing cycle
         AL = 6.*C+2.*A
         BL = 6.*D-2.*SPC(i)+2.*B
         SINIT = 0
         TINIT = 0
         XL = BL/(2.*D)
         if ( XL.gt.1.9 ) then
            PP = 13.7+31.75*(XL-1.9)**1.2
```

```
          else
             PP = .307*exp(2.*XL)
          endif
          ILOOP = 0
 400      continue
          ILOOP = ILOOP + 1
          TINIT = TINIT+1
          NT = CYCLES(i)*TINIT/4.
          XL = .5*(AL*NT+BL)/(C*NT+D)
          if ( XL.gt.1.9 ) then
             PL = 13.7+31.75*(XL-1.9)**1.2
          else
             PL = .307*exp(2.*XL)
          endif
          IA = (PL+PP)/2.
          SINIT = SINIT+IA
          AA = SINIT/TINIT
          if ( AA.lt.PPT(i) ) then
             PP = PL
             go to 400
          endif
C
C         Calculate the surfacing cycle in years
          SCYCL(i) = (TINIT-1)/4.
C
C         Ballast foul rate (in/MGT)
          BFR(i) = 3.73E-5 * BAI(i)**1.54 * BCI(i)
C
C         Required lift height
          LIFT(i) = 1.175*BFR(i)*SCYCL(i)*(TON(i)/1.e6)
C
410   continue
C
      write(11,3200)
      do 260 i = 1,NTRACK
         write(11,3202) i,CYCLES(i),BFR(i),SCYCL(i),LIFT(i),TON(i)
260   continue
      i = ITOT
      write(11,3203) CYCLES(i),BFR(i),SCYCL(i),LIFT(i),TON(i)
3200  format(//'Track   Tot ann.    Ballast Surface    Lift',
     :          '    Tot tons per',
     :         /'    i equiv. cyc  foul rate cyc(yr)    (in)',
     :          '     track class')
3202  format(i5,1x,f10.0,1x,e10.3,1x,f7.2,1x,f7.3,1x,f15.0)
3203  format(/'total',1x,f10.0,1x,e10.3,1x,f7.2,1x,f7.3,1x,f15.0)
C
C++++++++++++++++++++++++++++++++++++++++++++++++++++++++++++++++++++++++++++
C     End of routine.
C
      stop
      end
```

```
TRAFFIC DATA
Class     Wheel load        Ann. ton.
    j     (lb/wheel)         (mgt/yr)
    1        8000.00           10.728
    2       20000.00           11.622
    3       33000.00           22.350


TRACK DATA
Class TotTon Length            EI TrkMod   BAI    BCI    SPC   PPT
    i per yr (mile)    lb*in**2 lb.in/in
    1 44.700  78.00  .2640E+10 2000.0 61.00  1.00    .63 16.00
    2 44.700  25.00  .2640E+10 2000.0 61.00  1.00    .63 16.00
    3 44.700  37.00  .2640E+10 2000.0 61.00  1.00    .63 16.00
    4 44.700  25.00  .2640E+10 2000.0 61.00  1.00    .63 16.00


SPEED DATA
 Track      Traffic Class (mph)
 Class       1      2      3
     1   45.    45.    45.
     2   40.    40.    40.
     3   35.    35.    35.
     4   30.    30.    30.


CALIBRATION DATA
 A = .621E-07 B = .246E+00 C = .273E-07 D = .139E+00


DYNAMIC LOADS
 Load cycl  Static V  HR min D  HR max D  LR min D  LR max D
 per year   ld (lb)    ld (lb)   ld (lb)   ld (lb)   ld (lb)

  1341000.     8000.   7370.80   8629.20   7370.80   8629.20
   581100.    20000.  18427.00  21573.00  18427.00  21573.00
   677273.    33000.  30045.67  35954.33  30045.67  35954.33

  1341000.     8000.   7814.31   9037.71   7024.15   8123.83
   581100.    20000.  19535.78  22594.26  17560.37  20309.59
   677273.    33000.  31885.13  37629.43  28661.00  33824.44

  1341000.     8000.   8148.50   9414.46   6698.20   7738.84
   581100.    20000.  20371.23  23536.15  16745.50  19347.12
   677273.    33000.  33251.49  39195.69  27333.29  32219.53

  1341000.     8000.   8284.74   9434.90   6676.72   7603.64
   581100.    20000.  20711.86  23587.24  16691.81  19009.09
   677273.    33000.  33846.54  39246.96  27277.14  31629.36


LMBDA   trk def.    HR min    HR max    HR trk    LR min    LR max    LR trk
```

```
        / unit P   trk def    trk def        EGF    trk def    trk def        EGF

 .021  .789E-05   .58E-01    .68E-01    .76E-01    .58E-01    .68E-01    .76E-01
 .021  .789E-05   .15E+00    .17E+00    .48E+00    .15E+00    .17E+00    .48E+00
 .021  .789E-05   .24E+00    .28E+00    .15E+01    .24E+00    .28E+00    .15E+01

 .021  .789E-05   .62E-01    .71E-01    .78E-01    .55E-01    .64E-01    .63E-01
 .021  .789E-05   .15E+00    .18E+00    .49E+00    .14E+00    .16E+00    .40E+00
 .021  .789E-05   .25E+00    .30E+00    .15E+01    .23E+00    .27E+00    .12E+01

 .021  .789E-05   .64E-01    .74E-01    .84E-01    .53E-01    .61E-01    .57E-01
 .021  .789E-05   .16E+00    .19E+00    .53E+00    .13E+00    .15E+00    .36E+00
 .021  .789E-05   .26E+00    .31E+00    .16E+01    .22E+00    .25E+00    .11E+01

 .021  .789E-05   .65E-01    .74E-01    .77E-01    .53E-01    .60E-01    .50E-01
 .021  .789E-05   .16E+00    .19E+00    .48E+00    .13E+00    .15E+00    .31E+00
 .021  .789E-05   .27E+00    .31E+00    .15E+01    .22E+00    .25E+00    .97E+00


  avg trk    equiv.
      EGF    cycles

  .76E-01    129762.
  .48E+00    351437.
  .15E+01   1269331.

  .71E-01    120113.
  .44E+00    325307.
  .14E+01   1174953.

  .71E-01    120059.
  .44E+00    325161.
  .14E+01   1174429.

  .64E-01    108327.
  .40E+00    293384.
  .12E+01   1059659.


Track    Tot ann.    Ballast Surface     Lift     Tot tons per
    1 equiv. cyc  foul rate cyc(yr)      (in)     track class
    1   1750530.   .209E-01    2.75     3.025       44700000.
    2   1620373.   .209E-01    3.00     3.301       44700000.
    3   1619649.   .209E-01    3.00     3.301       44700000.
    4   1461371.   .209E-01    3.25     3.576       44700000.

total   1657648.   .209E-01    3.00     3.301       44700000.
```